

Electron Transfer at Iron Mineral Surface in the Presence of Aqueous Sulfide and Dissolved Organic Matter under Anoxic Condition

Dissertation

der Mathematisch-Naturwissenschaftlichen Fakultät

der Eberhard Karls Universität Tübingen

zur Erlangung des Grades eines Doktors der Naturwissenschaften

(Dr. rer. nat.)

vorgelegt von Shaojian Zhang

aus Jingmen, China

Tübingen 2018

Tag der mündlichen Qualifikation: 12.12.2018

Dekan: Prof. Dr. Wolfgang Rosenstiel

1. Berichterstatter: Prof. Dr. Stefan Haderlein

2. Berichterstatter: Prof. Dr. Stefan Peiffer

Table of contents

Table of contents.....	i
Abstract.....	v
Zusammenfassung.....	vii
1 Introduction.....	1
1.1 The significance of Fe(II) and iron (hydr)oxides.....	1
1.1.1 Cycling of iron in natural system.....	1
1.1.2 Reactivity of Fe(II) species associated with iron oxides	2
1.1.3 Sorption of Fe(II) on iron oxides	3
1.2 Aqueous sulfide	5
1.2.1 Origin of sulfide species	5
1.2.2 The interactions between sulfide and iron oxides.....	5
1.3 Natural Organic Matter	7
1.3.1 General information.....	7
1.3.2 The role of NOM in degradation of pollutants	9
1.3.3 The interactions of NOM with iron oxides/ aqueous sulfide.....	10
1.4 Scope of this dissertation	11
2 Effect of Fe(II) on geochemical interactions of iron minerals and aqueous sulfide in anoxic waters	15
2.1 Introduction.....	15
2.2 Materials and methods	17
2.2.1 Materials	17
2.2.2 Experimental setups	18
2.2.3 Sampling and analytical methods	19
2.3 Results and discussion	23

2.3.1 pH changes during the studied reactions	23
2.3.2 Evaluation of sulfur species during the reaction.....	24
2.3.3 Evaluation of Fe(II) species during the reaction.....	27
2.3.4 Mössbauer spectroscopy	30
2.3.5 Evaluation of acid volatile sulfide and S distribution.....	32
2.4 Conclusions.....	36
3 Reaction of aqueous sulfide with goethite/Fe(II) in the presence of natural organic matter at neutral pH under anoxic conditions	39
3.1 Introduction.....	39
3.2 Materials and Methods.....	40
3.2.1 Materials	40
3.2.2 Experimental setups	41
3.2.3 Sampling and analytical methods	45
3.3 Results and discussion	49
3.3.1 pH changes during the reaction.....	49
3.3.2 Evaluation of sulfur species during the reaction.....	50
3.3.3 Evaluation of Fe(II) species during the reaction.....	52
3.3.4 Acid volatile sulfide.....	55
3.3.5 Sulfur atoms mass balance.....	57
3.4 Conclusions and outlook.....	60
4 The abiotic sulfur cycle revisited – Disproportionation of elemental sulfur by surface-bound Fe(II) at goethite	61
4.1 Introduction.....	61
4.2 Materials and methods	62
4.2.1 Materials	62
4.2.2 Experimental setup.....	63
4.2.3 Analytical methods	63

4.3 Results and discussion	67
4.3.1 Changes in pH, S ⁰ and Fe(II) in suspension	67
4.3.2 Formation of reduced sulfur species (polysulfides, FeS, FeS _n)	69
4.3.3 Formation of oxidized sulfur species (sulfate and thiosulfate).....	71
4.3.4 Sulfur-mass balance	73
4.3.5 Reaction mechanisms and electron balance.....	75
4.5 Environmental implications	79
5 Conclusions and Outlook.....	81
5.1 Conclusions.....	81
5.2 Outlook	82
6 References.....	85
Statement of Personal Contribution.....	93
Acknowledgement	94
Curriculum Vitae	95

Abstract

The interaction between iron oxides and aqueous sulfide is an important biogeochemical process under anoxic water conditions. The main reaction products are elemental sulfur and ferrous iron with the formation of metastable iron sulfide minerals, which may transform to thermodynamically stable pyrite. Thus, these reactions play a significant role in the cycling of iron and sulfur in natural system. In anoxic aquatic systems, Fe(II) and natural organic matter (NOM) are ubiquitously present and likely interfere with the reaction of iron oxides and sulfide. Little is known, however, how and to what extent Fe(II) and NOM affect the interactions between iron oxides and aqueous sulfide. Therefore, the role of Fe(II) and NOM on the redox reactions between iron oxides and sulfide was investigated in this dissertation. Considering that mineral adsorbed Fe(II) ($\text{Fe(II)}_{\text{sorb}}$) exhibits a high reducing power and elemental sulfur is a main product in the oxidation of sulfide, it was also investigated if and under which conditions elemental sulfur can be reduced by Fe(II) adsorbed at iron mineral surfaces. Wet chemical analysis was used to determine the main sulfur and iron species. In addition, Mössbauer spectroscopy was used to check the formation of potential secondary iron mineral.

The presence and speciation of Fe(II) strongly affected the pathways, rates and products of reactions between goethite and aqueous sulfide. In the absence of Fe(II) the redox reaction between structural Fe(III) of goethite and sulfide was significant and gave high yields of elemental sulfur. When suspended goethite completely adsorbed aqueous Fe(II) ($\text{Fe(II)}_{\text{aq}}$) so that no detectable $\text{Fe(II)}_{\text{aq}}$ was present, the oxidation of sulfide was severely inhibited. In the presence of significant concentrations of both $\text{Fe(II)}_{\text{sorb}}$ and $\text{Fe(II)}_{\text{aq}}$, however, the oxidation of sulfide to elemental sulfur occurred. It is proposed that under such conditions, sulfide reacted with Fe(III) surface species that dynamically formed. The presence of $\text{Fe(II)}_{\text{aq}}$ is required to renew $\text{Fe(II)}_{\text{sorb}}$ species that partially inject electrons into bulk goethite thereby being transiently oxidized to reactive Fe(III) at the goethite surface. Thus, the significant reaction between sulfide and goethite in the presence of $\text{Fe(II)}_{\text{aq}}$ was attributed to the continuous regeneration of reactive Fe(III) species at goethite surface. No secondary iron mineral was detectable by Mössbauer spectroscopy.

The presence of Aldrich humic acid (AHA) inhibited the redox reaction between sulfide with goethite in the presence of Fe(II) due to its sorption at goethite surface, leading to a lower amount of transformation products (thiosulfate and sulfate were not detected). Within the range of applied AHA concentrations (10 mg C/L – 40 mg C/L), the coating effect of AHA played

the major role in the whole reaction process, while, the redox state of AHA was insignificant. Furthermore, a small fraction of sulfide was incorporated into the AHA structure, which also contributed to the inhibition of the reaction of sulfide with goethite.

Finally the reduction of elemental sulfur by $\text{Fe(II)}_{\text{sorb}}$ at goethite surface was investigated at neutral pH under anoxic conditions. It was found that parallel to the reduction of S^0 to sulfide by $\text{Fe(II)}_{\text{sorb}}$ and subsequent formation of FeS and polysulfides, S^0 also was oxidized to sulfate. The occurrence of sulfur oxidation suggested the presence of reactive surface Fe(III) species. Due to scavenging effect of goethite and Fe(II), the buildup of polysulfides was inhibited as they readily decomposed to sulfide and elemental sulfur.

The results of this thesis revealed new and significant insights in the interactions of goethite with sulfide in the presence of Fe(II) and NOM. Furthermore, the disproportionation of sulfur in goethite/Fe(II) suspension not only demonstrated the high reducing potential of $\text{Fe(II)}_{\text{sorb}}$, but also the oxidation capability of Fe(III) surface species under reducing anoxic conditions. Therefore the findings of this dissertation can help us to improve our understanding of the geochemical interactions in natural anoxic waters, thus eventually enabling us to apply these findings to develop techniques of pollutant transformation in anoxic groundwater systems.

Zusammenfassung

Die Wechselwirkung zwischen Eisenoxiden und gelöstem Sulfid ist ein wichtiger biogeochemischer Prozess in anoxischen Wässern. Die Hauptprodukte dieser Reaktion sind elementarer Schwefel und zweiwertiges Eisen, sowie gebildete metastabile Eisensulfid-Mineraie, welche zu thermodynamisch stabilem Pyrit umgewandelt werden können.

Daher spielen diese Reaktionen eine wichtige Rolle im Eisen- und Schwefelkreislauf in natürlichen Systemen. In anoxischen aquatischen Systemen sind Fe(II) und natürliches organisches Material (NOM) stets vorhanden und es ist wahrscheinlich, dass diese die Reaktion zwischen Eisenoxiden und Sulfid beeinflussen. Jedoch ist wenig darüber bekannt, wie und in welchem Ausmaß dies der Fall ist. Deshalb wurde in dieser Arbeit die Rolle von Fe(II) und NOM auf die Wechselwirkung von Eisenoxiden und Sulfid untersucht. In Anbetracht der Tatsache, dass an Minerale adsorbiertes Fe(II) ($\text{Fe(II)}_{\text{sorb}}$) ein hohes Reduktionspotential aufweist und elementarer Schwefel das Hauptprodukt der Oxidation von Sulfid ist, wurde ebenfalls untersucht, ob und unter welchen Bedingungen elementarer Schwefel durch Fe(II) reduziert werden kann, welches an Eisenmineralen adsorbiert ist. Die Hauptspezies von Schwefel und Eisen wurden mittels nasschemischer Analyse bestimmt. Zusätzlich wurde Mössbauer-Spektroskopie angewendet, um die mögliche Bildung sekundärer Eisenminerale zu untersuchen.

Die Anwesenheit und Spezierung von Fe(II) hatte einen großen Einfluss auf den Reaktionsverlauf, und Rate, sowie die Produkte der Reaktion zwischen Goethit und gelöstem Sulfid. In der Abwesenheit von Fe(II) war die Reaktion zwischen strukturellem Fe(III) in Goethit und Sulfid ausgeprägt und hatte die Bildung hoher Konzentrationen an elementarem Schwefel zur Folge. Im Falle kompletter Adsorption von gelöstem Fe(II) ($\text{Fe(II)}_{\text{aq}}$) an Goethit wurde die Oxidation von Sulfid merklich gehemmt. Jedoch fand die Oxidation von Sulfid zu elementarem Schwefel statt, wenn signifikante Mengen an $\text{Fe(II)}_{\text{sorb}}$ und $\text{Fe(II)}_{\text{aq}}$ vorhanden waren. Für dieses System wurde eine Reaktion von Sulfid mit dynamisch gebildeten Fe(III)-Oberflächenspezies hypothesiert. Hierbei ist die Anwesenheit von $\text{Fe(II)}_{\text{aq}}$ nötig, um erneut $\text{Fe(II)}_{\text{sorb}}$ -Spezies zu bilden, welche partiell Elektronen in das Goethit überführen und dadurch zu Fe(III) oxidiert wurden. Somit wurde die Reaktion von Sulfid mit Goethit in der Anwesenheit von $\text{Fe(II)}_{\text{aq}}$ auf die kontinuierliche Regeneration von reaktiven Fe(III)-Spezies auf der Goethit-Oberfläche zurückgeführt. Hierbei konnten keine sekundären Eisenminerale mittels Mössbauer-Spektroskopie nachgewiesen werden.

Die Anwesenheit von Aldrich Humins äure (AHA) verhinderte die Redoxreaktion zwischen Sulfid und Goethit in der Anwesenheit von Fe(II) aufgrund der Adsorption der Humins äure an die Goethit-Oberfl äche. Dies führte zu geringeren Konzentrationen an Transformationsprodukten (Thiosulfat und Sulfat wurden nicht nachgewiesen). Im untersuchten AHA-Konzentrationsbereich (10 mgC/L – 40 mgC/L) spielte die Bildung einer Humins äureschicht auf der Mineraloberfl äche eine ausschlaggebende Rolle für den gesamten Reaktionsprozess, wohingegen der Einfluss des Redoxzustands unerheblich war. Zudem wurde ein kleiner Teil des Sulfids in die AHA-Struktur eingebaut, was zusätzlich zu der Hemmung der Reaktion zwischen Sulfid und Goethit beitrug.

Schlussendlich wurde die Reduktion von elementarem Schwefel durch Fe(II)_{sorb} auf Goethit unter anoxischen Bedingungen und im neutralen pH-Bereich untersucht. Neben der Reduktion von S⁰ zu Sulfid durch Fe(II)_{sorb} und der darauf folgenden Bildung von FeS und Polysulfiden, wurde zudem die Oxidation von S⁰ zu Sulfat gezeigt. Diese Oxidation deutete auf die Anwesenheit reaktiver Fe(III)-Spezies auf der Goethit-Oberfl äche hin. Goethit und Fe(II) hemmten die Bildung von Polysulfiden, da diese schnell zu Sulfid und elementarem Schwefel zerfielen.

Die Ergebnisse dieser Arbeit geben neue und wichtige Einblicke in die Wechselwirkung zwischen Goethit und Sulfid in der Anwesenheit von Fe(II) und NOM. Zudem, konnte anhand der Disproportionierung von Schwefel im Goethit/Fe(II)-System nicht nur das hohe Reduktionspotential von Fe(II)_{sorb}, sondern auch das Oxidationspotential von Fe(III)-Oberfl ächenspezies unter anoxischen Bedingungen gezeigt werden. Somit helfen die Ergebnisse der vorgestellten Arbeit, das Verständnis über geochemische Prozesse zu verbessern und somit möglicherweise Techniken für den Schadstoffabbau in anoxischen Grundwassersystemen zu entwickeln.

1 Introduction

1.1 The significance of Fe(II) and iron (hydr)oxides

1.1.1 Cycling of iron in natural system

Oxygen and iron are the most and the fourth most abundant elements by mass in the earth's crust, in which their respective proportions amount to 46.6 % and 5.0 %. It is therefore not surprising that compounds made up of these two elements are common in natural system (Murad and Cashion, 2004). They can form iron oxides, iron oxyhydroxides and iron hydroxides, which are often grounded under the general term "iron oxides". So iron oxides are one of the most common compounds in the earth and readily synthesized in laboratory. They can be found in almost all of the different compartments of the global system (Cornell and Schwertmann, 2003). These iron oxides profoundly influence the quality of our water, air and soil through the biologically-driven redox cycling between ferric iron (Fe(III)) and ferrous iron (Fe(II)).

The biogeochemical interactions play a vital role in the cycling of elements and behavior of inorganic and organic contaminants. They can reduce iron oxides to Fe(II) and reduce sulfur containing compounds to hydrogen sulfide (Cline and Richards, 1972; Fonselius et al., 2007), thus conserving energy to support growth by completely oxidizing organic compounds to carbon dioxide. The redox cycling of organic compounds and nitrogen through biogeochemical interaction not only influence the micro- and macro-biological environment, but also exert implications for global balances and climate change. For example, the emission of methane and carbon dioxide contributes significantly to the overall greenhouse gas budget on Earth (Borch et al., 2009; Lovley, 1997; Schmidt et al., 2010). Microbial oxidation of organic contaminants coupled to Fe(III) reduction removes significant amounts of pollutants from many contaminated waters (Lovley, 1997). Thus, Lovley proposed that the metabolism can be useful for the remediation of metal-contaminated subsurface environment and the subsequent insoluble Fe(II) products of Fe(III) reduction can reductively dechlorinate chlorinated contaminants, which lead to a lot of investigations on this aspect. Therefore, the cycling of iron oxides is of great importance for the environment, and the investigations related to iron redox reaction obtained mass interest.

1.1.2 Reactivity of Fe(II) species associated with iron oxides

In anoxic aqueous environments Fe(II) can be produced through microbial reduction of iron oxides. The Fe(II) released into the groundwater is a main groundwater quality problem in many waters. Fe(II) is also an important reductant in natural environment, particularly when it is associated with iron oxides. Numerous lab-based experiments and field studies have demonstrated the high reactivity of surface sorbed Fe(II) ($\text{Fe(II)}_{\text{sorb}}$) towards reducible compounds (Elsner et al., 2004; Glass, 1972; Haderlein and Pecher, 1998; Hofstetter et al., 2006; Hofstetter et al., 2003). Several studies found that the rates of contaminants degradation could be expressed as a linear function of the concentration of $\text{Fe(II)}_{\text{sorb}}$ (Amonette et al., 2000; Cui and Eriksen, 1996; Gregory et al., 2004; Klausen et al., 1995). A general scheme for reduction of pollutants by reactive $\text{Fe(II)}_{\text{sorb}}$ was proposed by Haderlein and Pecher (1998) as follows:

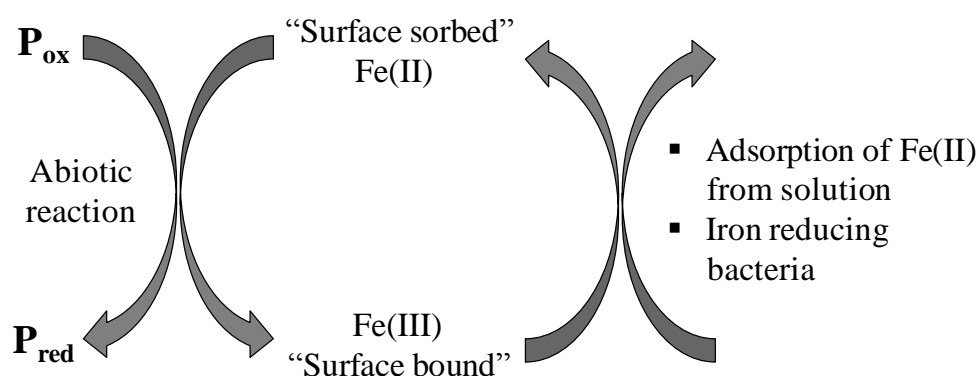


Figure 1.1: General scheme for reduction of pollutants by reactive Fe(II) surface sites and processes that regenerate such reductants.

Previous researches have demonstrated that the $\text{Fe(II)}_{\text{sorb}}$ is reactive towards reducible organic pollutants such as dichlorodiphenyltrichloroethane (DDT), 4-chloronitrobenzene (4-Cl-NB) and nitrobenzenes (NBs) (Glass, 1972; Heijman et al., 1995; Heijman et al., 1993; Klausen et al., 1995). The reduction was surface mediated and the reduction rate increased with the loading of $\text{Fe(II)}_{\text{sorb}}$. No reaction occurred when only Fe(II) was present and iron oxides were absent. The contaminants degradation had a second-order reaction rate with respect with the density of $\text{Fe(II)}_{\text{sorb}}$. Similar observations have also been found by Elsner et al. (2004) and Shao (2007).

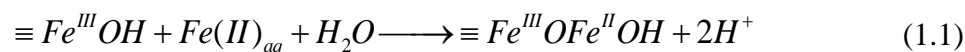
Regarding the contaminant metals and metalloids such as uranium, technetium, cobalt, chromium and selenium, a significant amount of investigations have also been conducted. The reduction of U(VI) by Fe(II) sorbed at iron oxides surface has been widely observed (Chakraborty et al., 2010; Fox et al., 2013; Liger et al., 1999). Williams and Scherer (2001) observed that the heterogeneous reduction by Fe(II) associated with the carbonate green rust appears to be the dominant pathway controlling Cr(VI) loss from solution. Huang and Zhang (2016) observed the nitrate reduction by magnetite associated Fe(II) at near-neutral pH.

In summary, the Fe(II) can not only contribute to the degradation of organic pollutants, but also is useful for remediation of heavy metals pollutions. Due to the significant characteristic of Fe(II), researches related to the reaction between Fe(II) with iron oxides and their reaction (iron oxides/ Fe(II)) with other reactant have always been hot research targets.

1.1.3 Sorption of Fe(II) on iron oxides

The sorption of Fe(II) at iron oxides surface is a complicated process between Fe(II) and iron oxides, comprising sorption, electron transfer, atom exchange and in some cases reductive dissolution and transformation to secondary minerals.

The increased reactivity of $Fe(II)_{sorb}$ relative to aqueous Fe(II) ($Fe(II)_{aq}$) was attributed to hydroxyl ligands (-OH) at the iron oxides surface acting as sigma donor ligands, which increased the electron density of the Fe(II) atoms (Stumm, 1987; Stumm and Sulzberger, 1992). It was proposed that the specific surface species $\equiv Fe^{III}OFe^{II}OH$ was responsible for contaminant reduction, allowing more Fe(II) adsorption (Liger et al., 1999). A reaction of Fe(II) sorption at Fe minerals surface is provided by Elsner et al. (2004), which can be represented as:



Where $\equiv Fe^{III}OH$ refers to as a surface adsorption site. The surface complex of Fe(II) on mineral surface is $\equiv Fe^{III}OFe^{II}OH$, which is neutral charged, rather than surface-Fe(II), suggesting that further adsorption of Fe(II) from solution is not prevented by electrostatic repulsion.

The electron transfer reaction between sorbed Fe(II) and the underlying iron oxides occurs as following (Coughlin and Stone, 1995):



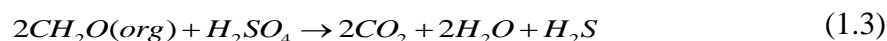
Larese-Casanova and Scherer (2007) investigated the interaction of $^{57}\text{Fe}(\text{II})$ with ^{56}Fe hematite using Mössbauer spectroscopy. Their finding demonstrated that at low $\text{Fe}(\text{II})$ concentrations, sorbed $\text{Fe}(\text{II})$ species were transient and quickly underwent electron transfer with structural $\text{Fe}(\text{III})$ in hematite. Other researches using Mössbauer spectroscopy revealed that electron transfer took place between sorbed $^{57}\text{Fe}(\text{II})$ and structural $\text{Fe}(\text{III})$ (e.g. goethite, hematite and magnetite), and that the $^{57}\text{Fe}(\text{II})$ was oxidized to form similar underlying minerals (Gorski and Scherer, 2009; Larese-Casanova and Scherer, 2007; Williams and Scherer, 2004). Due to electron transfer between $\text{Fe}(\text{II})_{\text{sorb}}$ and structural $\text{Fe}(\text{III})$ in iron oxides, the electron migrates from $\text{Fe}(\text{II})_{\text{sorb}}$ to the oxide structure, reducing structure $\text{Fe}(\text{III})$ to structural $\text{Fe}(\text{II})$. The reduced $\text{Fe}(\text{II})$ may be released into solution as an $\text{Fe}(\text{II})$ atoms (Gorski and Scherer, 2011; Pedersen et al., 2005). Pedersen et al. (2005) investigated isotopic exchange between aqueous $\text{Fe}(\text{II})$ (0 – 1.0 mM) with ^{55}Fe enriched oxides with different crystallinities (e.g. ferrihydrite, lepidocrocite, goethite, hematite) at 25 °C and pH 6.5, and observed the continuous release of ^{55}Fe from the investigated minerals into solution with time, and the rate and extent of atom exchange varies significantly due to different crystallinities. Handler et al. (2009) demonstrated a complete atom exchange between enriched $^{57}\text{Fe}(\text{II})_{\text{aq}}$ with natural abundant nano-goethite through measuring $\delta^{57/56}\text{Fe}$ values in both $\text{Fe}(\text{II})_{\text{aq}}$ and goethite. Electron transfer and atom exchange lead to the reductive dissolution of iron oxides and growth of an $\text{Fe}(\text{III})$ layer at the oxide surface that is similar to the bulk oxides (Pedersen et al., 2005; Williams and Scherer, 2004). The resulting surface sorbed $\text{Fe}(\text{II})$ species is capable of reducing organic contaminants.

Previous literatures have proved that electron transfer and atom exchange are the main interactions between $\text{Fe}(\text{II})_{\text{aq}}$ and iron oxides, thus playing a vital role regarding the reactivity of $\text{Fe}(\text{II})_{\text{sorb}}$ and subsequent reactions related to $\text{Fe}(\text{II})$ and $\text{Fe}(\text{III})$. In natural anoxic water systems, $\text{Fe}(\text{II})$ along with many other components are present. $\text{Fe}(\text{II})$ sorbs at mineral surface as coating, preventing the direct reaction between iron oxides with the adjacent components (e.g sulfide, metal ion or organic matter). On the other hand, sorbed $\text{Fe}(\text{II})$ can also react with them or act as an electron transfer mediator to stimulate the reaction between these adjacent components with iron oxides. While the overall effect of $\text{Fe}(\text{II})$ on the reaction between iron oxides and other component is not clear. Thus it is necessary to investigate the interaction between iron oxides with other reactants in the presence of $\text{Fe}(\text{II})$.

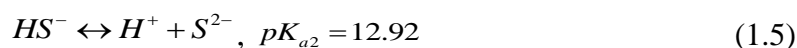
1.2 Aqueous sulfide

1.2.1 Origin of sulfide species

Hydrogen sulfide is an important reductant in anoxic waters and sediments, it can be produced in groundwater through sulfate reduction by microorganisms, which requires the presence of both sulfate and organic matter in the absence of oxygen and other oxides in groundwater (see Eq 1.3) (Fonselius et al., 2007; Kamyshny Jr et al., 2008).



The speciation of sulfide is strong pH dependent. Sulfide exists mainly in two forms in water: undissociated hydrogen sulfide (H_2S) and bisulfide ion (HS^-), the form of S^{2-} is never a dominating aqueous speciation (Duranceau and Faborode, 2012).



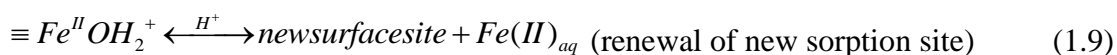
At pH 8.0 (typical of seawater), about 9 % of sulfide is in the form of H_2S , whereas at pH 6.0, approximate 91 % of sulfide is in the form of H_2S . At pH 7.0, both H_2S and HS^- are present at the same amount (Wang and Chapman, 1999).

1.2.2 The interactions between sulfide and iron oxides

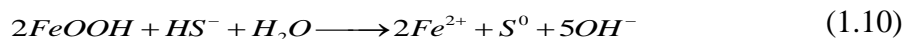
The presence of sulfide species can significantly interfere with the redox chemistry of iron oxides and the composition of the mineral-water interface. Thus the investigations on the kinetic and mechanisms of the reaction between aqueous sulfide and iron oxides have been widely conducted (Dos Santos Afonso and Stumm, 1992; Peiffer et al., 2015; Peiffer et al., 1992; Poulton, 2003; Wan et al., 2014).

Hydrogen sulfide can reductively dissolve iron oxides, which is of great importance in the cycling of electrons and sulfur element, as well as the diagenesis in water-sediment systems and in soil systems. Since the main redox products from reaction between sulfide and iron oxides are elemental sulfur and Fe(II), the Fe(II) would precipitate sulfide to form FeS. While FeS is a metastable iron monosulfide mineral, which can react with elemental sulfur and transform to thermodynamically stable pyrite (Hunger and Benning, 2007; Pyzik and Sommer, 1981; Wan et al., 2014).

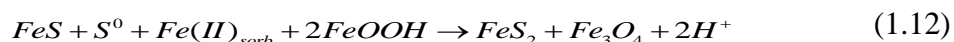
The interactions between sulfide and iron oxides have been proposed to proceed via the following reaction sequences (Dos Santos Afonso and Stumm, 1992):



The surface complex between bisulfide and reactive surface sites can form an inner sphere complex, which is expected to result in the fast transfer of electrons (Poulton, 2003). The reaction between hydrogen sulfide and lepidocrocite exhibits a strong pH dependence with a maximum rate at pH 7 (Peiffer et al., 1992). The overall reaction follows the stoichiometry:



The yield of iron monosulfide (FeS) depends on the initial sulfide concentration and reactive mineral surface sites concentrations (Hellige et al., 2012; Peiffer et al., 2015). Hellige and Peiffer proposed that under conditions where the initial sulfide concentration is relatively lower compared to the amount of reactive sites, the oxidation of sulfide is fast and thus the association of sulfide with generated Fe(II) is slow, leading to low FeS concentration but high S^0 concentration. Meanwhile, the generated Fe(II) would bind at mineral surface forming $Fe(II)_{sorb}$. While under conditions where the sulfide concentration is very high, the detachment rate of Fe(II) is high enough to channel Fe(II) into FeS formation. The precipitated FeS is supposed to sorb at iron oxides surface and to transfer electrons to structural Fe(III) in a similar way as adsorbed sulfide does (Hellige et al., 2012). Peiffer et al. (2015) observed the yield of pyrite was high in experiments in which high concentrations of $Fe(II)_{sorb}$ was intermediately formed. It is believed that $Fe(II)_{sorb}$ can trigger transformation of mineral and accelerate the formation of pyrite via Eq 1.12 (Hellige et al., 2012; Peiffer et al., 2015).



In summary, the main reaction products between aqueous sulfide and iron oxides are elemental sulfur and Fe(II). The rate and extent of iron sulfide minerals transformation varies significantly with the crystallinities of iron oxides and the concentration of sulfide. As a main

product of the interaction, Fe(II) plays a vital role in the subsequent reactions, affecting the reactions between sulfide and iron oxides and the formation of pyrite. Due to the wide presence of Fe(II) in natural anoxic water system, apart from the reaction between sulfide with iron oxides, the interaction of sulfide with Fe(II)_{aq} or Fe(II)_{sorb} is inevitable. However how Fe(II) affect the overall reactions is not clear yet. To this end, we investigated the effect of Fe(II) on the interaction between aqueous sulfide and goethite in this PhD research work, and to identify the role of Fe(II) in natural water systems.

1.3 Natural Organic Matter

1.3.1 General information

Natural organic matter (NOM) is a ubiquitous component of the lithosphere and hydrosphere, it can be found in soils, sediments, surface water and groundwater, and is known to influence groundwater quality and geochemical reactions taking place in these environments. NOM is one of the largest reservoirs of the carbon in the environment (Kosobucki and Buszewski, 2014). It is a highly heterogeneous mixture, since it is formed in soils by degradation/ decomposition of biomass consisting degradation products of plant and animal tissues as well as substances resulting from biochemical changes of plant and animal origin substrates and their transitional products (Kosobucki and Buszewski, 2014; Tan, 2014). Thus, it fulfills a wide range of important functions in environment.

Humic substances (HS) are one of the major fractions of NOM which are enriched in carbon and largely contribute to the organic carbon content on the earth's surface playing a significant ecological role in the natural environment (Kosobucki and Buszewski, 2014; Tan, 2014). They are highly resistant to the biodegradation, so they are found in almost all components of the natural terrestrial and marine environment. HS are redox-active compounds. Their major functional groups are carboxylic acids, phenolic and alcoholic hydroxyls, ketone and quinone groups. Quinone groups are usually considered as the main redox-active moieties of HS (Kappler and Haderlein, 2003). HS can be further divided in three main fractions based on their behavior in the acid-alkaline environment:

- ① Fulvic acids (lowest in molecular weight, lightest in brownish color and soluble in acids and alkalis).
- ② Humic acids (HA) (medium in molecular weight, medium in color and soluble in alkali only).

- ③ Humins (highest in molecular weight, darkest in color, insoluble in both).

Evidence has accumulated that HS play an important role as an electron shuttle to iron oxides in microbial redox processes and in the biodegradation of priority pollutants (Kappler and Haderlein, 2003). While the capacities of electron transfer vary significantly with different HS. This is not surprising since the chemical structure of HS is strongly dependent upon its source materials and the environmental conditions under which they were produced (Ratasuk and Nanny, 2007).

As we have already described above, HS contain a variety of different functional moieties, these moieties are very important elements of the HS structure that determine a wide range of properties of HS. Most moieties are chemically connected with the aromatic part, some of them are also connected with the alkyl group (Kosobucki and Buszewski, 2014). An example of schematic structure of HS is presented in Figure 1.2.

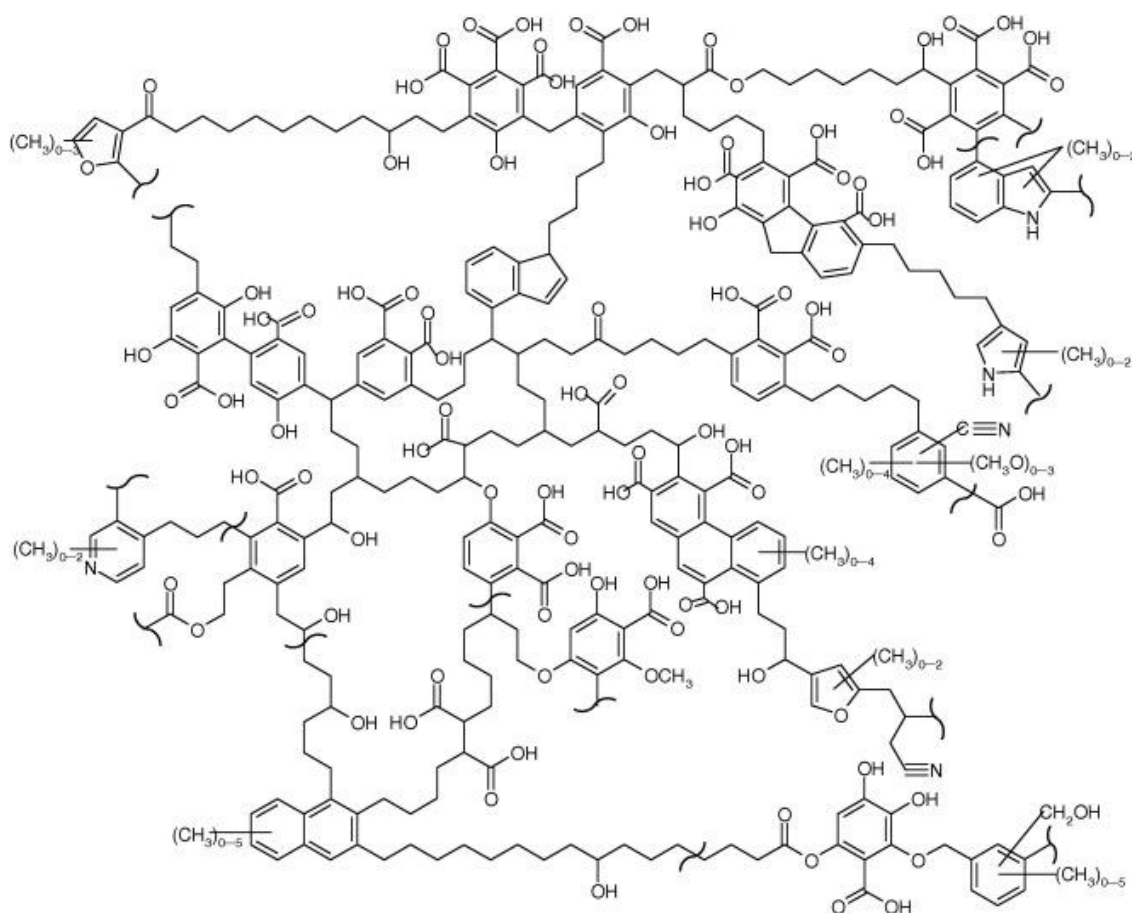


Figure 1.2: A model structure of humic acid (Schulten, 1995)

HS can accelerate reduction kinetics of Fe(III) minerals by acting as electron shuttle (Jiang and Kappler, 2008). They can serve as a terminal acceptor, which means they can be reduced by Fe(II) or sulfide (Heitmann and Blodau, 2006). On the other hand, HS can also decrease the reduction rate of organic pollutants at mineral surface due to competitive sorption and complexation of Fe(II)_{sorb} (Colón et al., 2008). As an important fraction of HS, HA are ubiquitous in the subsurface and aquifers where they undergo a variety of electron transfer reactions with their adjacent elements, thus HA have potential effects on surface catalyzed transformation processes in iron mineral redox systems (Kappler and Haderlein, 2003; Tratnyek et al., 2001).

1.3.2 The role of NOM in degradation of pollutants

HS can significantly influence oxidation and hydrolysis rate of organic contaminants by minerals. They compete with contaminants for adsorption sites on mineral surfaces and participate in or accelerate mineral dissolution. Thus these processes can affect the fate and environmental behavior of organic or inorganic contaminants (Polubesova and Chefetz, 2014). The impacts of HS on the transformation of contaminants by minerals manifest in three major processes: (a) competition for surface active sites on mineral surface, (b) dissolution of minerals and exposing new surface sites on the minerals, and (c) electron shuttling (Polubesova and Chefetz, 2014).

Stimulating role: Due to a wide range of functional moieties, HS can act as electron accepting/donating agents, which can contribute to redox reactions of redox-active inorganic contaminants (Polubesova and Chefetz, 2014), thus promoting the transformation of pollutants (Curtis and Reinhard, 1994; Dunnivant et al., 1992; O'Loughlin et al., 1999). Kappler and Haderlein (2003) investigated the potential of HA as reductant for chlorinated aliphatic pollutants, revealing that not only the electrochemically reduced HA but also the HA of natural redox-state can reduce hexachloroethane, indicating a wide range of redox-active moieties contained in HA even under oxic conditions. Guo and Jans (2006) investigated the influence of NOM on the degradation of methyl parathion in the presence of hydrogen, finding that the observed pseudo-first-order reaction rate constants were proportional to NOM concentration.

Inhibitory role: The inhibitory effect of HS on the decomposition of organic contaminants by mineral has been amply demonstrated. In most cases the inhibitory role is attributed to their sorption at mineral surface (Klausen et al., 1997; Zhang and Huang, 2003). Feitosa-Felizzola

et al. (2009) demonstrated that the presence of dissolved Aldrich humic acid (AHA) (10 mg/L) decreased the transformation rate of macrolide antibacterial agents by a factor of 10 to 15 by Fe(III) and Mn(IV) oxides, suggesting that the dissolved AHA molecules compete with the studied compounds for the reactive mineral surface sites. Vindedahl et al. (2016) investigated the influence of HS on the goethite nanoparticle reactivity and aggregation, demonstrating that fulvic-like substances more strongly inhibited goethite nanoparticle aggregation and reactivity than did humic-like substances, and the reactivity decreased with increasing HS concentration from 0 – 50 mg/L. The loss of reactivity can be attributed to the loss of Fe(II) due to either complexation with HS or oxidation to Fe(III) by the HS, as well as the blockage or change of the surface reactive sites by HS.

1.3.3 The interactions of NOM with iron oxides/ aqueous sulfide

Interactions of NOM with iron oxides: Adsorption of NOM on mineral oxides, which is usually coupled with the redox reaction between NOM and iron oxides, plays an important role in the environment (Feng et al., 2005; Saito et al., 2004). Colón et al. (2008) investigated the role of Suwannee river humic acid (SRHA) in the reduction of chemicals in anoxic environment. Their work showed that the presence of SRHA can reduce the reactivity of goethite/Fe(II) towards the reduction of p-substituted nitrobenzene due to oxidizing or complexing the Fe(II)_{sorb}, which is the main reactive element to reduce chemical under anoxic conditions. The SRHA can also act as coating to hindering the access of nitrobenzene to Fe(II)_{sorb}. Piepenbrock et al. (2014) quantified the rate and extent of electron transfer from reduced and nonreduced Pahokee Peat humic acids (PPHA) and the fresh soil organic matter (SOM) extracts to different iron oxides. They found that SOM has a lower capacity of electron transfer with iron minerals compared to PPHA, indicating a difference in redox potential distribution of the redox-active functional groups in SOM and PPHA. Their study demonstrated that HS electron shuttling can contribute to iron redox processes in environments where biogenic Fe(III) mineral are present.

Interactions of NOM with sulfide: The interactions of NOM with sulfide have been investigated during the last decades. Apart from the inorganic transformation products of elemental sulfur and thiosulfate, the incorporation of sulfide into organic matter has been previously amply demonstrated (Casagrande et al., 1980; Henneke et al., 1997). Heitmann and Blodau (2006) investigated the reaction of hydrogen sulfide with peat HA at pH 6, finding that

small fraction of sulfide got oxidized with the main oxidation product of thiosulfate and large fraction (61 %) was incorporated into the organic structure. Yu et al. (2015) investigated the transformation of aqueous sulfide with both chemically reduced AHA and nonreduced AHA at pH 6 under anoxic condition, revealing that apart from the incorporation of sulfide into NOM structure, inorganic transformation products (elemental sulfur and thiosulfate) was detected in the reaction with non-reduced AHA solution, while in the reaction with reduced AHA, no inorganic transformation products were observed. Yu et al. (2016) also investigated the reactivities of H_2/Pd reduced AHA and electrochemical reduced AHA towards sulfide. Their results revealed that compared to electrochemical reduction, H_2/Pd reduced AHA alters redox properties and reactivity of organic matter and may therefore lead to results that cannot be transferred in natural systems. Therefore, the electrochemical reduced NOM can be more representative of the natural NOM.

In summary, NOM plays a vital role in regulating the interactions between iron oxides with other reactants. As a ubiquitous and reactive component in anoxic waters, NOM can sorb at mineral surface to inhibit the reaction with the adjacent components (e.g. inhibiting the degradation of organic pollutants). On the other hand, some reactive NOM can react with iron oxides to generate Fe(II), which can contribute to the degradation of organic pollutants. Thus the overall effect of NOM is complicated. Furthermore, NOM can react with iron oxides and hydrogen sulfide, respectively. Therefore, the presence of NOM will affect the reaction between sulfide with iron oxides, altering the behavior of sulfide in natural environment, affecting the cycle of sulfur. So understanding the effect of NOM on interactions between iron mineral with sulfide is of significant importance.

1.4 Scope of this dissertation

So far, the interaction between sulfide and iron oxides has been extensively studied in the lab. While the influence of other components, e.g. Fe(II) and NOM, which are ubiquitous in anoxic groundwater remains unclear. Therefore, the goals of this study are to investigate the influence of Fe(II)/ NOM on the reaction between sulfide and goethite under anoxic condition (Figure 1.3), to track the fate of sulfide in the system, mimicking the interactions in groundwater. Answering these questions will help us to understand the geochemical interactions and the pollutants degradation in groundwater.

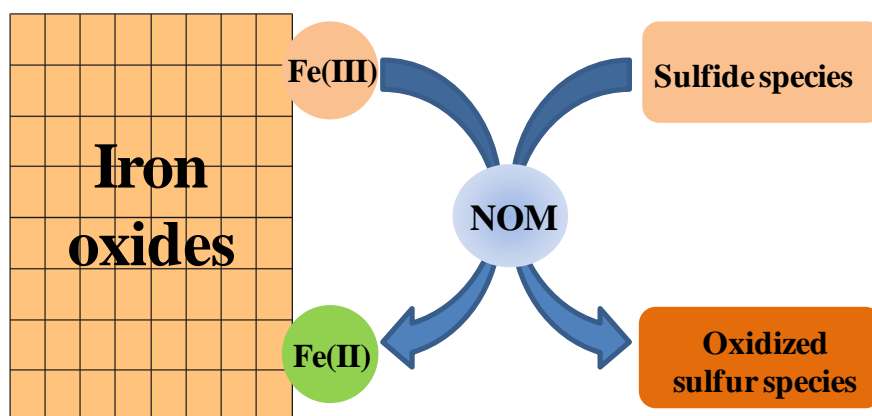


Figure 1.3: Influence of Fe(II) and NOM on the interaction between sulfide with iron oxides.

To this end, the pre-equilibrated goethite/Fe(II) suspension and goethite/Fe(II)/NOM suspension were prepared, followed by spiking of sulfide solution. After titrating pH to 7, samples were sacrificed at certain intervals for analysis. Wet chemical analysis were applied to determine the concentrations of Fe(II) and sulfur species and pH during the reaction process. The expected secondary sulfide iron minerals were characterized by using Mössbauer Spectroscopy.

This dissertation comprises the following chapters:

Chapter 1 presents a general introduction and research gap about the background of this study, and describes the objectives and structures of the dissertation.

In **Chapter 2**, the influence of Fe(II) on the interaction between sulfide with goethite is investigated at pH 7 under anoxic conditions. Different initial concentrations of Fe(II) (0 mM, 0.5 mM, 1.5 mM) were selected to check the role of Fe(II) in the reaction. Wet chemical analysis was applied to track the concentrations of Fe(II) species and sulfur species during the reaction process, Mössbauer spectroscopy was used to identify mineral products.

In **Chapter 3**, the influence of NOM on the reaction between sulfide with goethite/Fe(II) is investigated. AHA was selected as model NOM. We focused on the reaction at mineral surface, thus the investigations were conducted at conditions where the concentration of aqueous AHA was as low as possible. Since we investigated the reactions in anoxic conditions, the electrochemically reduced AHA (refers to as AHA_{red}) was used as well to check the effect of the redox state of NOM on the reactions. The influences of AHA concentration and redox state on the interaction between sulfide and goethite/Fe(II) are discussed.

It is confirmed that elemental sulfur is the main oxidation product of reaction between sulfide and iron oxides, and the yield of elemental sulfur also plays a role in the subsequent reactions as well. Hellige et al. (2012) proposed that the reactive $\text{Fe(II)}_{\text{sorb}}$ has the potential of reducing elemental sulfur to polysulfides. However, there is no direct experimental evidence to prove it. Therefore, in **Chapter 4** we studied the interaction between elemental sulfur and goethite/ Fe(II) under anoxic conditions. The objectives of this study are to identify whether $\text{Fe(II)}_{\text{sorb}}$ can reduce elemental sulfur and if there are any polysulfides formed in the reaction.

Finally, the conclusions and outlooks of this study are presented in **Chapter 5**.

2 Effect of Fe(II) on geochemical interactions of iron minerals and aqueous sulfide in anoxic waters

2.1 Introduction

The interaction between iron oxides and aqueous sulfide is closely linked to the cycling of iron and sulfur elements in natural systems, thus has been intensively studied (Dos Santos Afonso and Stumm, 1992; Hellige et al., 2012; Peiffer et al., 2015; Peiffer et al., 1992; Poulton, 2003; Wan et al., 2014). As an important parameter controlling reactions, the pH can affect the reaction significantly (Tratnyek et al., 2011), therefore most studies focus on the reaction at neutral pH. There are several reasons accounting for this selectivity: i) the pH of most natural waters are neutral, around pH 7 (Ben - Yaakov, 1973; Stumm and Morgan, 2012); ii) pH affects the reaction rate. Peiffer et al. (1992) investigated the initial reaction between hydrogen sulfide and lepidocrocite in the pH range between 4 – 8.6, revealing that the rate of sulfide oxidation was of a strong pH dependence with a maximum value at pH 7; iii) the adsorption of Fe(II) at mineral surface and its reactivity vary significantly with different pH values, thus it is necessary to conduct the experiment at fixed pH (Buchholz, 2009). So in many researches pH buffer is used to maintain the pH constant. It has been confirmed that at neutral pH elemental sulfur (S^0) and Fe(II) are the major redox products of the reaction, and iron monosulfide (FeS) would precipitate immediately and transforms to other iron sulfide minerals with the reaction proceeding.

To deeper understand the interaction between iron oxides and aqueous sulfide, in particular in the mineral transformation under the influence of $Fe(II)_{sorb}$, Hellige et al. (2012) and Peiffer et al. (2015) investigated the reaction between different iron oxides (e.g. lepidocrocite, ferrihydrite, goethite) and aqueous sulfide with varying concentrations at pH 7 and room temperature. They observed that the extent of FeS formation and yield of excess-Fe(II) which sorbs at mineral surface referred to as $Fe(II)_{sorb}$, strongly depend on the ratio between aqueous sulfide and surface sites of iron oxides (SS), as well as the characteristics of iron oxides. In the case of high ratios of sulfide: SS, the yield of FeS is significant, while $Fe(II)_{sorb}$ is negligible. In the case of low ratios of sulfide: SS, the results are the opposite: the yield of $Fe(II)_{sorb}$ exceeds the yield of FeS. Peiffer et al. (2015) also observed that in the reaction between sulfide and ferrihydrite, where the fraction of $Fe(II)_{sorb}$ was higher, pyrite formed faster. In reaction of sulfide and goethite, while, the concentration of $Fe(II)_{sorb}$ was negligible, the formation of

pyrite was slow. This is in line with Wan's research (2017), they proposed that the ratios of sulfide : SS is an import indicator for pyrite formation, and Fe(II)_{sorb} plays a significant driving role in the process of mineral transformation and cycling of sulfur.

Iron oxides are ubiquitous in natural system. Through iron oxides form when iron is exposed to oxygen, they are also present in anoxic environments, e.g. lake sediment, marine sediment, peatland, groundwaters (Cornell and Schwertmann, 2003). In anoxic aqueous systems, the Fe respiring bacteria, such as *Geobacter spp.* and *Shewanella spp.*, can reduce iron oxides to Fe(II) to obtain energy, providing a continuous flux of Fe(II) ions (Glasauer et al., 2002; Lovley, 1997). Due to the high surface area and sorptive capacities, iron oxides are dominant sorbents for cations (e.g. Mn²⁺, Cu²⁺, Cr³⁺, and Fe²⁺) in natural environments (Gorski and Scherer, 2011). Therefore in anoxic aqueous systems, the presence of Fe(II) and their sorption at mineral surface are inevitable. The Fe(II)_{sorb} exhibits a strong reducing capability towards organic pollutants and some toxic metal ions (already shown in Chapter 1), and it thus arised extensive and intensive researches about the interaction between aqueous Fe(II) and iron oxides, demonstrating electron transfer and atom exchange between Fe(II)_{sorb} and underlying iron oxides.

Despite the numerous published reports about the reactions of iron oxides and aqueous sulfide, the influence of Fe(II) on the interaction has not been investigated so far. Therefore, in this study we choose goethite as model iron oxides and investigated the interaction between goethite and aqueous sulfide under the influence of various amounts of Fe(II) at pH 7 under anoxic conditions. It can be envisioned that the sulfide can undergo two competitive reaction pathways: one is the reaction with Fe(II) to form FeS precipitate, another is the redox reaction with goethite with the formation of oxidation products of sulfide. Mineral transformation, e.g., the transformation of FeS to Fe₃S₄ or FeS₂ may also take place with reaction proceeding. The extent of these reactions and the fate of sulfide, however, are not clear. Thus the main objectives of this study are to ① check the extent of these geochemical reactions under the influence of Fe(II) and to ② identify the fate of aqueous sulfide. The pH, concentrations of iron species and sulfur species were monitored during the reaction process. The formation of secondary iron sulfide minerals was estimated via acid volatile sulfide (AVS) analysis, combined with application of Mössbauer Spectroscopy.

2.2 Materials and methods

2.2.1 Materials

Goethite: α -FeO(OH) occurs in rocks and throughout the various compartments of the global system. It is one of the most thermodynamically stable iron oxides at ambient temperature. In massive crystal aggregates goethite is dark brown or black, whereas the powder is yellow and responsible for the color of many rocks, soils and ochre deposits (Cornell and Schwertmann, 2003). Furthermore, goethite has an orthorhombic crystallographic system and is antiferromagnetic (Cornell and Schwertmann, 2003). The goethite structure, with the octahedral double chains, is shown in Figure 2.1.

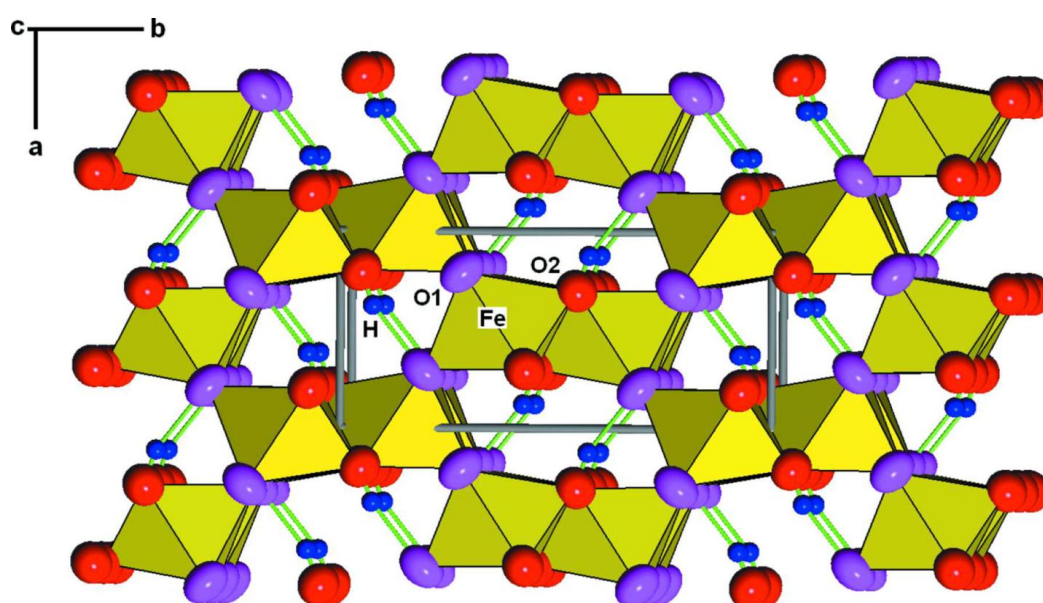


Figure 2.1: The crystal structure of goethite, α -FeO(OH). O atoms are drawn with anisotropic displacement ellipsoids at the 90% probability level and H atoms with arbitrary radii. Hydrogen bonding is indicated with green lines (Yang et al., 2006).

The specific surface area of goethite is one of the most important properties, determining its reactivity, particularly its dissolution and dehydroxylation behavior, interaction with sorbents, phase transformation and also thermodynamic stability. The goethite used in this study was purchased from Lanxess Germany GmbH, Leverkusen. Its specific surface area is about $9 \text{ m}^2/\text{g}$, pH_{pzc} (pH at point of zero charge) after washing is about 6.5 (Buchholz, 2009).

Fe(II) stock solution: The Fe(II) stock solution was prepared by adding 1.4 g of metal iron powder ($\geq 99\%$, Alfa Aesar) into a 50 mL of 1 M deoxygenated HCl solution under constant

gentle stirring in the glovebox (Braun, Germany, $O_2 < 1$ ppm). After the iron powder dissolved in acid, Fe(II) solution was filtered with 0.45 μm filter (with Hydrophobic Polytetrafluoroethylene (PTFE) Membrane, BGB Analytik) to remove the non-dissolved iron particles. The exact concentration of Fe(II) was determined using ferrozine assay (Stookey, 1970).

Sulfide solution: A sodium sulfide nonahydrate ($\text{Na}_2\text{S} \cdot 9\text{H}_2\text{O}$) crystal ($\geq 98\%$, Sigma-Aldrich) was rinsed with N_2 -purged Millipore water to remove the surface contaminants, followed by dissolving in N_2 -purged Millipore water under the flow of nitrogen gas. The exact concentration of sulfide solution was determined using iodometric method (Lawrence et al., 2000; Siegel, 1965).

2.2.2 Experimental setups

Goethite suspension with surface area concentration of 50 m^2/L (Fe atom concentration was about 60.1 mM) was prepared by adding 5.43 g goethite powder in Schott bottle with 1 L Millipore water and washed twice to remove the residual ions sorbed at goethite surface, then N_2 -purged before transferring into glovebox. In the glovebox, 250 mL of the prepared goethite suspension was transferred into Schott bottles, followed by addition of Fe(II) stock solution. The bottle with initial Fe(II) concentration of 0.4 mM was referred to as Fe(II)_{low} setup and the one with 1.5 mM Fe(II) was referred to as Fe(II)_{high} setup. The setup without addition of Fe(II) was referred to as Fe(II)_{no} setup.

For both Fe(II)_{low} and Fe(II)_{high} setups, the Fe(II) stock solution was added in three steps to prevent $\text{Fe}(\text{OH})_2$ precipitation and after each step the pH was titrated to 7.0 ± 0.1 by dropwise addition of 0.2 mM NaOH solution or 0.1 mM HCl solution. During the equilibration period of > 72 hours under constant stirring condition, the pH was titrated to 7.0 ± 0.1 regularly. After reaching pH equilibrium, both aqueous Fe(II) ($\text{Fe}(\text{II})_{\text{aq}}$) and total acid extractable Fe(II) ($\text{Fe}(\text{II})_{\text{tot}}$, including $\text{Fe}(\text{II})_{\text{aq}}$, surface associated Fe(II) extractable in 1 M HCl) concentrations were determined prior to addition of sulfide (see Table 2.1). In the glovebox anoxic sulfide stock solution was spiked slowly into suspension under constant stirring condition to achieve a concentration of 0.3 mM. After stirring for 30 minutes, suspensions were titrated to $\text{pH } 7.0 \pm 0.1$. After 5 hours samples were taken for analysis.

Table 2.1: Initial experimental conditions

Setups	Goethite concentration	Fe(II) concentration	S(-II)_{initial} concentration
Fe(II) _{no}	50 m ² /L	No Fe(II)	0.3 mM
Fe(II) _{low}	50 m ² /L	Initially added Fe(II): 0.4 mM; After equilibration: Fe(II) _{tot} , 377.6 ± 9.5 μM; Fe(II) _{aq} , 3.4 ± 0.4 μM	0.3 mM
Fe(II) _{high}	50 m ² /L	Initially added Fe(II): 1.5 mM; After equilibration: Fe(II) _{tot} , 1391.6 ± 136.2 μM; Fe(II) _{aq} , 883.3 ± 24.2 μM	0.3 mM

2.2.3 Sampling and analytical methods

There are several species needed to be sampled and analyzed. The details are shown in the following.

Iron species

Fe(II)_{aq} concentration was determined after filtration (0.45 μm, with Hydrophobic Polytetrafluoroethylene (PTFE) Membrane, BGB Analytik) using ferrozine method (Stookey, 1970). Fe(II)_{tot} concentration was determined after mixing 0.1 mL of unfiltered sample with 0.9 mL of 1 M HCl first. After incubation for 24 h, the suspension was centrifuged and the supernatant was analyzed. The difference between Fe(II)_{tot} and Fe(II)_{aq} is the concentration of Fe(II) in solid phase, including mineral surface bound Fe(II) (Fe(II)_{sorb}) and the Fe(II) associated with sulfide which is extractable in 1 M HCl.

Sulfur species

Aqueous sulfide: Aqueous sulfide (S(-II)_{aq}) was determined photometrically by methylene blue method after filtration (0.45 μm, with Hydrophobic PTFE Membrane, BGB Analytik) (Cline, 1969).

Elemental sulfur: Elemental sulfur (S^0) was extracted after treatment of 0.3 mL unfiltered suspension sample with 0.15 mL of zinc acetate (10 wt%) to precipitate free sulfide following a procedure modified after Kamyshny et al. (2009). After 15 minutes, 1.6 mL methanol was added into the suspension. After shaken for 3 hours, the suspension was centrifuged and the supernatant was measured by HPLC combined with Diode array detector after separation on a C18 column (Ultrasphere ODS 5 μ m, 250 by 4.6 mm) and isocratic elution by 98 % methanol with a flow rate of 0.8 mL/min. The detection was performed at a wavelength of 265 nm.

Thiosulfate: For thiosulfate samples, 0.1 mL zinc acetate (10 wt%) solution was added into 2.5 mL unfiltered samples to precipitate the residual sulfide. The filtered sample was measured by HPLC with a modification of the protocol published by Steudel et al. (1989) and Lohmayer et al. (2014). A reversed-phase C18 column (Ultrasphere ODS, 5 μ m, 250 by 4.6 mm) was used for separation. Elution was performed with eluent compositions with 2 mM tetrabutylammonium chloride ($[\text{CH}_3(\text{CH}_2)_3\text{NCl}]$) and 1 mM sodium carbonate (Na_2CO_3) in 77 % Millipore water and 23 % acetonitrile (CH_3CN), with the pH adjusted to 7.7 by the addition of 1 M HCl. Following parameters were used: a flow rate of 0.8 mL/min, the injection volume of 15 μ L, and the detection wavelength of 215 nm.

Sulfate: The sulfate concentration in samples was determined via ion chromatography (IC) (Metrohm AG). Since the Fe(II) present in the sample would block the IC column during measuring process, thus it is necessary to remove it prior to analysis. For this purpose, 5 mL of filtered sample was treated with adding 0.16 mL of 0.2 M NaOH solution to attain alkaline pH to stimulate Fe(II) oxidation as Fe(III) precipitate in the air. After approximately 30 min when all Fe(II) ion got oxidized to Fe(III), pH was lowered back to 7 – 8 by adding 0.44 mL of 0.1 M HCl to decrease the solubility of $\text{Fe}(\text{OH})_3$. Then the resulting sample was centrifuged to remove $\text{Fe}(\text{OH})_3$ precipitate and the supernatant was separated for further analysis.

Acid volatile sulfide(AVS)

The addition of HCl can release H_2S from sulfide-containing species including the metastable iron sulfide minerals. These substances can be divided into two groups: (1) dissolved iron and sulfur species and their complexes and (2) solid iron sulfides precipitate (e.g. FeS , Fe_3S_4 , FeS_2) (see Figure 2.2).

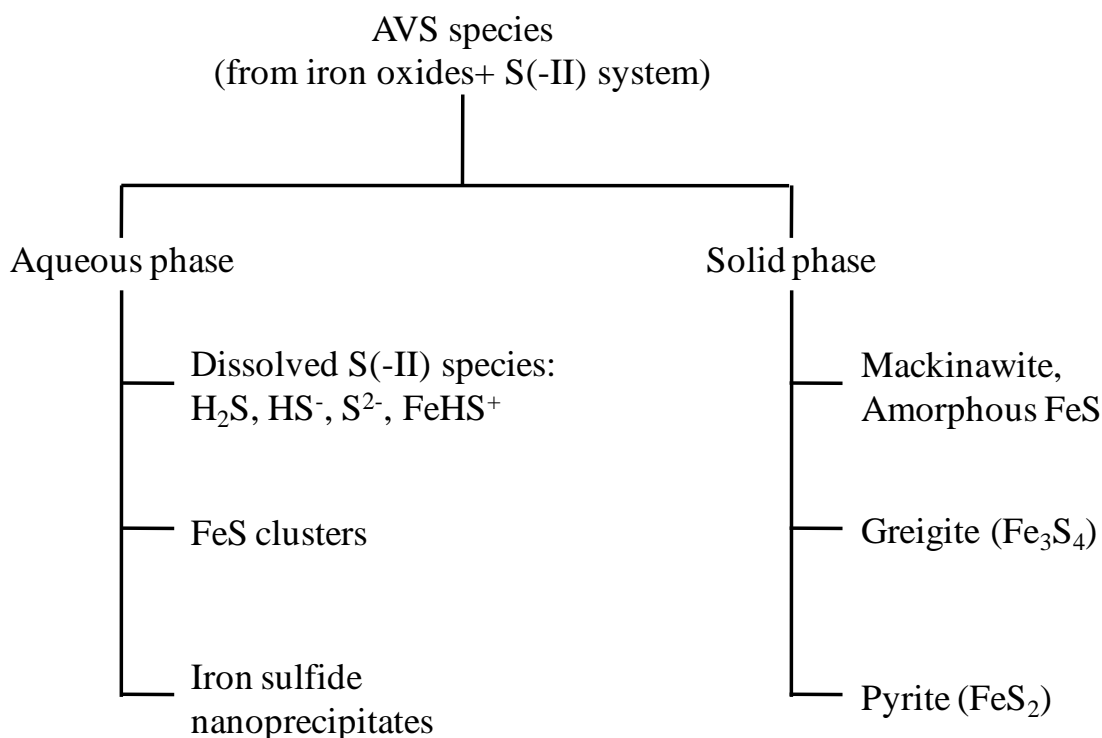


Figure 2.2: The potential sources of AVS (Rickard and Morse, 2005)

Although acid volatile sulfide (AVS) method has been proposed many years ago, many investigations have been conducted to develop this method, there is still no common method to be established as AVS extraction standard (Cornwell and Morse, 1987; Meysman and Middelburg, 2005; Rickard and Morse, 2005; Ulrich et al., 1997). This method suffers from a lack of absolute specificity in mineral phase separation. There are overlaps between different extraction reagents, operations, and the overlaps may not be constant between different studied samples (Cornwell and Morse, 1987).

Morse et al. (1987) summarized that the amorphous FeS can be completely dissolved in 1 M HCl and recovered, greigite (Fe₃S₄) does not entirely dissolve in simple HCl treatment and pyrite (FeS₂) does not dissolved in HCl (see Table 2.2). The different solubilities of iron sulfide minerals in acidic solution could be used experimentally to separate them from each other.

Table 2.2: The sulfide recovery from different minerals (Morse et al., 1987)

	Amorphous (FeS)	Mackinawite	Greigite	Synthetic pyrite	Pyrite
	%	%	%	%	%
1.0 M HCl	100	90	40 – 67	0	0
6.0 M HCl	100	98 – 102	60 – 69	0	0

Extraction method: In glovebox 5 mL unfiltered suspension sample was transferred in 100 mL serum bottle, and a tube containing 2 mL of 10 wt% zinc acetate solution was placed in the bottle as trapping solution and the bottle was sealed with rubber stopper. Outside the glovebox, 5 mL of anoxic HCl with concentration of 2 M or 12 M was injected via syringe. The trapping solution can precipitate the liberated H₂S as ZnS. After shaking gently on a horizontal shaker for 24 hours, the trapping tubes were removed from the serum bottles. A homogeneous ZnS suspension was ensured by treatment in sonication water bath for 5 minutes. The sulfide was measured with methylene blue method (Cline, 1969).

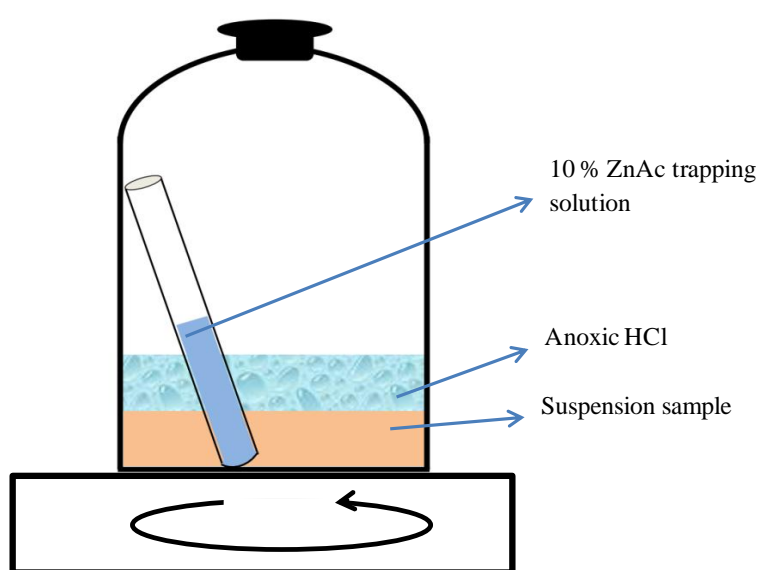


Figure 2.3: Scheme of AVS Extraction

Mössbauer Spectroscopy

Mössbauer spectroscopy is a useful analytical tool to estimate the type and fraction of iron minerals in research. Since only ⁵⁷Fe is visible in Mössbauer spectroscopy, samples of very low concentration can be detected by enriching the content of ⁵⁷Fe in target samples. Mössbauer uses ⁵⁷Co as radiation source to emit gamma-ray and is equipped with a constant acceleration drive system in transmission mode. Spectra are calibrated against a spectrum of alpha-Fe(0) foil at room temperature (Hellige et al., 2012). Data acquisition times are usually 12–20 h per spectrum. Spectral fitting is performed using Recoil software (University of Ottawa, Canada) and Voigt-based spectral lines. Since Mössbauer only detects ⁵⁷Fe in sample, we used pure ⁵⁷Fe(II) solution in a pretest experiment to increase the signal of ⁵⁷Fe-containing products.

Approximately 30 mL of suspension was filtered through a membrane filter in the glovebox. The solid sample clinging on the membrane was sealed between two layers of Kapton tape for Mössbauer spectroscopy analysis. The Mössbauer spectra were collected at different temperatures (77 and 4.2 K). Obtained spectra were calibrated against a spectrum of alpha Fe(0) foil at 297 K.

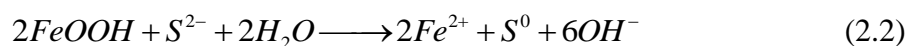
2.3 Results and discussion

2.3.1 pH changes during the studied reactions

After spiking of sulfide solution, the color of goethite suspension changed immediately from yellow to black. The pH values in all setups increased: the pH value were > 9.8 for the Fe(II)_{no} setup, > 9.5 for the Fe(II)_{low} setup, > 9.5 for the Fe(II)_{high} setup, respectively. The alkaline sulfide stock solution contributed to the pH increase. The color change was attributed to the formation of FeS precipitate. Since the sulfide solution was of high pH, sulfide ion (S^{2-}) is the dominating sulfide species in the solution (Broderius and Smith, 1977; Olson, 2005). The formation of FeS can be presented as follows (see Eq 2.1):



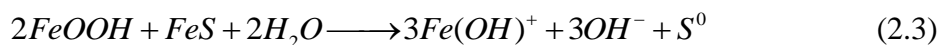
Although there was not initial Fe(II) present in the Fe(II)_{no} setup, the spiked sulfide reduced goethite rapidly to release Fe(II), followed by precipitation with remaining sulfide. Considering that in the goethite suspension, the pH was titrated to 7, bisulfide ion (HS^-) and sulfide ion (S^{2-}) would be the main species (Broderius and Smith, 1977; Olson, 2005). Thus, the reduction of goethite by sulfide occur like the following reaction (Eq 2.2) (Dos Santos Afonso and Stumm, 1992; Peiffer and Gade, 2007).



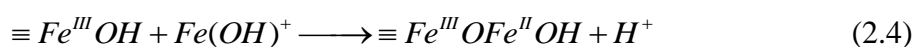
It seems that the alkaline sulfide solution and the redox reaction between goethite and sulfide contributed to the increase in pH.

To maintain the pH constant at 7 during the reaction process, suspensions were titrated to $pH\ 7.0 \pm 0.1$ using 0.1 M HCl solution. The amounts were around 1.16 mL for the Fe(II)_{no} setup, 0.87 mL for the Fe(II)_{low} setup and 0.13 mL for the Fe(II)_{high} setup, respectively. Thereafter, the pH values in all setups were quite stable during the whole reaction process.

In all setups, aqueous sulfide was consumed within 6 hours, but the yield of S⁰ continuously increased (shown later). It is proposed that after aqueous sulfide was consumed, FeS reacted with goethite with formation of S⁰ and Fe(II) (Eq 2.3).



The generated Fe(II) was supposed to sorb at the goethite surface. Because the increasing formation of S⁰ indicated the continuous generation of Fe(II). However, no increase in the Fe(II)_{aq} concentration was observed (shown in Figure 2.7), therefore it was concluded that the generated Fe(II) sorbed at goethite surface. Sorption of Fe(II)_{aq} at goethite surface can also decrease the pH (Elsner et al., 2004).



The sorption of Fe(II) generate H⁺, which can compensate the generated OH⁻ from the redox reaction. Therefore after pH titration to 7, the reaction in the suspensions did not produce significant amounts of OH⁻ or H⁺ ions to change pH.

2.3.2 Evaluation of sulfur species during the reaction

Concentrations of aqueous sulfide and oxidation products of sulfide were monitored during the reaction process. In all setups, aqueous sulfide was consumed within 6 hours and cannot be detected afterwards. Thiosulfate and sulfate were not detected with detection limits of 6.0 μM and 7.6 μM respectively.

In the Fe(II)_{no} setup the reaction between sulfide and bare goethite was very fast (see Figure 2.4), consistent with previous findings (Hellige et al., 2012; Peiffer et al., 2015; Peiffer et al., 1992; Wan et al., 2014). The S⁰ concentration was already high (around 64 μM) after 7 hours and increased slowly to 75 – 80 μM towards the end of the experiment. In the Fe(II)_{high} setup, the S⁰ concentration was only 24 μM after 7 hours, but increased steadily to 65 – 70 μM after 4 days, which was only slightly lower than that in the Fe(II)_{no} setup. In the Fe(II)_{low} setup, there was no S⁰ detected in the early phase (7 – 24 hours). While after 24 hours, S⁰ was detected and the concentration remained at 15 – 20 μM, accounting for 3.3 % – 6.6 % of initially added sulfide.

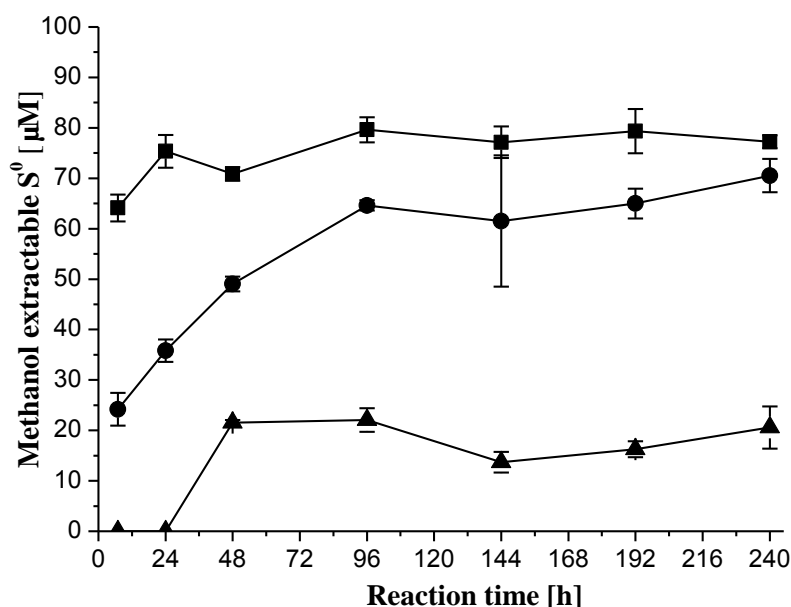


Figure 2.4: The evolution of S^0 concentration in reactions between goethite and aqueous sulfide at pH 7 under anoxic condition. The symbols represent: ■ for Fe(II)_{no} setup (without initially added Fe(II)); ▲ for Fe(II)_{low} setup (with initially added Fe(II) concentration of 0.4 mM); ● for Fe(II)_{high} setup (with initially added Fe(II) concentration of 1.5 mM).

In the Fe(II)_{high} setup, even in the case of aqueous sulfide was completed, concentration of S^0 still increased. The continuous generation of S^0 suggested that in the early phase with presence of aqueous sulfide, the reaction took place between aqueous sulfide and the bare goethite surface with fast formation of S^0 . While after the surface bound sulfide was consumed, the reaction took place between FeS and goethite. However, compared to FeS, aqueous sulfide transfer electrons to iron oxides faster (Hellige et al., 2012), so after consumption of aqueous sulfide the formation slowed down.

Regarding why the yield of S^0 in the Fe(II)_{low} setup was much less than that in the Fe(II)_{high} setup, it is proposed that in the Fe(II)_{low} setup the reaction between FeS and goethite was slow. Because goethite is one of the most crystalline iron oxides in natural environment, the tendency of electron transfer of structure Fe(III) in goethite is slower compared to other less crystalline iron oxides, e.g. ferrihydrite, lepidocrocite (Cornell and Schwertmann, 2003; Wan et al., 2014), thus the interaction between FeS and goethite was not significant. However, this explanation is not convincing enough to interpret the high yield of S^0 in the Fe(II)_{high} setup. Therefore the reaction mechanism for S^0 formation may be different in the Fe(II)_{high} setup. Previous studies

demonstrated that an un-identified surface Fe(III) species forms during the reaction of Fe(II) sorption at iron oxides surface. Electron transfer and atom exchange between Fe(II)_{sorb} and structural Fe(III) in iron oxides leads to the formation of Fe(III) species (Boland et al., 2014; Coughlin and Stone, 1995; Handler et al., 2009; Larese-Casanova and Scherer, 2007). Amstatter et al. (2009) reported the oxidation of As(III) to As(V) in Fe(II) treated goethite suspension, and proposed that this surface Fe(III) species contributed to the oxidation of As(III) to As(V). Accordingly, it is also possible that this Fe(III) species can oxidize FeS in goethite/Fe(II) suspension. In the Fe(II)_{high} setup due to the presence of Fe(II)_{aq}, the reactive Fe(III) species can be continuously regenerated. Because the continuous re-sorption of Fe(II)_{aq} can generate the fresh reactive Fe(II)_{sorb} at goethite surface. Then electron transfer between Fe(II)_{sorb} with structural Fe(III) leads to formation of reactive Fe(III) species, thus allowing the oxidation of FeS at goethite surface. Thus, it is proposed that the presence of Fe(II)_{aq} allows for the continuous regeneration of reactive Fe(III) species at goethite surface, which stimulates the oxidation of FeS.

To test the above hypothesis, an additional experiment was performed. Two goethite suspensions were prepared at neutral pH under anoxic condition, one was with the addition of Fe(II), the other was not. In both two setups, the goethite surface area concentration were 50 m²/L, the initial added FeS concentration was around 0.3 mM. In the setup with Fe(II), the initially added Fe(II) concentration was 1.5 mM. After sorption equilibrium, the Fe(II)_{sorb} and Fe(II)_{aq} were around 0.5 mM and 1.0 mM respectively, which was the same as the conditions in the Fe(II)_{high} setup. After addition of FeS, in the Fe(II)-containing setup, the S⁰ concentration was higher than that in the setup without addition of Fe(II) (see Figure 2.5), which further demonstrated that the presence of both Fe(II)_{sorb} and Fe(II)_{aq} could stimulate the reaction between FeS and goethite.

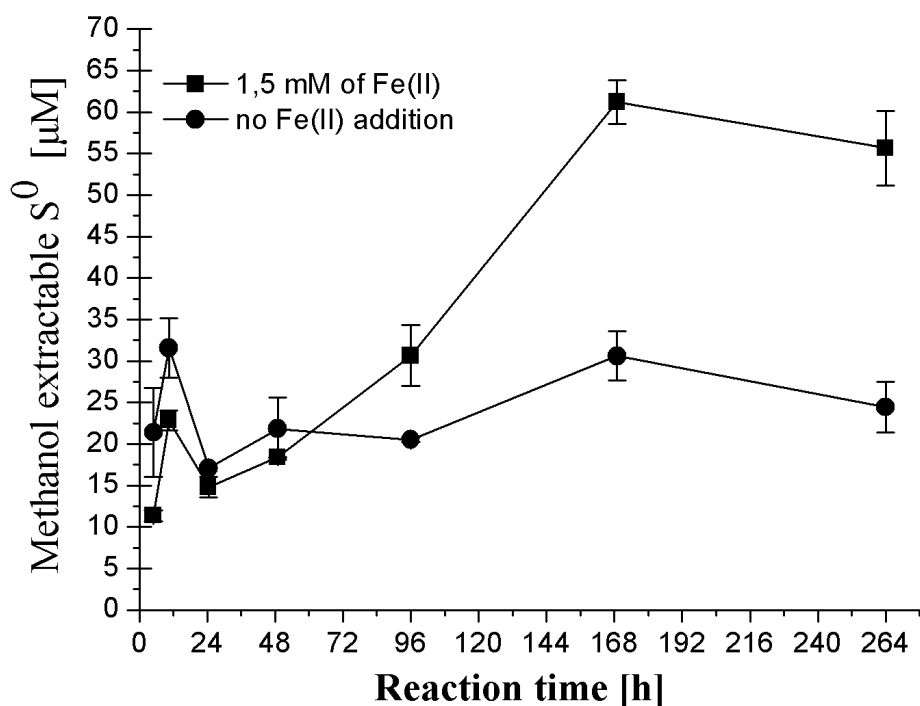


Figure 2.5: The evolution of S^0 concentration in the reactions between FeS and goethite at pH 7 under anoxic condition.

2.3.3 Evaluation of Fe(II) species during the reaction

The Fe(II) species undergo various and complicated pathways in this experimental system (see Figure 2.6). Fe(II) can be consumed by precipitation with sulfide (see **a** and **b** in Figure 2.6), and can also be generated from Fe(III) reduction by sulfide (see **c** in Figure 2.6), Fe(II)_{sorb} participates in the transformation of iron sulfide minerals as well (Hellige et al., 2012; Peiffer et al., 2015). Apart from these reactions, dynamic sorption between Fe(II)_{aq} and goethite/Fe(II) occurs at goethite surface (see **d** in Figure 2.6).

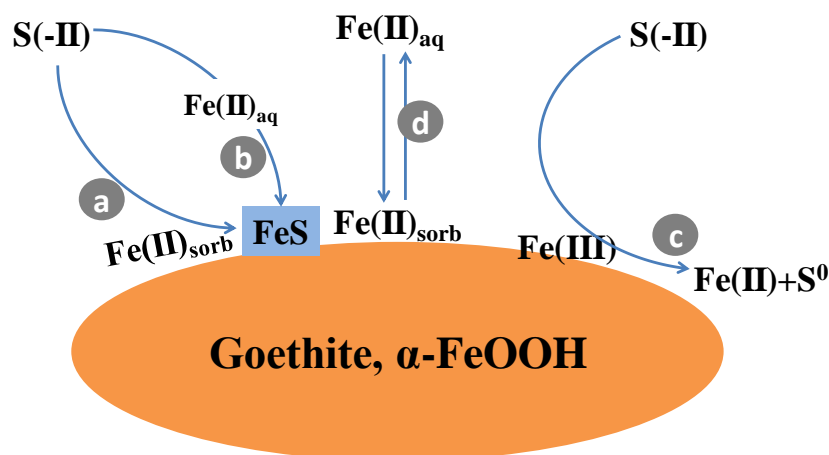


Figure 2.6: Interactions between goethite and sulfide in the presence of Fe(II) at pH 7 under anoxic conditions. Pathways of a) and b) represent the FeS precipitation reaction between aqueous sulfide and Fe(II). Pathway of c) is the redox reaction between sulfide and goethite with formation of Fe(II) and S⁰. Pathway of d) shows the dynamic sorption between Fe(II)_{aq} and goethite leading to the regeneration of reactive Fe(II)_{sorb}.

Figure 2.7 shows the evolution of Fe(II) concentration in reactions between goethite and sulfide at pH 7 under anoxic conditions. We can see that after sulfide spiking, in the Fe(II)_{high} setup Fe(II)_{aq} concentration decreased by 140 μM immediately due to precipitation with sulfide (there were no Fe(II)_{aq} present in the other two setups). Afterwards, the Fe(II)_{aq} concentration remained constant.

Fe(II)_{tot} concentration increased fast due to goethite reduction by sulfide in all the three setups, then it started to decrease slowly with the reaction proceeding. In the Fe(II)_{high} setup, Fe(II)_{tot} rapidly increased by 160 μM within 7 hours and remained almost unchanged in the early phase of the reaction (within 4 days) but decreased slightly thereafter. In the Fe(II)_{no} setup, 300 μM of Fe(II)_{tot} were formed after 7 hours of reaction, and decreased slowly to 200 μM after 10 days. In the Fe(II)_{low} setup, Fe(II)_{tot} increased up to 568 μM after 7 hours and decreased slightly thereafter to remain at approximately 500 μM after 10 days.

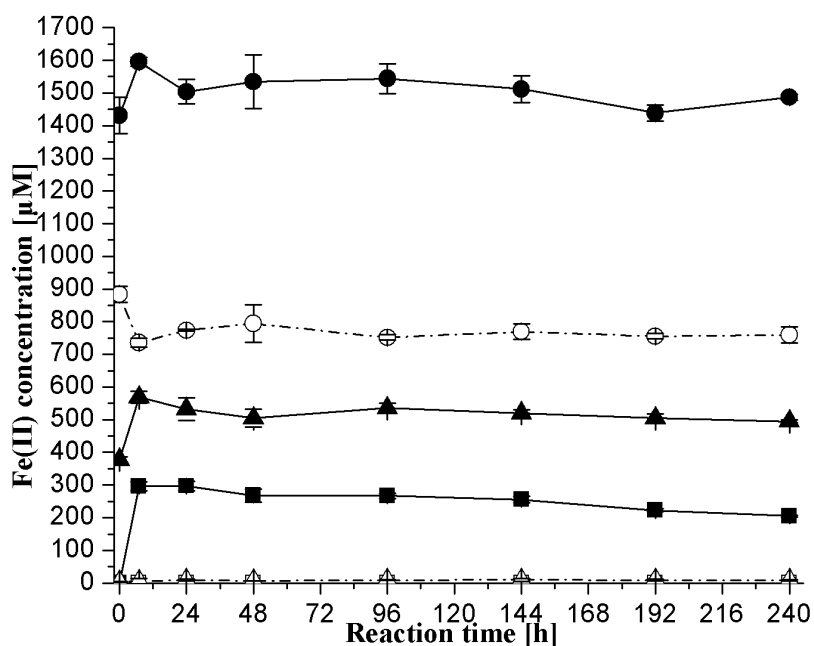
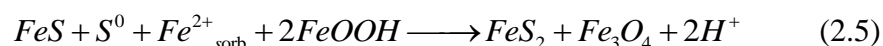


Figure 2.7: The evolution of aqueous and total Fe(II) concentrations in reactions between goethite and sulfide at pH 7 under anoxic conditions. The symbols represent: ■ and □: Fe(II)_{no} setup (without initially added Fe(II)); ▲ and △: Fe(II)_{low} setup (with initially added Fe(II) of 0.5 mM); ● and ○: Fe(II)_{high} setup (with initially added Fe(II) of 1.5 mM). Dashed line with open symbols represent Fe(II)_{aq}, solid line with filled symbols represent Fe(II)_{tot}.

The observed decrease in Fe(II)_{tot} concentration is in agreement with the finding by Hellige et al. (2012), who observed a decrease in Fe(II)_{tot} in the reaction between aqueous sulfide and lepidocrocite under similar experimental conditions. Since they also observed a consumption of S⁰ and the formation of pyrite and magnetite, they proposed the following reaction mechanism:



In our research Fe(II)_{tot} decreased during the course of the reaction whereas S⁰ accumulated. Thus, overall the rate of S⁰ formation processes exceeded the rate of S⁰ consuming processes. The decrease in Fe(II)_{tot} can be rationalized by two processes. During the course of the reaction, especially in the Fe(II)_{high} setup, Fe(II)_{tot} may have transformed via Eq 2.5 into a more crystalline Fe(II) mineral (e.g. Fe₃O₄, FeS₂ or some other FeS_n), which cannot completely dissolve in 1 M HCl. Alternatively, the electrons donated by Fe(II)_{sorb} to structural Fe(III) of goethite migrated into goethite structure, leading to incomplete recovery of Fe(II)_{tot}.

2.3.4 Mössbauer spectroscopy

The formation of secondary iron phase was identified by Mössbauer spectroscopy. In a test experiment with addition of 0.5 mM $^{57}\text{Fe(II)}$ solution, the reaction was conducted under the same conditions of the $\text{Fe(II)}_{\text{low}}$ setup as we described in this experiment, the only difference was that pure $^{57}\text{Fe(II)}$ solution was used in this experiment to increase the Mössbauer signal. According to the AVS analysis, the FeS concentration was estimated to be 151 μM after one week of reaction. Compared with the total goethite- ^{57}Fe concentration of 1266.3 μM (the goethite concentration was 60.3 mM, abundance of ^{57}Fe in goethite was 2.1 % (Handler et al., 2009)) and initial added $^{57}\text{Fe(II)}_{\text{sorb}}$ concentration of 500 μM in the system, the fraction of ^{57}FeS was 8.5 % (Eq 2.6) which was higher than the Mössbauer detection limit of 2 – 5 %. The fractions of other secondary minerals such as FeS_n were even lower, which is unlikely detectable.

$$f = \frac{C(^{57}\text{FeS})}{60.3\text{mM} * 2.1\% + 500\mu\text{M}} \quad (2.6)$$

Where f is the estimated fraction of ^{57}FeS in sample and $C(^{57}\text{FeS})$ is the estimated FeS concentration of 151 μM .

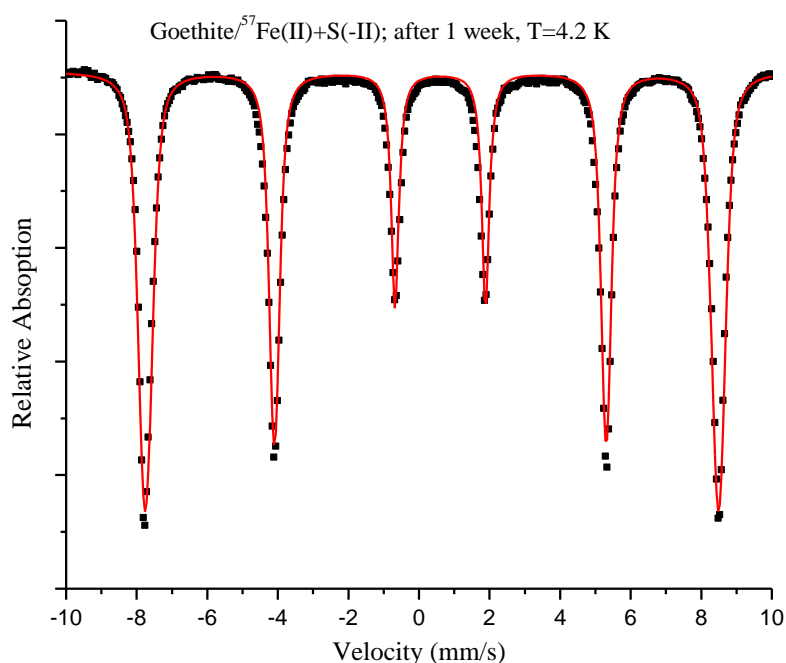


Figure 2.8: Mössbauer spectrum of goethite/ $^{57}\text{Fe(II)}$ reacted with sulfide after 1 week, measured at 4.2 K.

Table 2.3: Model parameters for Mössbauer spectrum of goethite/ $^{57}\text{Fe}(\text{II})$ reacted with sulfide after 1 week. Spectrum was collected at 4.2 K.

	I ^a (mm/s)	χ^2 ^b	<CS> ^c (mm/s)	<QS> ^d (mm/s)	<H> ^e T	#of comp. ^f	Hp ^g T
Goethite	0.097	3.1	0.48	-0.13	49.9	1	50.6

^a Lorentzian half-width at half-maximum.

^b Reduced chi-squared goodness of fit value.

^c Average center shift.

^d Average quadrupole splitting.

^e Average hyperfine magnetic field.

^f Number of Voigt-based fitting used to model the hyperfine magnetic field.

^g Most probable hyperfine magnetic field value.

The results showed that there were no secondary iron mineral phases except goethite observed by Mössbauer spectrum measured at 4.2 K (see Figure 2.8 and Table 2.3). This could be interpreted by the low fraction of secondary iron (^{57}Fe) mineral compared to the underlying goethite, which was caused by the atom exchange between $^{57}\text{Fe}(\text{II})_{\text{sorb}}$ and $^{56}\text{Fe}(\text{III})$ in goethite crystalline structure during the equilibration period of $^{57}\text{Fe}(\text{II})$ sorption at goethite surface. Due to atom exchange, the ^{57}Fe in $\text{Fe}(\text{II})_{\text{sorb}}$ transferred into goethite and $^{56}\text{Fe}(\text{III})$ contained in goethite structure released out to be $\text{Fe}(\text{II})_{\text{sorb}}$, which reduced the content of ^{57}Fe in $\text{Fe}(\text{II})_{\text{sorb}}$ (Handler et al., 2009; Neumann et al., 2015; Williams and Scherer, 2004). Another reason contributing to the lower fraction of $^{57}\text{Fe}(\text{II})$ mineral was that sulfide reduced the goethite-structural $^{56}\text{Fe}(\text{III})$ to $^{56}\text{Fe}(\text{II})$, and this sort of $^{56}\text{Fe}(\text{II})$ was subsequently released to mineral surface, binding with sulfide in the form of iron sulfide minerals. Fe atom exchange and reductive dissolution of $\text{Fe}(\text{III})$ by sulfide reduced the content of ^{57}Fe in secondary mineral, leading to its invisibility. Furthermore, from the viewpoint of crystallinity, the poor crystallinity of secondary mineral can also cause the invisibility. Although Mössbauer spectroscopy can detect nonstructured and amorphous mineral phase, it is possible only in the case of sufficient concentration of target mineral (Hunger and Benning, 2007; Larese-Casanova and Scherer,

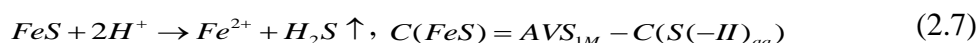
2007; Murad, 2010). So if the material is less crystalline and the amount is not sufficient to produce a detectable signal, it still could not be observed in Mössbauer spectra.

In the Fe(II)-containing setups we used normal Fe(II) solution, therefore it is not likely to observe secondary iron mineral in studied setups using Mössbauer spectroscopy, so it was not applied.

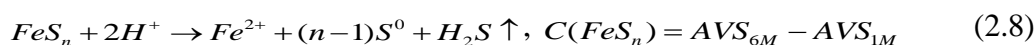
2.3.5 Evaluation of acid volatile sulfide and S distribution

According to previous studies (Cornwell and Morse, 1987; Kang et al., 2014; Rickard and Morse, 2005; Williams and Scherer, 2001), we conclude that even pyrite may form in this experiment, it does not dissolve and thus does not contribute to AVS data. While, some other less crystalline iron sulfide minerals which can dissolve in 6 M HCl, contributed to the AVS_{6M} data. Therefore, we assumed that the AVS released from 1 M HCl is FeS precipitate and dissolved S(-II) species, in 6 M HCl sulfide contained in less crystalline polysulfide minerals is released and trapped as well. To simplify the evaluation of concentration and fractions of iron sulfide minerals dissolving in different HCl concentrations, we account pyrite together with less crystalline polysulfide minerals (which do not dissolve in 1 M HCl but in 6 M HCl) as FeS_n. Considering in this way, pyrite is included in the term of FeS_n. The calculations are shown as below:

In 1 M HCl,



In 6 M HCl,



Where C(FeS), C(S(-II)_{aq}) and C(FeS_n) are concentrations of FeS, S(-II)_{aq} and FeS_n, respectively. AVS_{1M} and AVS_{6M} are sulfide concentration extracted in 1M HCl and 6 M HCl, respectively.

Considering that S(-II)_{aq} was not detected in all setups, AVS_{1M} was equal to the FeS concentration, thus it was assigned to correspond to FeS concentration. The difference of AVS_{6M} and AVS_{1M} was assumed to be the concentration of FeS_n. So the concentration of FeS and FeS_n can be obtained through the above calculations. The stoichiometric factor (n value)

of FeS_n can be calculated through a sulfur mass balance. Since dissolved sulfide, sulfate and thiosulfate were not detected, the concentrations of these sulfur species can be neglected. The calculation of n is presented as follows:

$$C(S(-II)_{\text{initial}}) = C(S^0) + C(\text{FeS}) + n * C(\text{FeS}_n) \quad (2.9)$$

Where $C(S(-II)_{\text{initial}})$ is the initially spiked sulfide concentration of $300 \mu\text{M}$. $C(S^0)$ is the methanol extractable S^0 concentration. $C(\text{FeS})$ and $C(\text{FeS}_n)$ are concentrations of FeS and FeS_n , respectively.

After 10 days of reaction, samples for AVS measurement were taken and analyzed. All samples were measured in triplicate. In the $\text{Fe(II)}_{\text{no}}$ setup, the AVS extracted in 1 M HCl was below detection limit ($6 \mu\text{M}$) and AVS in 6 M HCl was $27.6 \pm 5.6 \mu\text{M}$; In the $\text{Fe(II)}_{\text{low}}$ setup, the results were $62.1 \pm 10.2 \mu\text{M}$ for $\text{AVS}_{1\text{M}}$ and $140.1 \pm 43.5 \mu\text{M}$ for $\text{AVS}_{6\text{M}}$; In the $\text{Fe(II)}_{\text{high}}$ setup, the results were $159.8 \pm 55.8 \mu\text{M}$ for $\text{AVS}_{1\text{M}}$ and $229.2 \pm 30.8 \mu\text{M}$ for $\text{AVS}_{6\text{M}}$ (see Figure 2.9).

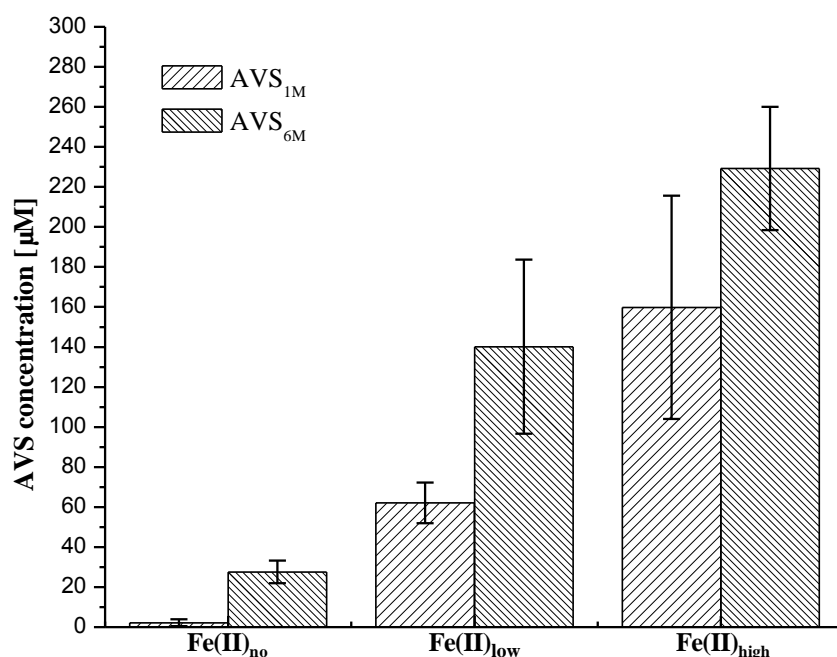


Figure 2.9: The AVS extracted in 1 M HCl and 6 M HCl solutions in the reaction between goethite and sulfide at pH 7 under anoxic condition, extracted at 240 h.

According to the assumptions that $\text{AVS}_{1\text{M}}$ was assigned to correspond to FeS concentration, the difference between $\text{AVS}_{6\text{M}}$ and $\text{AVS}_{1\text{M}}$ was assigned to FeS_n concentration, the concentrations of FeS and FeS_n could be obtained through calculation (Eqs 2.7 and 2.8). So in the $\text{Fe(II)}_{\text{no}}$ setup, the concentrations of FeS and FeS_n were 0 and $27 \mu\text{M}$, respectively. In the

Fe(II)_{low} setup, the concentrations of FeS and FeS_n were 62 μM and 78 μM, respectively. In the Fe(II)_{high} setup, the concentrations of FeS and FeS_n were 160 μM and 70 μM, respectively. Correspondingly, the S(-II) concentration contained in FeS_n are 27 μM in the Fe(II)_{no} setup, 78 μM in the Fe(II)_{low} setup, 70 μM in the Fe(II)_{high} setup. The other S atoms contained in FeS_n are assumed to be zero-valent sulfur (S(0)), and their concentration can be calculated via Eq 2.10.

$$C(S(0)) = C(FeS_n) * (n - 1) \quad (2.10)$$

Based on S mass balance and the proposed calculation of Eq 2.9, the calculated n values of FeS_n were 8.2 for the Fe(II)_{no} setup, 2.8 for the Fe(II)_{low} setup, and 1.0 for the Fe(II)_{high} setup, respectively. To differentiate the fractions of FeS from two different HCl extraction in the Fe(II)_{high} setup, we refer the FeS extracted in 1 M HCl to amorphous FeS (FeS_a), the FeS extracted 6 M HCl to crystalline FeS (FeS_c). Being calculated via Eq 2.10, the zero-valent S atoms contained in FeS_n were 194.4 μM in the Fe(II)_{no} setup, 140.4 μM in the Fe(II)_{low} setup. In the Fe(II)_{high} setup, there was no zero-valent S binding with FeS_c. The S distributions in three different setups are presented in Figure 2.10.

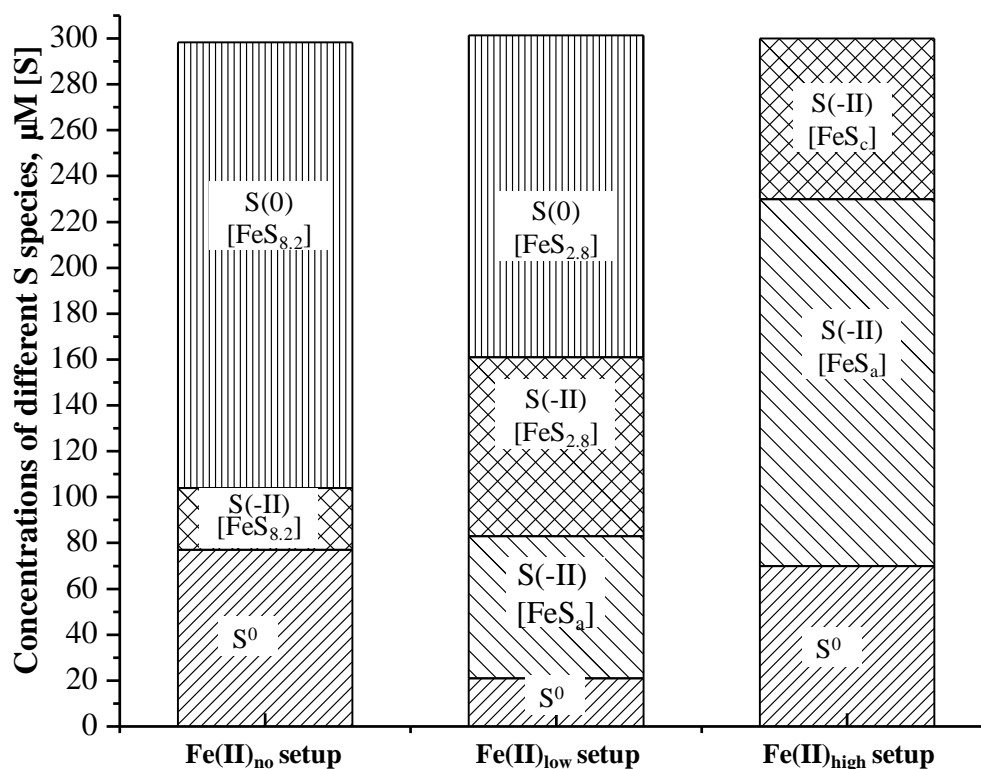


Figure 2.10: Sulfur atoms distribution in the reactions of sulfide with goethite under the influence of Fe(II) at pH 7 under anoxic conditions. The individual fraction represents the S atoms from their corresponding sulfur species, e.g the S(-II)[FeS_{8.2}] fraction represents the S atoms with redox state of -2 contained in FeS_{8.2}, S(0)[FeS_{8.2}] fraction represents the S atoms with redox state of zero contained in FeS_{8.2}. FeS_a is the amorphous FeS extractable in 1 M HCl, FeS_c is the crystalline FeS extractable in 6 M HCl. The other sulfur species such as aqueous sulfide and thiosulfate were not detected, therefore they were not shown in this graph.

From Figure 2.10, we can see that S⁰ was the main redox product in the interaction between goethite and aqueous sulfide, the presence of Fe(II) affected the yield of S⁰. In the absence of Fe(II) and in the presence of high concentration of Fe(II) where the generation of reactive surface Fe(III) species was allowed, the yield of S⁰ was high. While in the case of only Fe(II)_{sorb} present and Fe(II)_{aq} absent, goethite was covered by Fe(II) and subsequent FeS precipitate, once reactive surface Fe(III) species was consumed, the redox reaction between FeS and goethite ceased as well. The formation of iron sulfide minerals was also affected by Fe(II). During the whole reaction process, the AVS concentration in the Fe(II)_{no} setup was always very low: not detectable in 1 M HCl, less than 10 % of the initially added amount of sulfide in

6 M HCl. This is in the line with the previous literatures (Hellige et al., 2012; Peiffer et al., 2015; Wan et al., 2014). They observed that under experimental conditions of low ratios of sulfide : mineral surface sites (the Fe(II)_{no} setup matched this condition), the yield of FeS was negligible and most sulfide transferred to zero-valent sulfur associated with solid phase. In the Fe(II)_{low} and the Fe(II)_{high} setups, due to the pre-existence of Fe(II), large fraction of spiked sulfide immediately precipitated as FeS with concentrations of 62 μM in the Fe(II)_{low} setup and 160 μM in the Fe(II)_{high} setup.

The amount of zero-valent sulfur binding FeS_n decreased in the order of Fe(II)_{no} setup > Fe(II)_{low} setup > Fe(II)_{high} setup. In the Fe(II)_{no} setup, the calculated n value of FeS_n is 8.2. In the absence of Fe(II) the spiked sulfide bound to bare goethite surface and reduced goethite through an inner-sphere coordination of sulfide to Fe(III) followed by fast electron transfer (Dos Santos Afonso and Stumm, 1992). This is a faster reaction than an out-sphere process alone, so Fe(II) and S⁰ were produced immediately after sulfide spiking. However, a significant fraction of this S⁰ was supposedly still bound firmly to the FeS precipitate at the goethite surface, and was not extracted in methanol. In the Fe(II) containing setups, however, due to the presence of Fe(II) at goethite surface, the adhesion of the formed elemental sulfur bound at goethite apparently was weaker, so the it was extractable by methanol.

2.4 Conclusions

In this chapter, we investigated the effect of Fe(II) on the reaction between aqueous sulfide and goethite at pH 7 under anoxic conditions. Results indicated that S⁰ and Fe(II) are still the main redox reaction products in all setups. The presence of Fe(II) affected the reaction and the products of the subsequent reactions of sulfide with goethite. When there is only Fe(II)_{sorb} but in the absence of Fe(II)_{aq}, the reactivity and amount of reactive surface Fe(III) species was limited due to the consumption by reaction with sulfide. So in the case of low Fe(II) concentration, Fe(II)_{sorb} acted more as passivating coating at the goethite surface, inhibiting the reaction between sulfide/FeS and goethite. While under conditions where both Fe(II)_{sorb} and Fe(II)_{aq} are present, a dynamic sorption between Fe(II)_{aq} and Fe(II)_{sorb} occurs during the reaction process, keeping the Fe(II)_{sorb} fresh and reactive. Then electron transfer and atom exchange between reactive Fe(II)_{sorb} and structural Fe(III) led to the formation of reactive Fe(III) species at goethite surface, which subsequently reacted with FeS. Therefore, compared to conditions where there is only Fe(II)_{sorb}, under conditions where Fe(II)_{aq} is present as well,

$\text{Fe(II)}_{\text{sorb}}$ can remain fresh and act more as a stimulating role in the reaction between goethite and FeS .

Apart from methanol extractable S^0 , most spiked sulfide exist in the form of iron sulfide minerals. In the $\text{Fe(II)}_{\text{no}}$ setup in which there was no interference of Fe(II) , one quarter of spiked sulfide ($77 \mu\text{M}$) was methanol extractable S^0 . The other S atoms combined with iron sulfide minerals, which cannot be released as acid volatile sulfide in 1 M HCl. In the $\text{Fe(II)}_{\text{high}}$ setup in which $\text{Fe(II)}_{\text{aq}}$ and $\text{Fe(II)}_{\text{sorb}}$ are present, the distribution of S are similar with that in the $\text{Fe(II)}_{\text{no}}$ setup, but among the S binding to iron sulfide minerals, a large fraction of S ($160 \mu\text{M}$) are FeS , which can be released in 1 M HCl, another quarter of sulfide ($70 \mu\text{M}$) was strongly bound with iron sulfide mineral neither can be recovered in methanol nor be released in 1 M HCl. Under conditions where there was only $\text{Fe(II)}_{\text{sorb}}$ but no $\text{Fe(II)}_{\text{aq}}$, the formation of methanol extractable S^0 took up only 6.7 % of the initially spiked sulfide. The other S existed in the form of iron sulfide minerals.

As main reaction products between sulfide and iron oxides, Fe(II) and S^0 are commonly present in natural system. Hellige (2012) proposed the reduction of S^0 by $\text{Fe(II)}_{\text{sorb}}$ at lepidocrocite surface, however, there is no direct lab experiment available to support this hypothesis, the mechanism of interaction between $\text{Fe(II)}_{\text{sorb}}$ and S^0 is missing. In later chapter, this question will be addressed by investigating the reaction between goethite/ Fe(II) and S^0 at pH 7 under anoxic condition.

3 Reaction of aqueous sulfide with goethite/Fe(II) in the presence of natural organic matter at neutral pH under anoxic conditions

3.1 Introduction

The interaction between iron oxides and aqueous sulfide plays an important role in the cycling of iron and sulfur elements in natural systems and thus has been intensively studied (Dos Santos Afonso and Stumm, 1992; Hellige et al., 2012; Peiffer et al., 2015; Peiffer et al., 1992; Poulton, 2003; Wan et al., 2014). In natural anoxic water environments, Fe(II) is ubiquitously present (Glasauer et al., 2002; Lovley, 1997) and it would sorb at iron oxides surface altering their surface reactivity by complexation and transformation into secondary mineral phases (Handler et al., 2009; Handler et al., 2014).

Natural organic matter (NOM) is abundant in natural waters and plays important roles in both sorption and electron transfer processes. NOM can sorb at iron oxides surface, reduce iron oxides, complex with Fe(II), oxidize sulfide and incorporate sulfur, therefore exerting a significant influence on the degradation of organic pollutants at iron oxides, controlling the S cycle and supporting the growth of bacteria (see section of natural organic matter in chapter 1). Although interaction between NOM, iron oxides and sulfide have been extensively studied, the influence of NOM on the interaction between iron oxides and sulfide under environmentally relevant conditions remains enigmatic. It is not yet clear if NOM would act potentially as coating or electron transfer mediator in the reactions, and the extent of coating or electron transfer is also a mystery. Hence, the goal of this study is to investigate the influence of NOM on the interaction between iron oxides and aqueous sulfide under anoxic conditions at neutral pH, and how it affects the reaction while keeping track of sulfur species. Considering that in anoxic aquatic systems dominated by iron or sulfate reducing conditions, organic matter can be reduced by a variety of microorganisms (e.g., G. metallireducers) and geochemical-reducing species (e.g., sulfide) (Benz et al., 1998), thus aside from the natural-state of NOM, reduced redox state is present as well. Electrochemical reduction of NOM is a novel method to evaluate reversible electron transfer from and to NOM, which would reversibly reduce quinone moieties to hydroquinone moieties, resulting in less molecular alternation of NOM structure and its redox moieties, such as cleavage of quinones (Aeschbacher et al., 2009; Yu et al., 2016). Therefore, in this study electrochemically reduced NOM was used as well.

To complete these tasks, we studied the interactions between sulfide and goethite/Fe(II) suspension in the presence of Aldrich humic acid (AHA) (as representative of NOM of various concentrations and redox states). All the related experiments were performed at pH 7 under anoxic conditions. Geochemical evolutions were monitored by using wet chemical analysis.

3.2 Materials and Methods

All solutions were prepared with Millipore water and purged with N₂ to remove oxygen. The oxygen-sensitive procedures were conducted in anoxic glovebox. All chemical reagents were of analytical grade.

3.2.1 Materials

Fe(II) stock solution: The Fe(II) stock solution was prepared by adding 1.4 g of metal iron powder ($\geq 99\%$, Alfa Aesar) into a 50 mL of 1 M deoxygenated HCl with constant gentle stirring in the glovebox. After the iron powder dissolved in HCl solution, Fe(II) solution was filtered with 0.45 μm filter (with Hydrophobic PTFE Membrane, BGB Analytik) to remove the non-dissolved iron particles. The final exact concentration was measured using ferrozine assay (Stookey, 1970).

Goethite/Fe(II) stock solution: Goethite suspension with surface area concentration of 100 m^2/L was prepared by adding 10.86 g goethite powder (9.2 m^2/g) into 1 L Millipore water and washed twice with Millipore water to remove the residual ions sorbed at mineral surface. Then, goethite suspension was N₂-purged before transferring into a glovebox. In the glovebox, Fe(II) stock solution was spiked into goethite suspension thrice to reach an initial total concentration of 3.0 mM whereby pH was adjusted to 7.0 ± 0.1 after each step by using 0.1 M HCl or 0.2 M NaOH solution. The pH was titrated regularly until the sorption of Fe(II) at goethite attained an equilibrium and there was no further change in pH.

Sulfide solution: A sodium sulfide nonahydrate crystal ($\text{Na}_2\text{S} \cdot 9\text{H}_2\text{O}$) ($\geq 98\%$, Sigma-Aldrich) was rinsed with N₂-purged water to remove the surface contaminants, followed by dissolving in N₂-purged Millipore water under the flow of nitrogen gas. The exact concentration of sulfide solution was determined using iodometric method (Lawrence et al., 2000; Siegel, 1965).

Aldrich Humic Acid solution

AHA_{nat}: The Sigma Aldrich humic acid (AHA) with natural redox state was used as received and referred to as AHA_{nat}. AHA_{nat} stock solution was prepared by dissolving approximate 1g AHA powder in 1 L Millipore water at pH of around 7 with constant stirring. After 3 days until most solid dissolved, the AHA suspension was filtered through 0.45 µm filter (Whatman Sterile Mixed Cellulose Ester Membranes), and the filtrate was collected for future experiment. The AHA_{nat} stock solution was purged with N₂ (99.99 %) to remove oxygen and kept inside the glovebox for further experiment.

AHA_{red}: The electrochemical reduction of AHA_{nat} was conducted in the glovebox. The reduced AHA is referred to as AHA_{red}. Since the most widely accepted group of redox-active moieties in NOM are quinones or quinone-like moieties, the quinone in AHA_{nat} transforms via semiquinone intermediate to fully reduced hydroquinone. To prepare AHA_{red} solution, the AHA_{nat} stock solution was transferred into a 200 mL bulk electrolysis cell and electrochemically reduced at pH 7. The reduction of AHA solution was performed in 0.1 M KCl solution with the applied potential at -0.8 V by using potentiostat (Metrohm, Herisau, Switzerland) in the anoxic glovebox following Aeschbacher et al. (2009). The redox potential of HS mostly ranges between -0.3 V to +0.4 V (Aeschbacher et al., 2011; Kappler et al., 2004), thus under the applied potential of -0.8 V the AHA_{nat} is supposed to be completely reduced. The DOC concentrations in all AHA solutions were measured by High TOC analyzer (Elementar, Hanau, Germany).

3.2.2 Experimental setups

Concentration and redox states of NOM are two important factors affecting the interaction of NOM with other components (e.g. iron oxides and aqueous sulfide). To investigate the effect of NOM on the interaction between iron oxides and aqueous sulfide, initial total concentrations of 10 mg C/L and 40 mg C/L of AHA with different redox states were selected. Here the AHA concentrations of 10 mg DOC/L and 40 mg DOC/L were selected, because we focus on the reaction at the mineral surface, it is necessary to minimize the effect of aqueous AHA on the overall reactions. Based on Xue's (2018) results, under the similar conditions of goethite loading of 5.43 g/L (surface area concentration 50 m²/L), initial Fe(II) concentration of 1.5 mM and pH 7, when the initial AHA concentration was 40 mg DOC/L, regardless of the redox state, almost all AHA sorbs at goethite/Fe(II) mineral surface with only 5 – 9 mg C/L AHA

remaining in aqueous phase (see Figure 3.1). The points of L and H in Figure 3.1 are corresponding to low AHA concentrations of 10 mg C/L and high AHA concentration of 40 mg C/L conducted in this experiment (see Table 3.1). At point L (point of low AHA concentration), the sorbed AHA concentration was around 1.8 mg C/g with the goethite loading of 5.43 g/L, all AHA sorbs at goethite/Fe(II) surface, the corresponding sorbed AHA concentration was 9.8 mg C/L. At point H (point of high AHA concentration), in which the sorbed AHA concentration was around 7.1 mg C/g and aqueous AHA concentration was around 6 mg C/L, the sorption maintained a high level for both AHA_{nat} and AHA_{red}. Under this condition, the corresponding initial total AHA concentration is 40 mg C/L. Therefore, initial concentrations of 10 mg C/L AHA and 40 mg C/L AHA were chosen to achieve low and high AHA sorption, respectively.

For AHA containing setups, the prepared AHA solution was diluted to 20 mg C/L and 80 mg C/L first, and then 100 mL of the diluted AHA solutions was mixed with 100 mL of goethite/Fe(II) suspension (goethite surface area 100 m²/L, initial Fe(II) concentration of 3.0 mM) in 200 mL serum bottles (see Figure 3.2). The conditions of final suspensions are goethite surface concentration of 50 m²/L, Fe(II)_{tot} of 1.5 mM, AHA concentration of 10 mg C/L (referring to as AHA₁₀ setup) or 40 mg C/L (referring to as AHA₄₀ setup), respectively. Finally the pH was checked again and kept constant at 7.0 ± 0.1 by dropwise of 0.1 M HCl solution or 0.2 M NaOH solution until the pH reached a stable phase. For setups without addition of AHA (referred to as AHA₀ setup), 100 mL goethite/Fe(II) suspension was mixed with 100 mL Millipore water in 200 mL serum bottle.

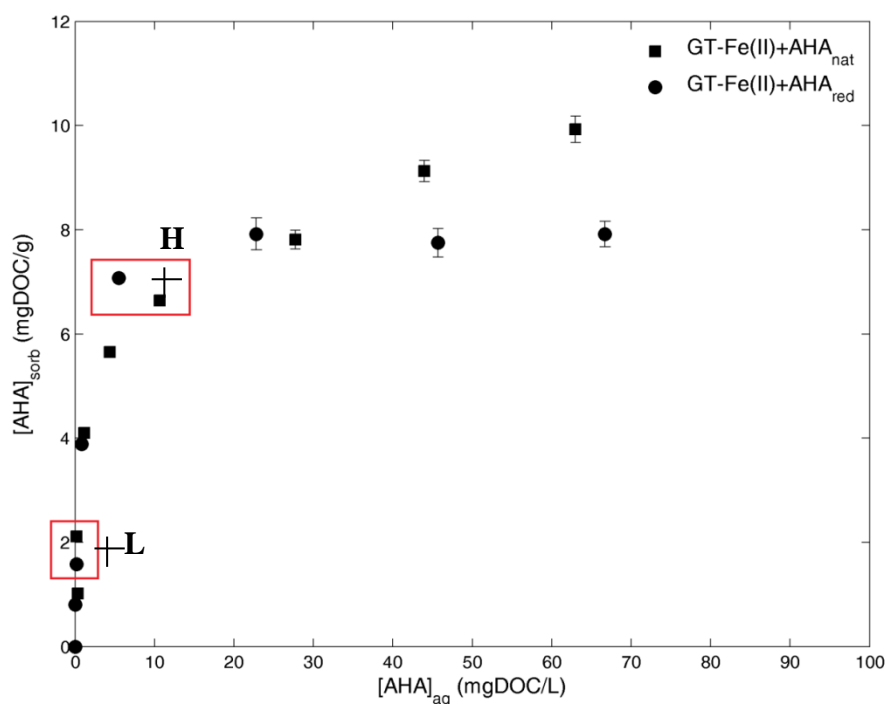


Figure 3.1: Sorption isotherm of AHA to goethite-Fe(II) with goethite loading of 5.43g/L and initial Fe(II) concentration of 1.5 mM at pH 7 under anoxic conditions (Xue, 2018).

Table 3.1: The selected AHA concentration in this experiment

Point in Figure 3.1	Sorbed AHA at goethite, mg C/g ^a	Aqueous AHA concentration, mg C/L	Total AHA concentration, mg C/L ^b
L	1.8	0	9.8
H	7.1	6	44.5

^a Goethite loading: 5.43 g/L; Specific surface area of goethite (N₂-BET): 9.2 m²/L.

^b The total AHA concentration is the sum amount of sorbed AHA and the aqueous AHA.

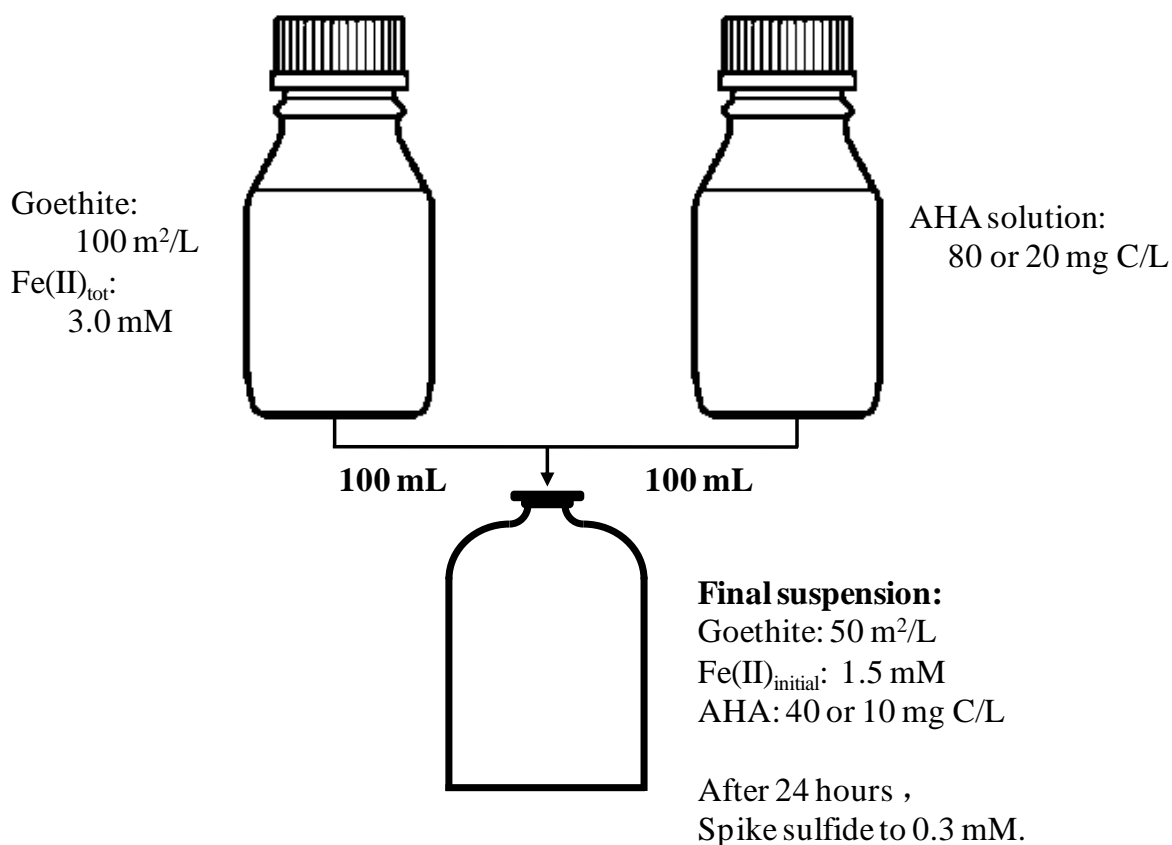


Figure 3.2: The procedure of experimental setups

When equilibrium of AHA solution (or water for AHA₀ setup) with goethite/Fe(II) suspension was built up, Fe(II)_{aq} and Fe(II)_{tot} concentrations were determined before spiking of sulfide. Then stock sulfide solution was spiked to reach an initial concentration of 0.3 mM, and pH was titrated to 7.0 ± 0.1 within 3 hours. The overview of the experiment of different setups is shown in Table 3.2. Samples were taken for analysis at intervals.

Table 3.2: Overview of the experiments conducted at neutral pH under anoxic conditions

Setups	Goethite, m ² /L	Fe(II), mM	Initial AHA, mg DOC/L	Sulfide, mM
AHA ₀			0	
AHA _{nat_10}			10	
AHA _{nat_40}	50	Fe(II) _{initial} : 1.5 mM; Fe(II) _{aq} : ≈ 1.0 mM	40	0.3
AHA _{red_10}			10	
AHA _{red_40}			40	

Note:

Both AHA_{nat_10} setup and AHA_{red_10} setup were referred to as AHA₁₀ setups; Both AHA_{nat_40} setup and AHA_{red_40} setup were referred to as AHA₄₀ setups.

3.2.3 Sampling and analytical methods

There are several species needed to be sampled and analyzed. The details are shown in the following.

Iron species: Fe(II)_{aq} was determined after filtration (0.45 μm, with Hydrophobic PTFE Membrane, BGB Analytik) using ferrozine method (Stookey, 1970). Fe(II)_{tot} was determined after mixing 0.1 mL of unfiltered sample with 0.9 mL of 1 M HCl first. After incubation for 24 h, the suspension was centrifuged and supernatant was analyzed. The difference between Fe(II)_{tot} and Fe(II)_{aq} is the concentration of Fe(II) in solid phase, including mineral surface bound Fe(II) (Fe(II)_{sorb}) and the Fe(II) associated with sulfide which is extractable in 1 M HCl.

Sulfur species

Aqueous sulfide: Aqueous sulfide (S(-II)_{aq}) was determined photometrically by methylene blue method after filtration (0.45 μm) (Cline, 1969).

Elemental sulfur: Elemental sulfur (S^0) was extracted after treatment of 0.3 mL unfiltered suspension sample with 0.15 mL of zinc acetate (10 wt %) to precipitate residual sulfide following a procedure modified after Kamyshny et al. (2009). After 15 minutes, 1.6 mL methanol was added into the suspension. After shaken for 3 hours, the suspension was centrifuged and the supernatant was measured by HPLC combined with Diode array detector after separation on a C18 column (Ultrasphere ODS 5 μ m, 250 by 4.6 mm) and isocratic elution by 98 % methanol with a flow rate of 0.8 mL/min. The detection was performed at a wavelength of 265 nm.

Thiosulfate: 0.1 mL zinc acetate solution was added into unfiltered 2.5 mL samples to precipitate the residual sulfide. After filtration the same was measured by HPLC with a modification of the protocol published by Lohmayer et al. (2014). A reversed-phase C18 column (Ultrasphere ODS, 5 μ m, 250 by 4.6 mm) was used for separation. Elution was performed with eluent composed with 2 mM tetrabutylammonium chloride ($[\text{CH}_3(\text{CH}_2)_3\text{NCl}]$) and 1 mM sodium carbonate (Na_2CO_3) in 77 % Millipore water and 23 % acetonitrile (CH_3CN), and the pH was adjusted to 7.7 by the addition of 1 M HCl. Following parameters were used: a flow rate of 0.8 mL/min, the injection volume of 15 μ L, and the detection wavelength of 215 nm.

Sulfate: The sulfate concentration in samples was determined via ion chromatography (IC) (Metrohm AG). Since the Fe(II) present in the sample would block the IC column during measuring process, thus it is necessary to remove it prior to analysis. For this purpose, 5 mL of filtered sample was treated with adding 0.16 mL of 0.2 M NaOH solution to attain alkaline pH to stimulate Fe(II) oxidation as Fe(III) precipitate in the air. After approximately 30 min until all Fe(II) ion got oxidized to Fe(III), pH was lowered back to 7 – 8 by adding 0.44 mL of 0.1 M HCl (to decrease the solubility of $\text{Fe}(\text{OH})_3$). Then the resulting sample was centrifuged to remove $\text{Fe}(\text{OH})_3$ precipitate and the supernatant was separated for further analysis.

Acid volatile sulfide (AVS)

The addition of HCl can release H_2S from sulfide-containing species including the metastable iron sulfide minerals and some organic sulfur (Rickard and Morse, 2005). In general, these substances can be divided into two groups: (1) dissolved iron and sulfur species and their complexes and (2) solid iron sulfides precipitate (e.g. FeS , Fe_3S_4 , FeS_2) (see Figure 3.3). In

addition, in the presence of organic matter, aqueous sulfide can be incorporated into organic matter ($S(-II)_{org}$), which can also contribute to AVS (Rickard and Morse, 2005).

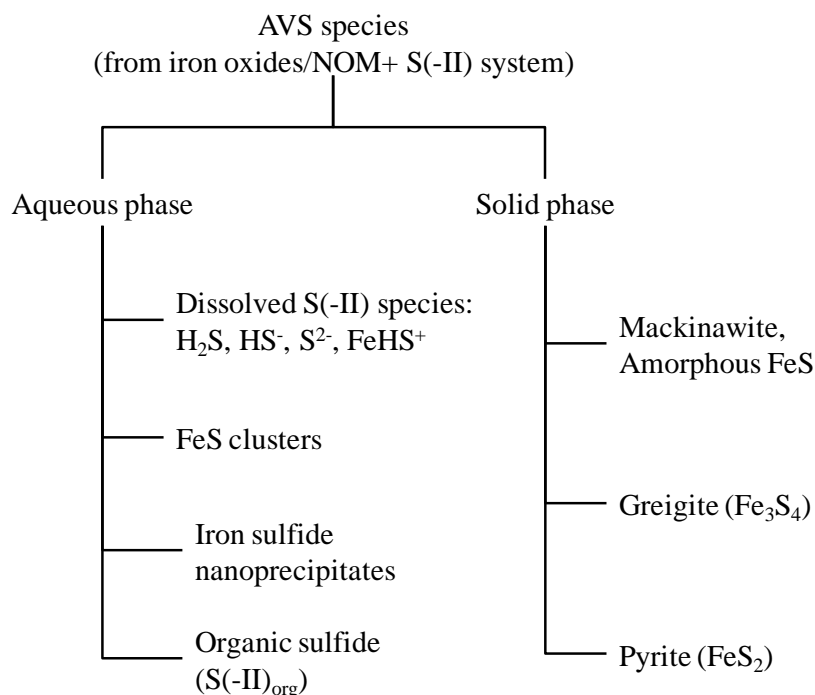


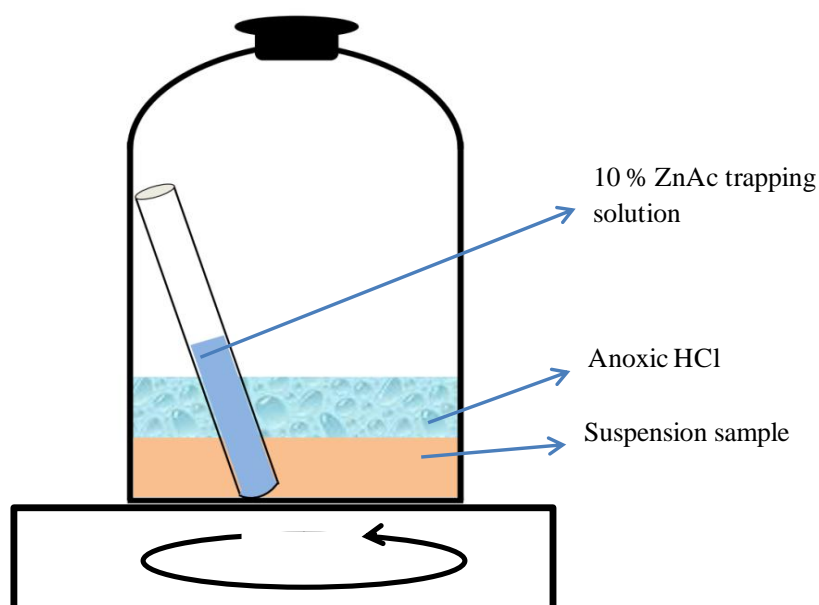
Figure 3.3: The potential sources of AVS modified after Rickard and Morse (2005)

Although AVS extraction method was proposed many years ago, and many investigations have been conducted to develop this method, there is still no common standard method established as AVS extraction method (Cornwell and Morse, 1987; Meysman and Middelburg, 2005; Rickard and Morse, 2005; Ulrich et al., 1997). Since this method suffers from a lack of absolute specificity in mineral phase separation, there are overlaps between different extraction reagents, operations, and the overlaps may not be constant between different studied samples (Cornwell and Morse, 1987). Morse et al. (1987) summarized that the amorphous FeS can be completely dissolved in 1 M HCl and recovered, greigite (Fe_3S_4) does not entirely dissolve in simple HCl treatment and pyrite (FeS_2) does not dissolve in HCl (see Table 3.3). The different solubility of iron sulfide minerals in acidic solution could be used experimentally to separate them from each other.

Table 3.3: The sulfide recovery from different minerals (Morse et al., 1987)

	Amorphous (FeS) %	Mackinawite %	Greigite %	Synthetic pyrite %	Pyrite %
1.0 M HCl	100	90	40 – 67	0	0
6.0 M HCl	100	98 – 102	60 – 69	0	0

Extraction method: The extraction of AVS was operated like the following: In glovebox 5 mL unfiltered suspension sample was transferred in 100 mL serum bottle, and a tube already containing 2 mL of 10 wt% zinc acetate solution was placed in the bottle as trapping solution and the bottle was sealed with rubber stopper. Outside the glovebox, 5 mL of anoxic HCl with concentration of 2 M or 12 M was injected via syringe. The trapping solution can precipitate the liberated H_2S as ZnS. After shaking gently on a horizontal shaker for 24 hours, the trapping tubes were removed from the serum bottles. A homogeneous ZnS suspension was ensured by treatment in sonication water bath for 5 minutes. The sulfide was measured by using methylene blue method (Cline, 1969).

**Figure 3.4: Scheme of AVS Extraction**

3.3 Results and discussion

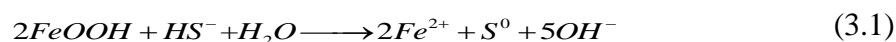
All the measured terms mentioned in previous sections are summarized and discussed separately in the following.

3.3.1 pH changes during the reaction

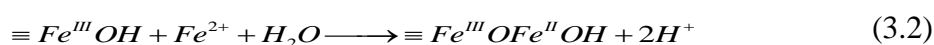
Upon the sulfide spiking, black precipitate, which was FeS precipitate, formed immediately in all setups. The intensity of black color increased in the order of:

AHA₄₀ setups < AHA₁₀ setups < AHA₀ setup (goethite/Fe(II) + sulfide). No matter the AHA were reduced or non-reduced.

Aside from the color changes, the pH increased to > 9.2 in all setups after sulfide spiking. The increase can be caused by two ways. First the sulfide stock solution was very alkaline with high pH value of > 12.8, thus the addition of sulfide solution increased the pH of suspension. The reaction between sulfide and goethite can produce OH⁻ as well (Eq 3.1) (Hellige et al., 2012; Peiffer et al., 1992).



The reaction between aqueous sulfide and iron oxides is a fast reaction (Peiffer et al., 1992; Wan et al., 2014), thus the pH increased immediately with the addition of sulfide. To maintain the reaction taking place at constant pH of 7, the pH was titrated back to 7 with dropwise of 0.1 M HCl solution. The titration process was finished in 3 hours. During the process of pH titration, the complementary amount of HCl added in the suspension ranged from 5 – 20 μM. After titration the pH values in all setups were quite stable (ranging between 6.8 – 7.0). This is in agreement with the observation in Chapter 2, where the interaction between goethite and aqueous sulfide was investigated in the presence of Fe(II). Even under conditions where aqueous sulfide was consumed but oxidation of sulfide to S⁰ was continuing, the pH remained stable. This scenario could be attributed to the sorption of newly generated Fe(II) at goethite surface. Because with the increasing formation of S⁰, no increase of Fe(II)_{aq} concentration was observed in all setups (shown in later section). Therefore, it could be inferred that the generated Fe(II) from Eq 3.1 sorbed at goethite surface (Eq 3.2) (Elsner et al., 2004).



The sorption of Fe(II) at goethite surface released H^+ , which can compensate the generated OH^- from the redox reaction. Therefore after pH titration to 7, the reaction in the suspensions did not produce significant amounts of OH^- or H^+ ions to change pH.

3.3.2 Evaluation of sulfur species during the reaction

Sulfide reacts with iron oxides and NOM rapidly. In this study, after 7 hours of reaction, there was no aqueous sulfide detected with detection limit of $6 \mu M$. During the whole reaction process thiosulfate and sulfate were not detected with detection limits of $6 \mu M$ and $7.6 \mu M$, respectively. The formation of elemental sulfur continued towards the end of reaction process.

The concentration of methanol extractable S^0 is highest in the AHA_0 setup, followed by setups with AHA concentration of 10 mg C/L , the setups with AHA concentration of 40 mg C/L had the lowest S^0 concentration (Figure 3.5). These results indicated that the presence of AHA significantly inhibited the formation of S^0 .

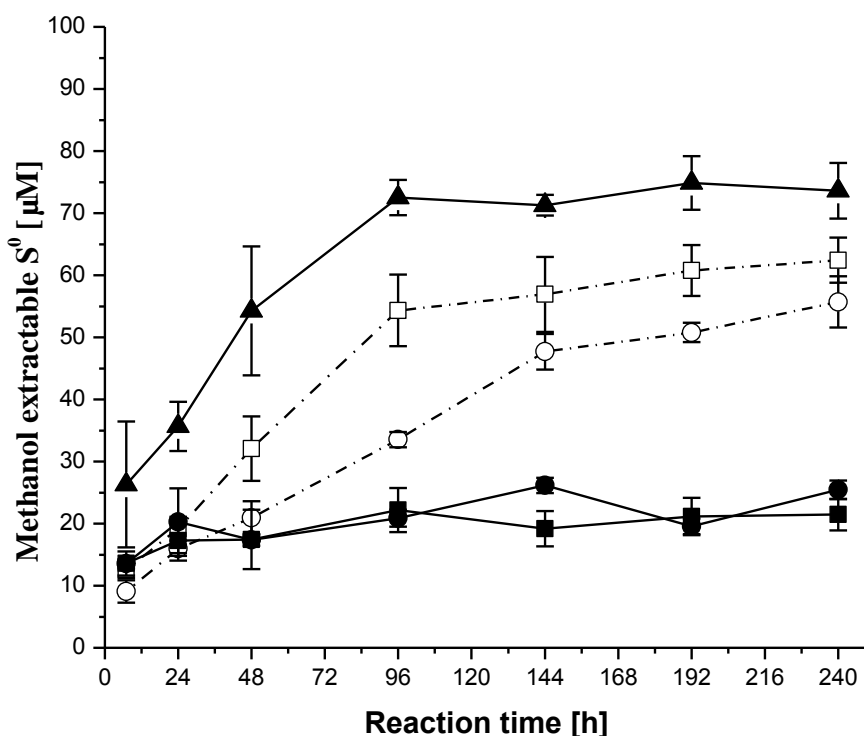


Figure 3.5: The evaluation of S^0 concentration during the reaction between aqueous sulfide and Fe(II) treated goethite suspension under the influence of AHA. The symbols represent: ▲ for the AHA_0 setup (in the absence of AHA); □ for the AHA_{nat_10} setup (10

mg C/L AHA with natural state); ○ for the AHA_{red_10} setup (10 mg C/L AHA with reduced state); ■ for the AHA_{nat_40} setup (40 mg C/L AHA with natural state); ● for the AHA_{red_40} setup (40 mg C/L AHA with reduced state).

In the AHA₀ setup, 20 μM of S⁰ formed after 7 hours of sulfide addition. The S⁰ concentration increased to 70 – 75 μM towards the end of experiment even in the case of all aqueous sulfide had been completely consumed. It is believed that the reaction between aqueous sulfide and iron mineral proceeds by the first adsorption step of sulfide at mineral surface (Dos Santos Afonso and Stumm, 1992; Wan et al., 2014). In the presence of Fe(II) both in aqueous phase and at goethite surface, the initially added aqueous sulfide can also be precipitated by Fe(II) to form FeS. Therefore, it can be inferred that after consumption of aqueous sulfide it was FeS that reacted with goethite to generate S⁰ in a similar way as sulfide did (Eq 3.3).



In AHA₄₀ setups, regardless the redox state of AHA, the formation of S⁰ was much lower than that in other setups with low AHA concentration, suggesting that sorption of AHA at goethite/Fe(II) surface significantly inhibited the interaction of FeS with goethite. Furthermore, the S⁰ concentration was similar (20 – 25 μM) in the AHA_{red_40} setup and AHA_{nat_40} setup, indicating that the redox state of AHA played insignificant role in the formation of S⁰ at high AHA concentration. Figure 3.1 and Table 3.1 show that under studied conditions (50 m²/L goethite surface concentration, 1.5 mM initial Fe(II) concentration and pH 7), when the initially added AHA concentration was 40 mg C/L, almost all AHA sorbed at goethite surface, approaching the saturation of AHA under these conditions. It is reasonable to conclude that 40mg C/L AHA covered the surface of goethite/Fe(II) significantly, regardless of the redox state. Therefore, it is likely that the sorption of AHA at goethite surface prevented the reaction of S(-II) with goethite, leading to low yield of S⁰.

In the setups with AHA concentration of 10 mg C/L, all AHA sorbed at goethite/Fe(II) surface, but goethite were not fully covered, so the coating effect of AHA at goethite/Fe(II) surface was limited. Therefore, the yield of S⁰ was slightly lower than that in the AHA₀ setups. Under conditions of such low AHA concentration, the effect of redox state of AHA started to be observable. The S⁰ concentration in the AHA_{nat_10} was approximately 10 μM higher than that in the AHA_{red_10} setup. It is likely that in the AHA_{nat_10} setup the AHA_{nat} oxidized Fe(II)_{sorb} to Fe(III) at goethite surface, the generated Fe(III) subsequently oxidized S(-II) to S⁰. This

assumption is in agreement with the measured electron accepting capability (EAC) of AHA in its natural redox state. The measured EAC in this study is $2.74 \pm 0.36 \mu\text{mol e}^- (\text{mg C})^{-1}$. In the AHA_{nat_10} setup, 27.4 μM Fe(II) could be oxidized to Fe(III) by AHA_{nat} then this Fe(III) subsequently oxidized approximately 14 μM S(-II) to S⁰. While in the AHA_{red_10} setup, there was no electron transfer between AHA and goethite/Fe(II) (Xue, 2018), the amount of reactive Fe(III) at goethite surface did not increase. In the AHA_{nat_40} setup, although more Fe(III) might be formed due to oxidation of Fe(II) by AHA_{nat}, they were significantly covered by AHA which prevented the access of sulfide to reactive Fe(III) at goethite surface. Therefore, the yields of S⁰ in the AHA_{nat_40} setup and the AHA_{red_40} setup were almost the same.

In summary, AHA sorbs at goethite/Fe(II) surface, exerting an inhibitory effect on the interaction between aqueous sulfide and goethite. Although it has been reported that NOM can act as electron transfer mediator between microorganism/ organic pollutants and iron oxides (Jiang and Kappler, 2008), in the case of high sorption (40 mg C/L) the inhibitory effect dominates among the overall effects and the redox state of AHA played a negligible role. Likewise, under conditions of low sorption (10 mg C/L) the inhibitory effect of AHA is correspondingly lower. The redox-active moieties in AHA cannot be regenerated under the studied experimental conditions, therefore, the redox state of AHA plays a negligible role in the whole reaction. While, at low AHA concentration AHA sorbed at goethite at a low level, AHA_{nat} can oxidize Fe(II)_{sorb} to Fe(III), enhancing the S⁰ formation. Since the effect of redox state of AHA only exhibits at low concentration, the overall effect of AHA is limited when it is of low concentration.

3.3.3 Evaluation of Fe(II) species during the reaction

The evaluations on Fe(II) species can be divided into two phases. The first is the reactions between goethite/Fe(II) with AHA, prior to spiking of sulfide. Second phase is after spiking of sulfide, in which sulfide got oxidized to S⁰ with formation of Fe(II).

Reactions of goethite/Fe(II) with AHA. After mixing with AHA solution, Fe(II)_{aq} decreased with increasing AHA concentration (Figure 3.6). Moreover, in setups with same AHA concentration, Fe(II)_{aq} concentration decreased more in the AHA_{nat} setups than in the AHA_{red} setups. It can be explained by that AHA_{nat} oxidized Fe(II)_{sorb} to Fe(III), which provided new surface sites for Fe(II)_{aq} sorption, thus the Fe(II)_{aq} in AHA_{nat} setups were lower than that in the

AHA_{red} setups (Xue, 2018). Regarding the decrease in Fe(II)_{aq} concentration in AHA_{red} setups, although it is reported that there is no electron transfer between AHA_{red} and goethite/Fe(II) complex under similar conditions (Xue, 2018), it is likely that Fe(II)_{aq} formed complex with AHA, followed by the adsorption of AHA-Fe(II) complex at goethite surface (Luan et al., 2013). The AHA_{red}-Fe(II) complex is less positive charged than AHA_{nat}-Fe(II) complex, so it can sorb at goethite/Fe(II) surface due to electron attraction.

No obvious effect of AHA was observed on Fe(II)_{tot} concentration, suggesting significant electron transfer did not occur between AHA and goethite/Fe(II) complex, even at high AHA concentrations (will be interpreted later).

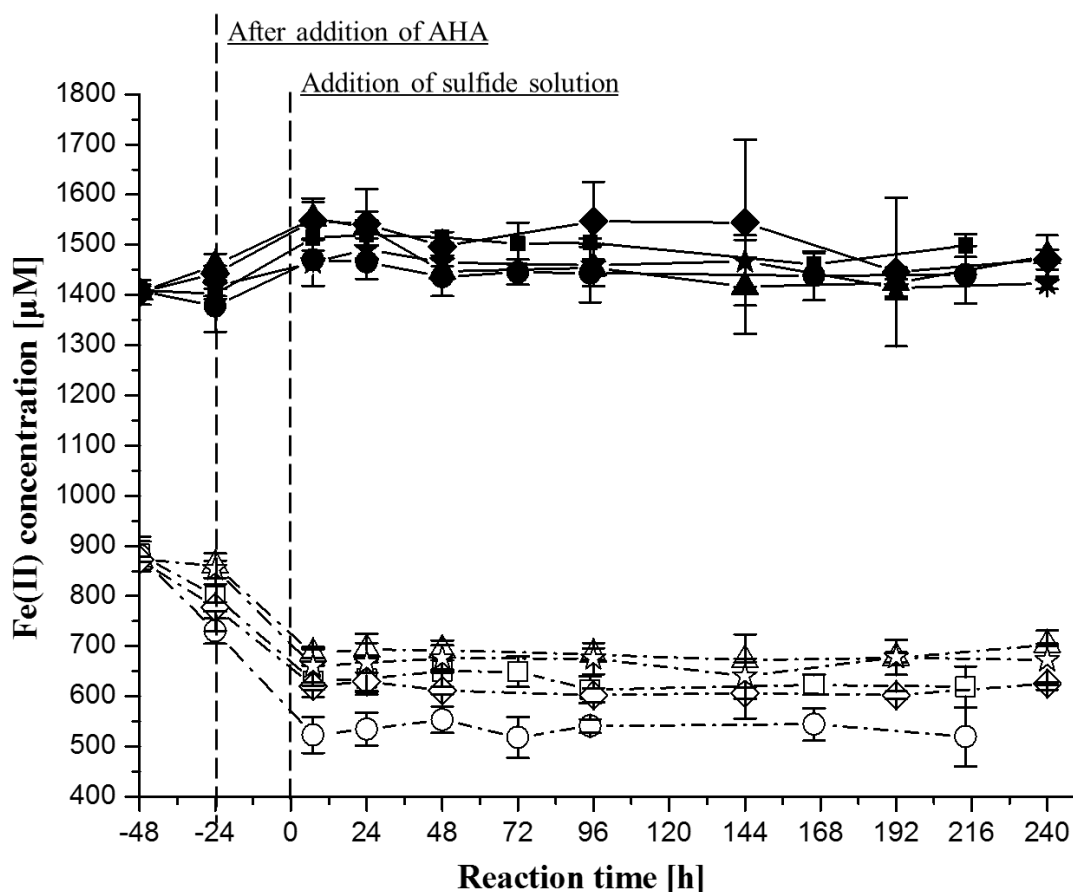
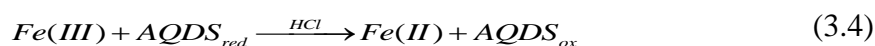


Figure 3.6: The evaluation of Fe(II) concentration during reactions between aqueous sulfide and Fe(II) treated goethite suspension under the influence of AHA at pH 7 under anoxic conditions. Sampling point at -48 h represents the initial Fe(II) concentration before mixing with AHA solution; at -24 h represent the concentration after equilibrium with AHA. Zero h is the point of adding aqueous sulfide.

Dashed line with ☆ and solid line with ★ are for Fe(II)_{aq} and Fe(II)_{tot} in the AHA₀ setup; Dashed line with □ and solid line with ■ for Fe(II)_{aq} and Fe(II)_{tot} in the AHA_{nat_10} setup; Dashed line with ○ and solid line with ● are for Fe(II)_{aq} and Fe(II)_{tot} in the AHA_{nat_40} setup; Dashed line with △ and solid line with ▲ for Fe(II)_{aq} and Fe(II)_{tot} in the AHA_{red_10} setup; Dashed line with ◇ and solid line with ◆ are for Fe(II)_{aq} and Fe(II)_{tot} in the AHA_{red_40} setup.

Reactions of Fe(II)/AHA treated goethite with aqueous sulfide. After spiking of 300 μM sulfide solution, $\text{Fe(II)}_{\text{aq}}$ decreased rapidly by 160 – 210 μM due to formation of FeS in all setups (see Figure 3.6). There was no significant difference among different setups.

$\text{Fe(II)}_{\text{tot}}$ concentration increased in all setups due to reduction of Fe(III) by sulfide (see Eq 3.1 and Eq 3.3), but the difference between different setups was not significant, regardless of the amount of AHA and the redox state of AHA. This was surprising, because based on the yield of S^0 in different setups, such as in the AHA_0 and AHA_{10} setups, in which the yield of S^0 were high, were supposed to show a high increase in Fe(II) concentration (see Eq 3.3). Likewise, in the AHA_{40} setups, the yield of S^0 was very low, the increase of Fe(II) were supposed to be small. However, the measured difference in $\text{Fe(II)}_{\text{tot}}$ concentrations between different setups were not significant due to relatively large measuring uncertainties. This is likely due to the presence of AHA, which made the $\text{Fe(II)}_{\text{tot}}$ measuring more challenging due to electron transfer and complexation between goethite/ Fe(II) and AHA. Xue (2018) investigated the electron transfer between goethite/ Fe(II) and AHA with different redox state under similar experimental conditions, revealing the reduction of AHA_{nat} by $\text{Fe(II)}_{\text{sorb}}$. Orsetti et al. (2013) observed that in goethite/ Fe(II) suspension, more Fe(II) was determined in the presence reduced anthraquinone-2,6-disulphonate (AQDS) during process of acidic extraction. The backward reaction can be expressed as in Eq 3.4.



Since the main redox functional groups in AQDS and AHA are quinone moieties (Aeschbacher et al., 2011; Tan, 2014), more Fe(II) formed in AHA-containing setups during the measuring of $\text{Fe(II)}_{\text{tot}}$ during process of acidic extraction. Therefore, the measuring of $\text{Fe(II)}_{\text{tot}}$ was affected by AHA, the $\text{Fe(II)}_{\text{tot}}$ thus contained uncertainty.

3.3.4 Acid volatile sulfide

As have been explained in the section of 3.2.3, the $\text{AVS}_{1\text{M}}$ and $\text{AVS}_{6\text{M}}$ are assigned to correspond to the concentrations of sulfide which can be released and recovered after acidification in 1 M HCl and 6 M HCl, respectively. Here due to the presence of NOM sulfide would be incorporated in NOM structure to form organic sulfur, referring to as $\text{S(-II)}_{\text{org}}$ which can contribute to AVS as well (Rickard and Morse, 2005). The constituents of AVS are different from that have been stated in Chapter 2, in which the AVS constitute only sulfide released from iron sulfide minerals. In this study, no dissolved sulfide was detected, so $\text{AVS}_{1\text{M}}$

is the S(-II) concentration of FeS and weakly NOM-bound sulfide (S(-II)_{org_w}) (Eq 3.5); in AVS_{6M} the sulfide of more crystalline iron sulfide minerals (FeS_n) and strongly NOM-bound sulfide (S(-II)_{org_s}) which were not released in 1 M HCl are released as well (Eq 3.6).

$$AVS_{1M} = C(S(-II)_{FeS}) + C(S(-II)_{org_w}) \quad (3.5)$$

$$AVS_{6M} = C(S(-II)_{FeS}) + C(S(-II)_{org_w}) + C(S(-II)_{FeS_n}) + C(S(-II)_{org_s}) \quad (3.6)$$

Thus the difference between AVS_{6M} and AVS_{1M} is the concentration of sulfide released from FeS_n and S(-II)_{org_s} (Eq 3.7). Subtracted the S(-II)_{org_s} concentration from the difference, the concentration of FeS_n can be obtained by Eq 3.8.

$$AVS_{6M} - AVS_{1M} = C(S(-II)_{FeS_n}) + C(S(-II)_{org_s}) \quad (3.7)$$

$$C(S(-II)_{FeS_n}) = AVS_{6M} - AVS_{1M} - C(S(-II)_{org_s}) \quad (3.8)$$

After 10 days of reaction between aqueous sulfide and Fe(II)/AHA covered goethite suspension, until the main oxidation products (S⁰ and Fe(II)) reached to a stable phase, the AVS concentrations in each setup were determined (see Figure 3.7). However, the AVS data contains a high level of uncertainty in setups of AHA₀ and AHA_{nat_10}, and there was overlap between AVS_{1M} and AVS_{6M}. Nevertheless, the AVS_{1M} and AVS_{6M} in AHA₁₀ setups were very close to the data of the AHA₀ setup. While in AHA₄₀ setups, both AVS_{1M} and AVS_{6M} decreased, implying that some sulfide incorporated in AHA structure, which was not easy to be extracted in 1 M HCl and 6 M HCl. In the setups with same AHA concentration (no matter 10 mg C/L or 40 mg C/L), the data from AHA_{nat} and AHA_{red} setups were close to each other, which is in agreement with the previous conclusion that redox state of AHA plays an insignificant role in the reaction between sulfide and goethite. It is likely that under conditions of high sorption, the sorption effect overwhelmingly exceeded the effect of redox state. At low concentrations the content of functional moieties in AHA was correspondingly low. Therefore, the redox of AHA does not play significant role under this studied condition.

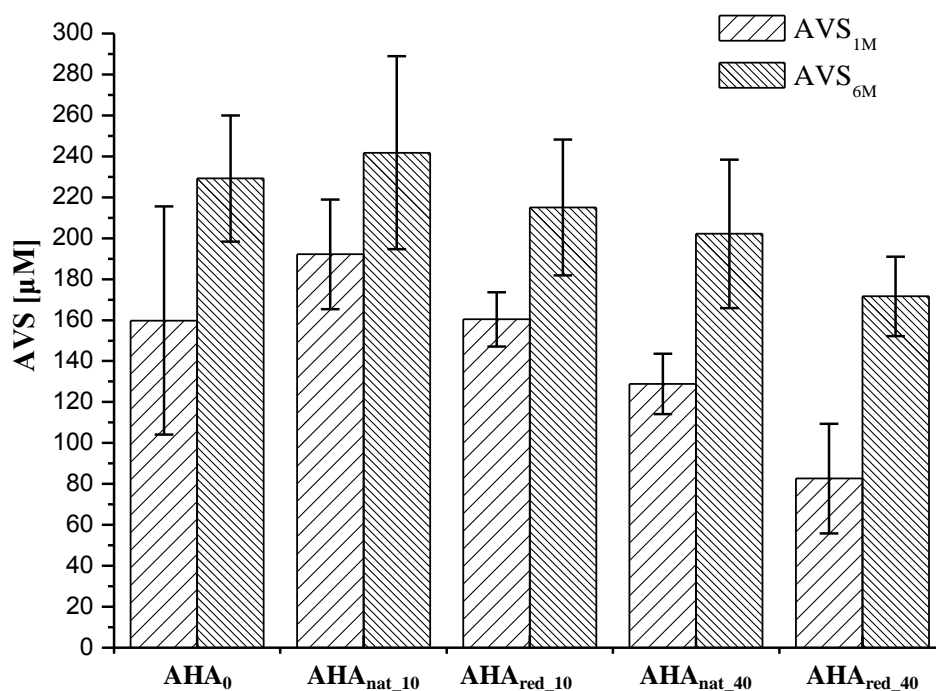


Figure 3.7: Acid volatile sulfide concentration in goethite/Fe(II) suspension reacted with aqueous sulfide under the influence of AHA with various concentrations and redox states.

3.3.5 Sulfur atoms mass balance

AVS method is a good way to estimate the sulfide concentration released from S(-II)-containing species, but from Figure 3.7 alone, it is impossible to estimate the exact individual fractions of FeS and S(-II)_{org_w} in AVS_{1M}, the fractions of FeS_n and S(-II)_{org_s} in AVS_{6M}. To evaluate this distribution of organic sulfur, investigation on the reaction between aqueous sulfide (initial concentration 150 μM) and electrochemical-reduced AHA (57.7 mg C/L, reduction potential applied at -0.8 V) solution was conducted at pH 7 under anoxic conditions. Results revealed that thiosulfate and S⁰ were not detected with the detection limit of 6 μM. The sulfide remaining in aqueous phase was 18.2 μM (12.2 %), the S(-II)_{org_w} recovered in 1 M HCl is 3.4 μM (2.3%), S(-II)_{org_s} recovered in 6 M HCl was 31.1 μM (20.7%), unrecovered sulfide was 97.2 μM (64.8%). Based on these datasets, the fractions of different organic sulfur species in the reaction of sulfide with different AHA solution can be roughly assessed. In 10 mg C/L AHA solution the S(-II)_{org_w} is 0.6 μM, S(-II)_{org_s} is 5.4 μM, unrecovered S is 16.8 μM. In 40 mg C/L AHA solution, S(-II)_{org_w}, S(-II)_{org_s} and uncovered S are 2.4 μM, 21.5 μM, and 68.1 μM, respectively.

However, there existed competitive reactions of sulfide with goethite/Fe(II) and with AHA at goethite surface (in AHA₄₀ setups dissolved AHA was around 6 mg C/L, therefore the reaction of sulfide with AHA in aqueous phase was negligible). The functional moieties in AHA, such as carboxyl or phenolic groups, have already been altered or occupied at goethite surface. The reaction of sulfide with goethite/Fe(II) is faster than the reaction of sulfide with NOM (Heitmann and Blodau, 2006), so it can be inferred that the fraction of sulfide reacted with AHA would be much lower than the amount reacted with goethite/Fe(II).

In the AHA₀ setup the S⁰ concentration was around 73 μM, the yield of S⁰ in AHA₁₀ setups were 56 μM – 63μM, while in AHA₄₀ setups the yield of S⁰ were only 22 μM – 25 μM. Regarding the AVS data, a similar trend was observed that AVS data from AHA₄₀ setups were lower than that from AHA₀ and AHA₁₀ setups. Compared to the AVA_{6M} in the AHA₀ setup, it were 15 μM – 20 μM lower for AHA₁₀ setups and 70 μM – 110 μM lower for AHA₄₀ setups. Therefore, it is reasonable to conclude that due to the sorption of AHA at goethite surface, some S(-II) reacted with AHA, leading to lower S⁰ formation. Based on the differences of S⁰ concentration in the AHA₀ setup and the other AHA-containing setups, we can roughly assess the amount of sulfide which reacted with AHA. Considering that the redox state of AHA exerted an unimportant influence on the interaction between sulfide and goethite/Fe(II), the effect of redox state of AHA on the reactions between sulfide and goethite/Fe(II) was ignored. We assumed that 10 μM sulfide reacted with AHA to form S(-II)_{org} in AHA₁₀ setups, 60 μM sulfide reacted with AHA to form S(-II)_{org} in AHA₄₀ setups. Here the S(-II)_{org} in AHA₁₀ setups was less than one quarter of that in AHA₄₀ setups. Because in AHA₁₀ setups goethite was slightly covered by AHA, it was much easier for sulfide to react with goethite. Based on the estimated S(-II)_{org} distribution in the reaction of sulfide with AHA in the pretest experiment, we assumed that in AHA₁₀ setups the AVS_{1M} and AVS_{6M} were negligible, all 10 μM sulfide were strongly combined with AHA and cannot be recovered. While in AHA₄₀ setups, the AVA_{1M} was negligible, around 15 μM sulfide was strongly bound to AHA (recovered in 6 M HCl), 45 μM was not recovered. With these assumptions, the concentrations of FeS and FeS_n in different setups can be calculated via Eq 3.5 and Eq 3.6. The obtained concentrations of different sulfur species in all setup are shown in Table 3.3. Based on sulfur mass balance, the n values of FeS_n can be calculated via Eq 3.9.

$$n = \frac{C(S(-II)_{initial}) - (C(S^0) + C(S(-II)_{FeS}) + C(S(-II)_{org}))}{C(FeS_n)} \quad (3.9)$$

Where $C(S(-II)_{initial})$ is the initially spiked sulfide concentration of 300 μM . $C(S^0)$ is the methanol extractable S^0 concentration. $C(\text{FeS})$ and $C(\text{FeS}_n)$ are concentrations of FeS and FeS_n , respectively. $C(S(-II)_{org})$ is estimated concentration of organic sulfide.

The calculated n values in FeS_n are 1.0 for AHA_0 setup, 0.7 for AHA_{nat_10} setup, 1.4 for AHA_{red_10} setup, 1.5 for AHA_{nat_40} setup, 1.8 for AHA_{red_40} setup (Table 3.3). There was no clear correlation shown up with different setups. It is likely that there is high uncertainty within AVS extraction method, therefore, it is a challenge to draw a general conclusion about the effect of NOM on the exact formation of AVS.

Table 3.3: Overview of concentrations of different sulfur species in all setups

Setups	S^0 , μM	$S(-II)_{org}$, μM			FeS, μM	FeS_n , μM	Calculated n
		$S(-II)_{org_w}$	$S(-II)_{org_s}$	$S(-II)_{unre}$			
AHA_0	73.6	0	0	0	159.8	69.4	1.0
AHA_{nat_10}	62.4	0	0	10	192.3	49.5	0.7
AHA_{red_10}	55.7	0	0	10	160.4	54.6	1.4
AHA_{nat_40}	21.5	0	15	45	128.8	58.4	1.5
AHA_{red_40}	25.4	0	15	45	82.6	74.0	1.8

In summary, the interactions among goethite/Fe(II), AHA and sulfide are complicated. Each component can react with the other one. AHA sorbed at the mineral surface to a large extent, and complexed with Fe(II) sorbing at goethite surface, electron transfer occurred between AHA_{nat} and goethite/Fe(II) complex, leading to re-sorption of Fe(II). With respect to AHA_{red} , complexation with Fe(II)_{aq} and the subsequent sorption of $\text{AHA}_{red}\text{-Fe(II)}$ resulted to the decreasing in Fe(II)_{aq} concentration. The AHA also affected the distribution of sulfide. The sorption of AHA prevented the access of sulfide to goethite, especially at high concentration of AHA (40 mg C/L), thus significantly inhibited the reaction. Due to the uncertainty coherent in AVS extraction, identifying the exact fraction of iron sulfide mineral is of high challenge.

3.4 Conclusions and outlook

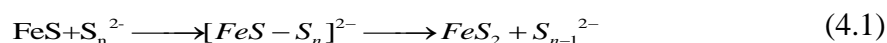
This effect of NOM on the reaction between goethite/Fe(II) and aqueous sulfide was investigated in this chapter. The data analysis demonstrated that AHA inhibited the redox reaction between sulfide with goethite due to sorption at goethite surface, leading to a lower amount of transformation products (thiosulfate and sulfate were not detected). Within the range of applied AHA concentration (10 mg C/L – 40 mg C/L), the coating effect of AHA played the major role in the whole reaction, while redox state of AHA played an unimportant role especially under conditions of high sorption. Furthermore, a fraction of sulfide incorporated into AHA structure, which further decreased the reaction of sulfide with goethite.

Although some studies reported that NOM acts as an electron transfer mediator between organic pollutants and the bulk electron acceptor like iron minerals, but all these studies were conducted in the presence of bacteria (Amstaetter et al., 2012; Jiang and Kappler, 2008; Klüpfel et al., 2014), where reduction of NOM by bacteria and re-oxidation of NOM by iron oxides took place. While, this presented study was performed in the absence of bacteria and thus the regeneration of functional moieties in AHA was not allowed, therefore, AHA cannot act as an electron transfer mediator to stimulate the reaction between goethite and sulfide. To better understand the role of AHA in a natural environment, some NOM-reduction bacteria can be introduced into the system in the future for further insights into the geochemical reactions in anoxic aqueous systems.

4 The abiotic sulfur cycle revisited – Disproportionation of elemental sulfur by surface-bound Fe(II) at goethite

4.1 Introduction

The interactions of iron oxides with sulfide have been widely studied as key processes in anoxic aqueous environments (e.g. marine sediments, aquifers, underground waters) in controlling the cycling of sulfur and iron (Dos Santos Afonso and Stumm, 1992; Peiffer et al., 1992; Poulton, 2003; Wan et al., 2014). Main products are elemental sulfur (S^0) and dissolved ferrous iron ($Fe(II)_{aq}$) (Dos Santos Afonso and Stumm, 1992; Hellige et al., 2012; Peiffer et al., 2015; Peiffer and Gade, 2007). The generated $Fe(II)_{aq}$ binds with sulfide to form a FeS precipitate which further evolves into more stable minerals like pyrite (Hellige et al., 2012; Peiffer et al., 2015; Wan et al., 2017). The reaction of FeS with polysulfides (S_n^{2-}) recently were identified as a key process in one of several routes of pyrite formation (Eq 4.1) (Luther, 1991; Rickard and Luther, 2007):



However, the formation pathway of polysulfides during the reaction of iron oxides with aqueous S(-II) and their contribution to pyrite formation remains enigmatic. Hellige et al. (2012) studied the reaction between lepidocrocite and elevated concentrations of aqueous sulfide at neutral pH under anoxic conditions. They found S^0 as a major sulfur product followed by the formation of pyrite and magnetite at the cost of FeS , sorbed $Fe(II)$ ($Fe(II)_{sorb}$) and S^0 . The concurrent disappearance of $Fe(II)_{sorb}$ and S^0 suggested that $Fe(II)_{sorb}$ has the potential to reduce S^0 to polysulfides (Eq 4.2). The resulting polysulfides subsequently participate in the formation of pyrite according to Eq 4.1.



Wan (2014) further investigated sulfur oxidation products during reaction of iron oxides (goethite and lepidocrocite) with aqueous sulfide under anoxic conditions at neutral pH. They demonstrated the formation of surface associated polysulfides as main oxidation product using cryogenic X-ray Photoelectron Spectroscopy. In Hellige's (2012) and Wan's (2014) studies, it was found that S^0 participated in the formation of polysulfides as a product of the reaction between iron oxides and sulfide and not as a starting reactant. Since a specific experimental

study directly addressing the interactions between S^0 and $Fe(II)_{sorb}$ is lacking, the major objective of this study is to fill this gap and evaluate the products of abiotic elemental sulfur transformation at iron reducing conditions. For this purpose, we investigated the reaction between S^0 and $Fe(II)_{sorb}$ by adding S^0 to goethite/ $Fe(II)$ suspensions. We focused on the role of S^0 as an initial reactant and not as a reaction product of interactions between iron oxides and sulfide. We stress on investigating whether $Fe(II)_{sorb}$ can reduce S^0 at appreciable rates, and to experimentally prove if there are any polysulfides formed during reaction. The concentrations of various $Fe(II)$ and sulfur species were monitored during this reaction.

4.2 Materials and methods

4.2.1 Materials

Fe(II) stock solution: The $Fe(II)$ stock solution was prepared by adding 1.4 g of metal iron powder ($\geq 99\%$, Alfa Aesar) into a 50 mL of 1 M deoxygenated HCl solution under constant gentle stirring in the glovebox (Braun, Germany, $O_2 < 1$ ppm). This solution was then filtered with 0.45 μm filter (with Hydrophobic PTFE membrane, BGB Analytik) to remove the non-dissolved iron particles. The exact concentration of $Fe(II)$ was determined using ferrozine assay (Stookey, 1970).

Goethite/ $Fe(II)$ suspension: Goethite suspension with surface area concentration of 100 m^2/L was prepared by adding 10.86 g goethite powder (N_2 -BET surface is 9.2 m^2/g , from Lanxess) into 1 L Millipore water and washed twice with Millipore water to remove the residual ions sorbed at mineral surface. The goethite solution was N_2 -purged and then transferring into glovebox. In the glovebox, $Fe(II)$ stock solution was spiked into goethite suspension thrice to obtain total concentration of 3.0 mM, and after each step titrated the suspension pH to 7.0 ± 0.1 by dropwise addition of 0.1 M HCl or 0.2 M NaOH solution. The pH was titrated regularly until the sorption of $Fe(II)$ at goethite attained an equilibrium and there was no further change in the pH. Once equilibrium was attained, the concentrations of aqueous $Fe(II)$ ($Fe(II)_{aq}$) and total acid extractable $Fe(II)$ ($Fe(II)_{tot}$) were measured again prior to reaction with S^0 .

Elemental sulfur solution: Approximately 100 mg of sulfur powder (Purity $\geq 99.5\%$, Fluka) was dissolved in 100 mL methanol (HPLC analysis grade, VWR Chemicals). After one day,

obtained solution was filtered through 0.45 μm PTFE filter (BGB Analytik) to remove undissolved sulfur powder. The determined S^0 concentration was 6.45 ± 0.36 mM (determined via a Shimadzu HPLC with Diode Array Detector as per Kamyshny et al. (2009), and transferred in glovebox after N_2 -purge.

4.2.2 Experimental setup

All air sensitive experiments were conducted in anoxic glovebox. In 250 mL serum bottle, 100 mL of prepared goethite/Fe(II) suspension was added, followed by addition of 90 mL of Millipore water, then 10 mL of methanol S^0 solution was added to reach a final volume of 200 mL with concentrations of 50 m^2/L goethite (Fe atom concentration was around 60.1 mM), 1.5 mM total Fe(II) and 322 μM S^0 . The final suspensions were titrated to $\text{pH } 7 \pm 0.1$ within 0.5 hour and stirred with a Teflon-coated stirring bar at a constant rate.

The pH value was kept constant at pH 7 by adding deoxygenated NaOH (0.01 M) with an automated pH-stat device (Titrande, Metrohm) during the whole reaction process. Based on pretest experiment of goethite/Fe(II)+ S^0 system, the pH would decrease significantly. Therefore, to maintain the pH at 7, acidic titrant was not needed.

4.2.3 Analytical methods

There are several species needed to be sampled and analyzed. The details are shown in the following.

Iron species: $\text{Fe(II)}_{\text{aq}}$ concentration was determined after filtration (0.45 μm , with Hydrophobic Polytetrafluoroethylene (PTFE) Membrane, BGB Analytik) using ferrozine method (Stookey, 1970). $\text{Fe(II)}_{\text{tot}}$ (including $\text{Fe(II)}_{\text{aq}}$, $\text{Fe(II)}_{\text{sorb}}$, and the Fe(II) associated with sulfide as FeS which were extracted in 1 M HCl) concentration was determined after mixing 0.1 mL of unfiltered sample with 0.9 mL of 1 M HCl first. After incubation for 24 h, the suspension was centrifuged and the supernatant was analyzed. The difference between $\text{Fe(II)}_{\text{tot}}$ and $\text{Fe(II)}_{\text{aq}}$ is the concentration of Fe(II) in solid phase, including $\text{Fe(II)}_{\text{sorb}}$ and FeS.

Aqueous sulfide: Aqueous sulfide ($\text{S(-II)}_{\text{aq}}$) was determined photometrically by methylene blue method after filtration (0.45 μm) (Cline, 1969).

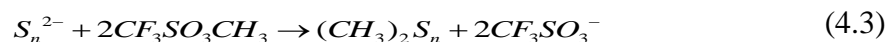
Elemental sulfur: Elemental sulfur (S^0) was extracted after treatment of 0.3 mL unfiltered suspension sample with 0.15 mL of zinc acetate (10 wt %) to precipitate free sulfide following

a procedure modified after Kamyshny et al. (2009). After 15 minutes, 1.6 mL methanol was added into the suspension. After shaken for 3 hours, the suspension was centrifuged and the supernatant was measured by HPLC combined with Diode array detector after separation on a C18 column (Ultrasphere ODS 5 μ m, 250 by 4.6 mm) and isocratic elution by 98 % methanol with a flow rate of 0.8 mL/ min. The detection was performed at a wavelength of 265 nm. Therefore, the measured S^0 concentration in this study is methanol extractable sulfur.

Thiosulfate: For thiosulfate samples, 0.1 mL zinc acetate (10 wt %) solution was added into unfiltered 2.5 mL samples to precipitate the residual sulfide. The filtered sample was measured by HPLC with a modification of the protocol published by Steudel et al. (1989) and Lohmayer et al. (2014). A reversed-phase C18 column (Ultrasphere ODS, 5 μ m, 250 by 4.6 mm) was used for separation. Elution was performed with eluent compositions with 2 mM tetrabutylammonium chloride ($[CH_3(CH_2)_3]_4NCl$) and 1 mM sodium carbonate (Na_2CO_3) in 77 % Millipore water and 23 % acetonitrile (CH_3CN), with the pH adjusted to 7.7 by the addition of 1 M HCl. Following parameters were used: a flow rate of 0.8 mL/min, the injection volume of 15 μ L, and the detection wavelength of 215 nm.

Sulfate: The sulfate concentration in samples was determined via ion chromatography (IC) (Metrohm AG). Since the Fe(II) present in the sample would block the IC column during measuring process, thus it is necessary to remove it prior to analysis. For this purpose, 5 mL of filtered sample was treated with adding 0.16 mL of 0.2 M NaOH solution to attain alkaline pH to stimulate Fe(II) oxidation as Fe(III) precipitate in the air. After approximately 30 min until all Fe(II) ion got oxidized to Fe(III), pH was lowered back to 7 – 8 by adding 0.44 mL of 0.1 M HCl (to decrease the solubility of $Fe(OH)_3$). Then the resulting sample was centrifuged to remove $Fe(OH)_3$ precipitate and the supernatant was separated for further analysis.

Polysulfides: Since polysulfide is an unstable component, we converted it into more stable dimethylpolysulfanes ($(CH_3)_2S_n$) for analysis following (see Eq 4.3) (Lohmayer et al., 2014).



The conversion was achieved by treatment with methyl trifluoromethanesulfane (methyl triflate; $CF_3SO_2OCH_3$) in a water-methanol solution, since methyl triflate is immiscible in water. For the unfiltered samples, the derivatization was performed by adding 1600 μ L of methanol in a 2.5 mL HPLC vial, then one hand added 400 μ L of unfiltered sample and the other hand added 12 μ L of methyl triflate simultaneously. The ratio of volume of sample solution and methanol volume was set to be 1: 4. After derivatization of approximate 20

seconds these solutions were filtered (0.45 μm , with PTFE filter, BGB Analytik) into 1.5 mL HPLC vials. The samples were kept frozen at $-20\text{ }^{\circ}\text{C}$ before analysis by HPLC-DAD.

Acid volatile sulfide(AVS)

The addition of HCl can release H_2S from sulfide-containing species including the metastable iron sulfide minerals. These substances can be divided into two groups: (1) dissolved iron and sulfur species and their complexes and (2) solid iron sulfides precipitate (e.g. FeS , Fe_3S_4 , FeS_2) (see Figure 4.1).

Although AVS method was proposed many years ago, many investigations have been conducted to develop this method, still there is no common method to be established as AVS extraction standard (Cornwell and Morse, 1987; Meysman and Middelburg, 2005; Rickard and Morse, 2005; Ulrich et al., 1997). Since this method suffers from a lack of absolute specificity in mineral phase separation, there are overlaps between different extraction reagents, operations, and the overlaps may not be constant between different studied samples (Cornwell and Morse, 1987).

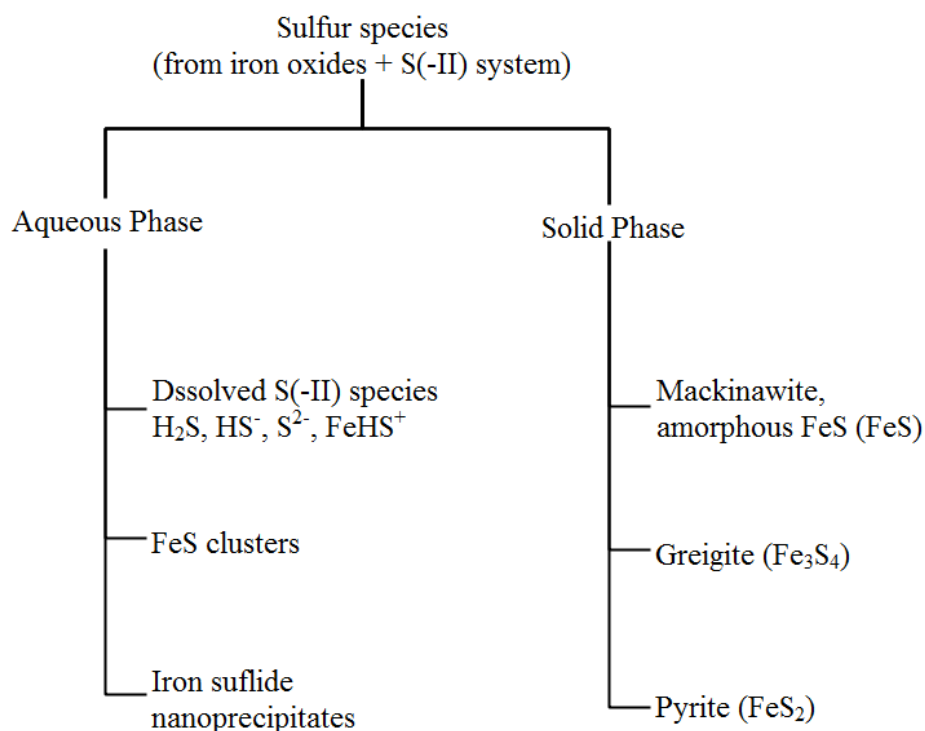


Figure 4.1: The potential sources of AVS (Rickard and Morse, 2005)

Morse et al. (1987) summarized that the amorphous FeS can be completely dissolved in 1 M HCl and recovered, greigite (Fe₃S₄) does not entirely dissolve in simple HCl treatment and pyrite (FeS₂) does not dissolved in HCl (see Table 4.1). The different solubility of iron sulfide minerals in acidic solution could be used experimentally to separate them from each other.

Table 4.1: The sulfide recovery from different minerals (Morse et al., 1987)

	Amorphous (FeS) %	Mackinawite %	Greigite %	Synthetic pyrite %	Pyrite %
1.0 M HCl	100	90	40 – 67	0	0
6.0 M HCl	100	98 – 102	60 – 69	0	0

Extraction method: In glovebox 5 mL unfiltered suspension sample was transferred in 100 mL serum bottle, and a tube already containing 2 mL of 10 wt % zinc acetate solution was placed in the bottle as trapping solution and the bottle was sealed with rubber stopper. Outside the glovebox, 5 mL of anoxic HCl with concentration of 2 M or 12 M was injected via syringe. The trapping solution can precipitate the liberated H₂S as ZnS. After shaking gently on a horizontal shaker for 24 hours, the trapping tubes were removed from the serum bottles. A homogeneous ZnS suspension was ensured by treatment in sonication water bath for 5 minutes. The sulfide was measured by using methylene blue method (Cline, 1969).

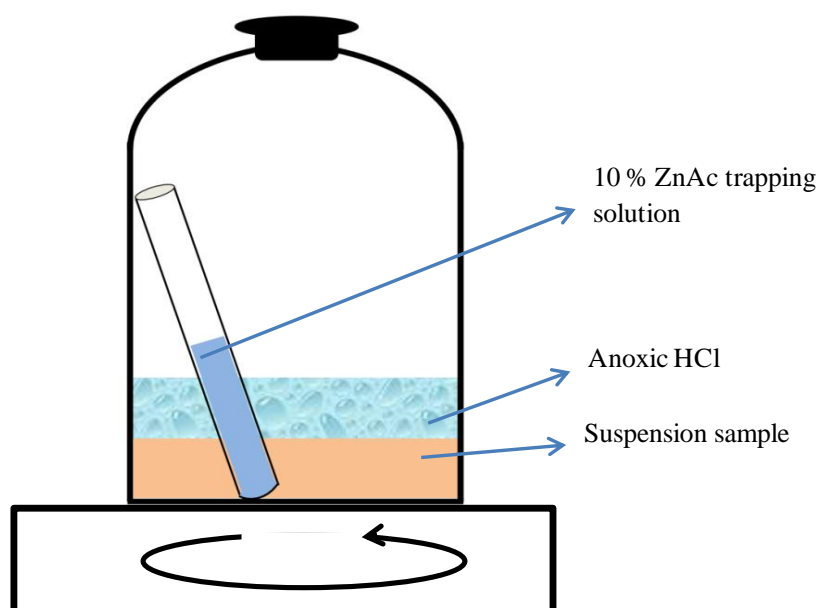


Figure 4.2: Scheme of AVS Extraction

4.3 Results and discussion

4.3.1 Changes in pH, S⁰ and Fe(II) in suspension

In our preliminary experiment, in which the reaction between goethite/Fe(II) and S⁰ was carried out without application of pH buffer solution nor automated pH-stat device, we observed a significant pH decrease due to the reaction between goethite/Fe(II) and S⁰. In order to prevent a pH drop with concomitant desorption of Fe(II) from goethite surface and a decrease of the reaction rate, automated titration with 0.01 M NaOH solution was used to keep the pH constant during the reaction process. Thus, changes in concentrations of Fe(II) and S⁰ are directly related to the interaction between Fe(II)_{sorb} and S⁰, not affected by the changes in pH. For this purpose, OH⁻ was rapidly consumed after addition of S⁰ into goethite/Fe(II) suspension to maintain the pH constant at 7 (Figure 4.3). The consumption of OH⁻ was observed within 3 days. No further consumption of OH⁻ was recorded beyond that. Concentration of S⁰ also decreased rapidly (from initial 322 μM to 105 μM) after 2 days of reaction (Figure 4.4) and only 23 μM of S⁰ was left in the suspension by the end of reaction. Thus, approximately 300 μM of S⁰ was transformed into other species during the reaction between Fe(II)_{sorb} and S⁰.

Fe(II)_{tot} along with Fe(II)_{aq} as main reactants followed the similar trend of S⁰ concentration and OH⁻ consumption as it decreased fast within the first 3 days (Figure 4.4). After 10 days, both Fe(II)_{tot} and Fe(II)_{aq} decreased to the similar extent (657 μM and 688 μM for Fe(II)_{tot} and Fe(II)_{aq}, respectively). The observed difference between Fe(II)_{tot} and Fe(II)_{aq} values is linked to the concentration of Fe(II) in the solid phase ((Fe(II)_{sorb} and FeS). Therefore, concentration of Fe(II) in solid phase remained almost unchanged. The Fe(II)_{sorb} concentration can be calculated via Eq 4.4.

$$C(\text{Fe(II)}_{\text{sorb}}) = C(\text{Fe(II)}_{\text{tot}}) - C(\text{Fe(II)}_{\text{aq}}) - C(\text{FeS}) \quad (4.4)$$

Where C(Fe(II)_{sorb}), C(Fe(II)_{tot}) and C(Fe(II)_{aq}) are the Fe(II) contents of Fe(II)_{sorb}, Fe(II)_{tot} and Fe(II)_{aq}, respectively. C(FeS) is the Fe(II) concentration in the form of FeS, which was appointed to AVS_{1M}. The values of AVS_{1M} were measured twice during the reaction process and were 131 ± 6 μM and 147 ± 16 μM at 24 h and 240 h, respectively. Since the concentrations of Fe(II)_{tot} and Fe(II)_{aq} were determined prior to the addition of S⁰ solution. Therefore, three Fe(II)_{sorb} concentrations were obtained: 565 μM, 615 μM and 450 μM at 0 h, 48 h and 240 h, respectively (Figure 4.4). During the whole reaction process, the amount of Fe(II)_{sorb} ranged 450 μM – 615 μM which allowed continuity of the reaction.

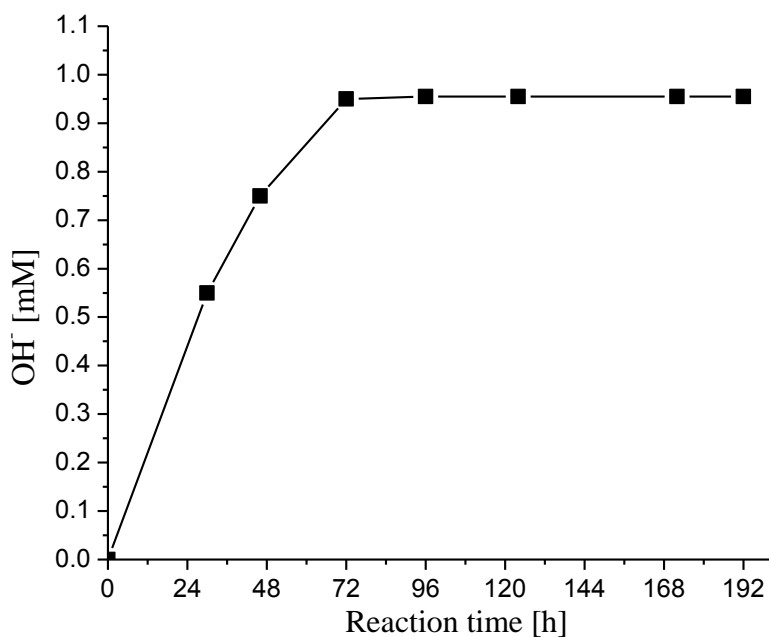


Figure 4.3: NaOH consumption during the reaction of S⁰ with surface bound Fe(II) at goethite surface to keep pH at 7.

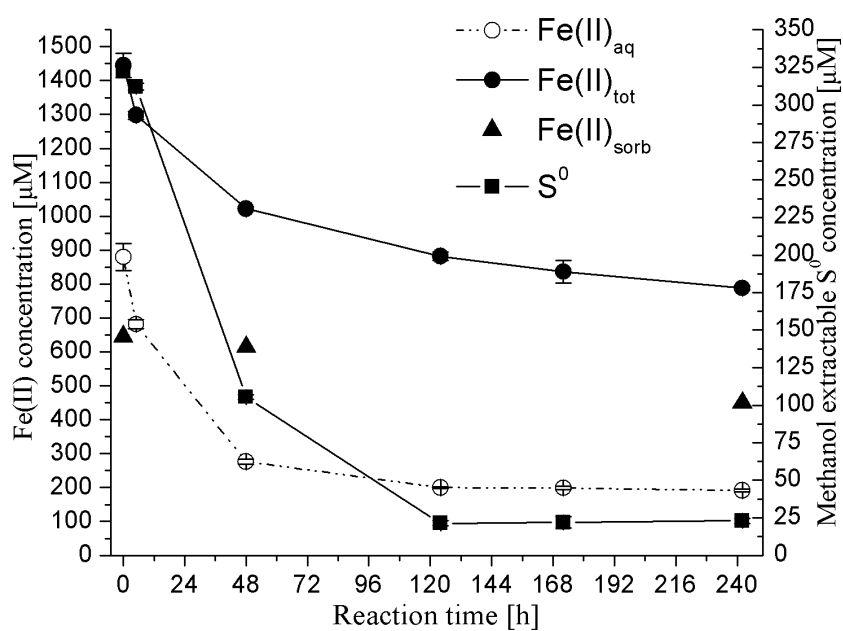
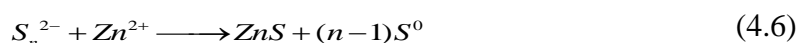
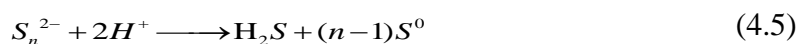


Figure 4.4: Time course of Fe(II) concentration (left axis) and S⁰ concentration (right axis) during the reaction of S⁰ with surface bound Fe(II) at goethite surface at pH 7.

The fast co-consumption of Fe(II) and S^0 , together with the OH^- , suggested the occurrence of the reaction between these components as reported in Eq 4.2. During the reaction process, $Fe(II)_{sorb}$ got oxidized to Fe(III) at goethite surface, providing new surface sites for $Fe(II)_{aq}$ sorption. The re-sorption of $Fe(II)_{aq}$ at goethite surface, on one hand, allowed the regeneration of new reactive surface Fe(II) complex and the proceeding of reaction (Amonette et al., 2000; Klausen et al., 1995).

4.3.2 Formation of reduced sulfur species (polysulfides, FeS, FeS_n)

The expected products of reaction among $Fe(II)_{sorb}$, S^0 and OH^- are polysulfides, which can be decomposed to S^0 and H_2S after treatment with acid (Eq 4.5) or with zinc salt solution (Eq 4.6) (Kamyshny et al., 2009). The released sulfide from Eq 4.5 contributes to AVS (Kamyshny et al., 2009; Rickard and Morse, 2005). Eq 4.6 is the pretreatment for S^0 sample measuring (Kamyshny et al., 2009; Wan et al., 2014).



The measured concentrations of polysulfides at different sampling times were very low, ranging from 9 – 20 μM [S] (Figure 4.5). Most polysulfide species were S_4^{2-} – S_7^{2-} in this study. Some of the individual polysulfides concentrations were even below detection limits, therefore, the obtained polysulfides concentration might bear some uncertainty. The detection limits of S_2^{2-} , S_3^{2-} and S_4^{2-} are 5 μM , 7.5 μM and 4.2 μM , respectively. For polysulfides with 5 – 8 S atoms, the detection limits were around 2.5 μM . Towards the end of reaction (10 days), the total polysulfides concentration (18 μM [S]) was very close to the determined methanol extractable S^0 concentration of 23 μM (Figure 4.4). During the process of sample processing for S^0 measuring, the sample was treated by addition of zinc acetate solution to decompose polysulfides to ZnS and elemental sulfur (Eq 4.6), followed by extraction in methanol. Wan et al. (2014) compared the S^0 concentration determined from HPLC (via extraction in methanol via ZnAc pretreatment) and the S^0 concentration derived from XPS measurement, found that the zero-valent sulfur in polysulfides was a significant fraction of methanol extractable sulfur. Therefore, it could be concluded that the 23 μM S^0 which remained in the suspension was probably from the polysulfides, which suggests that that all elemental sulfur transformed to other sulfur species under the studied conditions.

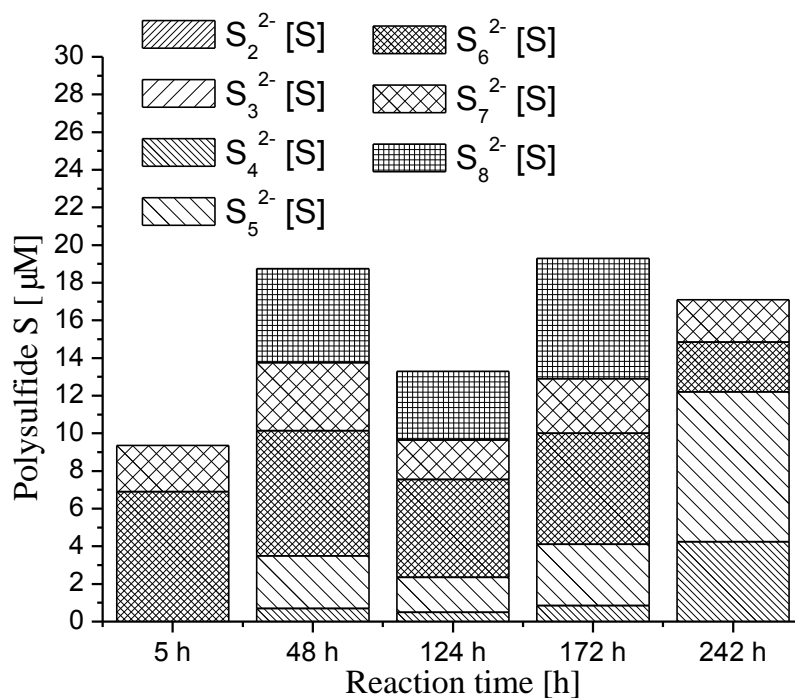
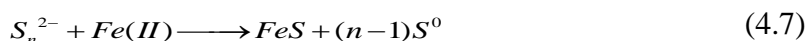


Figure 4.5: Concentrations of polysulfides with different chain-length (number of S atoms) measured at different sampling time. Note that the concentrations refer to S atoms present in the various polysulfide species, not to the concentration of molecular polysulfides species of different chain-lengths.

Regarding the low polysulfides concentration, it is likely due to the lack of aqueous sulfide which is essential for the formation of polysulfide (Kamyshny et al., 2009; Steudel, 2003). Although it was expected that the reduction of S^0 by Fe(II) occurred to a significant extent with the formation of S(-II), the resulting S(-II) was subsequently scavenged by excess of $Fe(II)_{aq}$ as FeS. This is in agreement with research by Poser et al. (2013). Poser et al. (2013) investigated the bio-disproportionation of elemental sulfur under the influence of iron oxides at pH 10 under anoxic conditions. Poser et al. (2013) reported a polysulfides concentration of only 0.85 mM in cultures supplemented with goethite, while a higher concentration (3 mM) in cultures without goethite. Therefore, Poser et al. (2013) proposed that iron oxides can precipitate sulfide to inhibit the formation of polysulfides. The inhibitory effect of goethite/Fe(II) on the yield of polysulfides can be interpreted by that Fe(II) decomposed polysulfides to S(-II) and elemental sulfur (Eq 4.7) in a similar way as Eq 4.6 did (Kamyshny et al., 2009; Poser et al., 2013).



Since polysulfides can release hydrogen sulfide after acidification (see Eq 4.5), the AVS_{1M} fraction comprised sulfide contained in FeS and polysulfides. The AVS measured in 6 M HCl (AVS_{6M}) is the sum concentration of AVS_{1M} and FeS_n . Thus, the difference between AVS_{6M} and AVS_{1M} is associated to be the concentration of FeS_n . We obtained values of $147 \pm 16 \mu M$ for AVS_{1M} and $237 \pm 3 \mu M$ for AVS_{6M} after 10 days of reaction. While polysulfides concentration was $18 \mu M$. We assumed an average chain length of such polysulfides to be 5, the amount of S(-II) released from polysulfides was only $3.6 \mu M$ (estimated using Eq 4.5) and thus was neglected for the calculation of S mass balance. Therefore, the concentrations of FeS and FeS_n were estimated to be $147 \mu M$ and $90 \mu M$, respectively.

The AVS_{6M} data indicated that most of the initially added S^0 was reduced to S(-II) by $Fe(II)_{sorb}$ at goethite surface. Reaction of reduced sulfide with S^0 resulted in the formation of polysulfides. However, due to the excess of Fe(II) in the suspension, the formation of polysulfides was inhibited and the generated polysulfides might also be decomposed to iron sulfide mineral and elemental sulfur.

4.3.3 Formation of oxidized sulfur species (sulfate and thiosulfate)

Addition of S^0 in goethite/Fe(II) suspension resulted in the formation of sulfate whose concentration increased slowly to $50 \mu M$ towards the end of reaction (Figure 4.6). However, no thiosulfate was detected (the detection limit of $6 \mu M$) in reaction medium. Since thiosulfate is reactive towards iron oxides, it might exist as a transient intermediate product but was consumed due to reaction with goethite (Elsgaard and Jørgensen, 1992), and thus it was not detected.

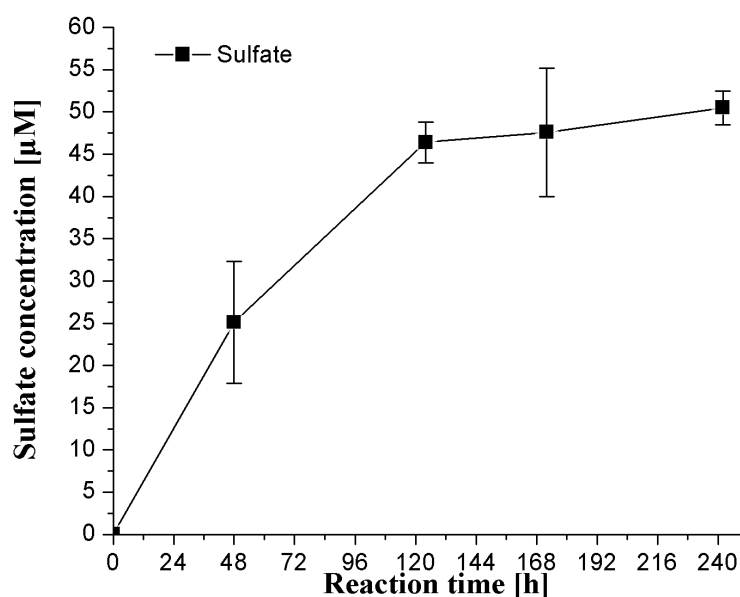


Figure 4.6: Time course of sulfate concentrations during the reaction of S^0 with surface sorbed Fe(II) at goethite surface

In previous studies on reactions between sulfide and iron oxides (in the absence of initial Fe(II)) at neutral pH (Hellige et al., 2012; Poulton, 2003; Poulton et al., 2004; Wan et al., 2017; Wan et al., 2014), neither sulfate nor thiosulfate were detectable. Only in the reactions between NOM and sulfide, trace amounts of sulfate and thiosulfate were detected (Heitmann and Blodau, 2006; Yu et al., 2015). Whereas in present study, 50 μM sulfate was formed in the suspension of goethite/Fe(II) after addition of elemental sulfur. On the other hand, no sulfate was detected in goethite suspension in the absence of Fe(II) under similar experimental conditions. Therefore, possibility of sulfur oxidation to sulfate by goethite alone can be ruled out in our system. Moreover, artifact of sulfate concentration during the IC analysis can also be excluded. Because the sulfate samples were treated after filtration in the glovebox, sulfur species of lower redox state (e.g. S^0 , polysulfide, iron sulfide minerals) existing in solid phase have already been removed from the sample and thus preventing their contribution in sulfate concentration by their oxidation to sulfate during analysis. So, it can be excluded that the sulfur species of lower redox state were oxidized to sulfate during the analysis. Therefore, it is reasonable to conclude that oxidation of elemental sulfur to sulfate observed in this study was caused by a reactive Fe(III) reactive species that were formed in goethite/Fe(II) suspension. The formation of sulfate is in line with the finding of a study conducted by Amstaetter et al. (2009), where As(III) was oxidized to As(V) in anoxic goethite/Fe(II) suspension. Since it has been observed that in goethite/Fe(II) suspension, a new intermediate Fe(III)-mineral phase or Fe(III)-Fe(II) mixed

mineral (usually magnetite) is formed due to electron transfer and atom exchange between surface bound Fe(II) and underlying goethite (Boland et al., 2014; Coughlin and Stone, 1995; Handler et al., 2009; Larese-Casanova and Scherer, 2007; Usman et al., 2018). Amstaetter et al. (2009) reported that newly formed intermediate Fe(III) species formed upon addition of Fe(II) and this unidentified Fe(III) species contributed to the oxidation of As(III) to As(V). This freshly formed surface-bound Fe(III) species is reactive and can also be responsible for the oxidation of S^0 to sulfate. Hellige et al. (2012) reported the formation of magnetite as a transient mineral phase in the reaction between sulfide and lepidocrocite, and they proposed that the magnetite served as electron mediator between lepidocrocite and FeS, promoting the oxidation of FeS to pyrite. Therefore, it can be interpreted that the transient magnetite sorbed at lepidocrocite oxidized FeS. Similar to previous studies (Amstaetter et al., 2009; Hellige et al., 2012), we propose that the transient Fe(III)-containing mineral oxidized S^0 to sulfate in our study. However, the exact nature of this oxidizing mineral could not be identified.

In Chapter 2, during the reaction of aqueous sulfide with goethite/Fe(II) suspension, significant amount of S^0 was yielded while no SO_4^{2-} was detected (detection limit of 7.6 μM). There are two possible explanations for this. Firstly, it could be the absence of elemental sulfur as initial substrate that ultimately transforms into sulfate. Other possible explanation could be that the reaction between goethite/Fe(II) complex with sulfide was faster and more favorable compared to the reaction between goethite/Fe(II) and S^0 . So goethite/Fe(II) complex got altered immediately upon the addition of sulfide with the formation of FeS and S^0 . Therefore, the oxidation of S^0 to sulfate by goethite/Fe(II) was significantly suppressed by the reaction of sulfide with goethite/Fe(II) complex. The alternation of goethite/Fe(II) complex can also explain the observed inhibition of sulfur oxidation to sulfate. The precipitates of FeS at goethite surface affect the oxidation capability of Fe(III) which is responsible for formation of sulfate. With the reaction proceeding and the formation of sulfate, the electron transfer between $Fe(II)_{\text{sorb}}$ and goethite reached to saturation phase (Amstaetter et al., 2009).

4.3.4 Sulfur-mass balance

Since the zero-valent sulfur contained in polysulfides can be captured by the methanol extractable sulfur analysis (Wan et al., 2014), there is no need to be accounted for as separate S-species to calculate sulfur balance. After 10 days of reaction, the concentrations of different sulfur species were 147 μM FeS, 90 μM FeS_n , 23 μM S^0 and 50 μM SO_4^{2-} . Taken the initial S^0

concentration of 322 μM into consideration, the n value of FeS_n can be calculated through Eq 4.8 and is 1.13. Therefore, the concentrations of S atoms in $\text{FeS}_{1.13}$ is 102 μM (90 μM of S(-II) and 12 μM of zero-valent sulfur).

$$n = \frac{C(S^0_{ini}) - (C(S^0_{residual}) + C(SO_4^{2-}) + C(FeS))}{C(FeS_n)} \quad (4.8)$$

$C(S^0_{ini})$ and $C(S^0_{residual})$ are the initially added S^0 concentration (322 μM) and the residual S^0 concentration (23 μM) after reaction, respectively; $C(FeS)$ and $C(FeS_n)$ are the FeS concentration (147 μM) and FeS_n concentration (90 μM) estimated from the AVS measurement. The distribution of different sulfur species are shown in Figure 4.7. We can see that most S^0 transformed to S(-II) which can be extracted after acidification. Fifty μM of S^0 was oxidized to SO_4^{2-} . The AVS results demonstrated that the reduction of S^0 by $\text{Fe(II)}_{\text{sorb}}$ at goethite surface occurred at neutral pH under anoxic conditions.

Since we classified the mixture of these iron sulfide minerals as FeS_n , the small n value of FeS_n indicates the low concentration of zero-valent sulfur that binds with FeS in the form of FeS_n . We proposed that due to the presence of $\text{Fe(II)}_{\text{aq}}$, the regeneration of reactive reducing $\text{Fe(II)}_{\text{sorb}}$ species continued and thus continuously reduced S^0 to sulfide. Simultaneously, the surface reactive Fe(III) species oxidized S^0 to sulfate. All S^0 transformed into other sulfur species, including reduced sulfur species (e.g. iron sulfide minerals) and oxidized sulfur species (e.g. sulfate). Even the 23 μM of S^0 remaining in the suspension has been originated from polysulfides. Therefore, it can be inferred that all the initially added elemental sulfur transformed to other species.

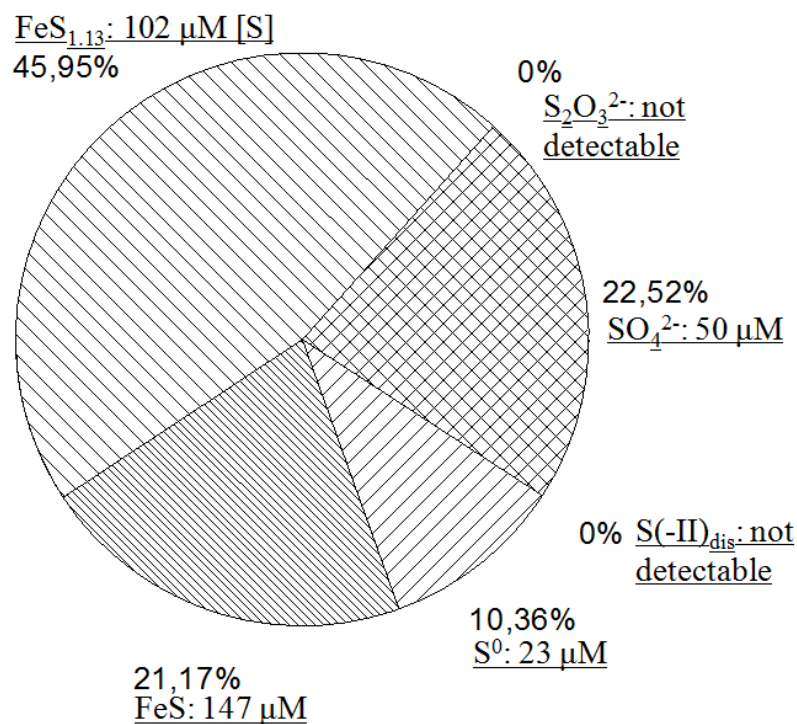


Figure 4.7: The S atom distribution of different sulfur species (23 μM for S^0 , 147 μM for FeS, 102 μM [S] for $\text{FeS}_{1.13}$, 50 μM for SO_4^{2-}). Note that the S in fraction of $\text{FeS}_{1.13}$ is the S atoms contained in $\text{FeS}_{1.13}$, not the concentration of $\text{FeS}_{1.13}$.

4.3.5 Reaction mechanisms and electron balance

In the suspension of goethite/Fe(II) at neutral pH under anoxic conditions, S^0 disproportionated into S(-II) and SO_4^{2-} . $\text{Fe(II)}_{\text{sorb}}$ reduced S^0 to S^{2-} (Figure 4.8 (a)). In the presence of S^0 , S^{2-} can react with S^0 to form S_n^{2-} . The generated sulfide can readily bind with $\text{Fe(II)}_{\text{sorb}}$ to form FeS, therefore, the extent of S_n^{2-} formation was limited. The scavenging of resulting sulfide by Fe(II) kept the sulfide concentration low and made the disproportionation energetically favorable (Wasmund et al., 2017). Furthermore, polysulfides can decompose to elemental sulfur and sulfide due to reaction with Fe(II), therefore the yield of polysulfide is not significant. On the other hand, due to electron transfer between $\text{Fe(II)}_{\text{sorb}}$ and structural Fe(III) in goethite (Figure 4.8 (b)), intermediate reactive Fe(III) surface species formed, and oxidized S^0 to SO_4^{2-} (see Figure 4.8 (c)).

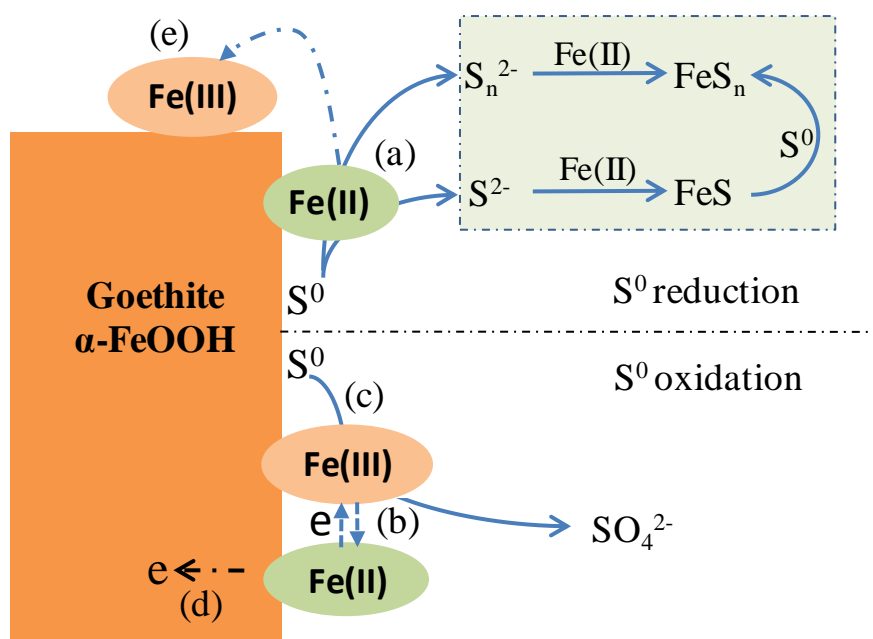
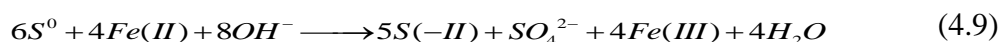


Figure 4.8: The reaction mechanisms between goethite/Fe(II) and S⁰: (a) Fe(II)_{sorb} reduce S⁰ to S(-II); (b) Due to electron transfer between Fe(II)_{sorb} and structural Fe(III) in goethite, (c) Fe(III) surface complex oxidizes S⁰ to SO₄²⁻, (d) the electron moves from Fe(II)_{sorb} into goethite structure, (e) Fe(II)_{sorb} transforms to Fe(III) minerals at goethite surface.

Since the measured S(-II) (AVS_{6M} data) and SO₄²⁻ concentrations are 237 μM and 50 μM, respectively, the ratio of S(-II) : SO₄²⁻ are approximately 5 : 1 in this system, the proposed reaction is obtained as follows:



In summary, Fe(II) was involved in different reaction pathways in this study. It acted as reactant to reduce S⁰ to S(-II), but also was generated as product in S⁰ oxidation by Fe(III) surface species, playing a vital role (Figure 4.8). The generation and consumption of Fe(II) in the reaction of S⁰ with goethite/Fe(II) complex is presented in Figure 4.9.

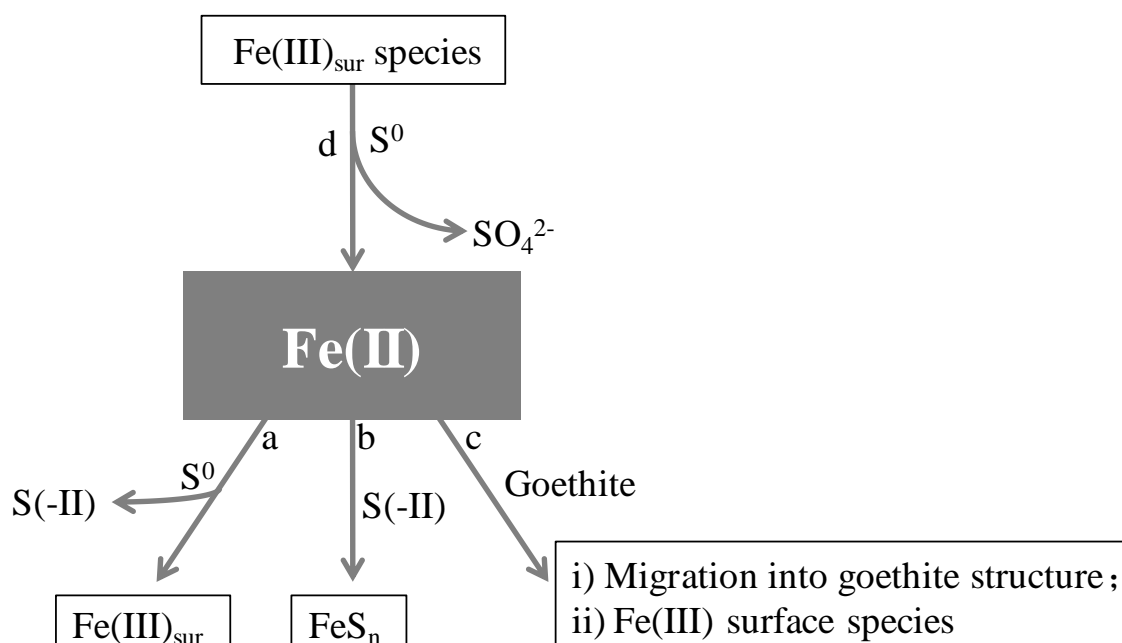


Figure 4.9: A simple “black box” model for Fe(II) species during reaction of S^0 goethite/Fe(II) at pH 7 under anoxic condition.

In the reduction of S^0 by $Fe(II)_{sorb}$ (Figure 4.9 a), the generated sulfide concentration was 237 μM (AVS_{6M}), indicating S^0 accepted around 474 μM electrons, which were mainly from Fe(II). Accordingly, theoretically 474 μM of Fe(II) was consumed due to oxidation to Fe(III) (Figure 4.9 a). In addition, Fe(II) can also precipitate with S(-II) to form FeS and further evolve to more stable iron sulfide minerals, such as Fe_3S_4 and FeS_2 , which are not extractable in 1 M HCl, leading to the unrecovery of Fe(II) (Figure 4.9 b). In this study, the estimated concentration of $FeS_{1.13}$, which can be expressed in the form of $Fe^n S \cdot S_{0.13}$, is 90 μM . Accordingly, the amount of Fe(II) contained in $FeS_{1.13}$ is 90 μM . However, this fraction of Fe(II) is assumed not to be extractable in 1 M HCl. These consumed Fe(II) represented the output of Fe(II) in Figure 4.9, they were referred to as $Fe(II)_{out}$. While on the side of oxidation of S^0 to SO_4^{2-} by Fe(III), 50 μM sulfate formed, theoretically 300 μM electron moved from S^0 to Fe(III) with formation of 300 μM Fe(II), representing the generated fraction of Fe(II) (Figure 4.9 d). Likewise, this newly generated Fe(II) represented the input of Fe(II) in Figure 4.9, they were referred to as $Fe(II)_{in}$. According to the Fe(II) measuring at 10 days of reaction, $Fe(II)_{tot}$ concentration decreased by approximately 657 μM . While the calculated Fe(II) above, accounting for the decrease in Fe(II), is not enough to account the decrease in $Fe(II)_{tot}$ concentration of 657 μM . There must be another output to meet the Fe(II) balance.

$$C(\text{Fe(II)}_{\text{out}}) - C(\text{Fe(II)}_{\text{in}}) = C(\text{Fe(II)}_{\text{decrease}}) \quad (4.10)$$

$C(\text{Fe(II)}_{\text{out}})$ and $C(\text{Fe(II)}_{\text{in}})$ are the amounts of Fe(II) consumed and generated in the system. $C(\text{Fe(II)}_{\text{decrease}})$ is the decrement of $\text{Fe(II)}_{\text{tot}}$ during the whole reaction process, which is 657 μM . According to Eq 4.10, there was approximately 390 μM Fe(II) representing another output of Fe(II) in Figure 4.9. This fraction of $\text{Fe(II)}_{\text{out}}$ was unrecovered in 1 M HCl, and was assumed to migrate into goethite structure due to electron transfer between $\text{Fe(II)}_{\text{sorb}}$ and structural Fe(III) in goethite (Figure 4.9 c). Compared to the background concentration (60.1 mM) of structural Fe(III) in goethite, this fraction of $\text{Fe(II)}_{\text{out}}$ accounted for 0.6 % of total Fe. During the whole reaction process, both $\text{Fe(II)}_{\text{aq}}$ and $\text{Fe(II)}_{\text{tot}}$ continuously consumed, while the $\text{Fe(II)}_{\text{sorb}}$ remained almost unchanged (Figure 4.4), indicating the continuous regeneration of $\text{Fe(II)}_{\text{sorb}}$. It has been widely observed that the sorption of Fe(II) at iron oxides surface resulted in electron transfer between $\text{Fe(II)}_{\text{sorb}}$ and structural Fe(III), in which electron would migrate into iron oxides structure and reduce a structural Fe(III) inside iron oxides, thus leading to recovery of Fe(II) in mild acid extraction (in 1 M HCl) (Gorski and Scherer, 2011; Jeon et al., 2001; Orsetti et al., 2013). We propose that during the reaction between Fe(II)/Fe(III) surface complex and elemental sulfur, electron transfer between $\text{Fe(II)}_{\text{sorb}}$ and structural Fe(III) in goethite was continuously occurring in this process, more electron migrated to bulk goethite, leading to incomplete recovery of Fe(II) in 1 M HCl. Another explanation for the incomplete recovery of Fe(II) is that Fe(II) strongly adsorbed at goethite surface and transformed to more crystalline iron mineral (e.g. magnetite) in the case of high $\text{Fe(II)}_{\text{aq}}$ concentration (Boland et al., 2014; Jeon et al., 2003). Jeon et al. (2003) investigated the reaction between Fe(II) and hematite at pH 6.8 under anoxic condition, revealing the oxidation of $\text{Fe(II)}_{\text{sorb}}$ and formation of secondary iron oxide (e.g. magnetite) due to electron transfer from $\text{Fe(II)}_{\text{sorb}}$ and structural Fe(III) in hematite. Boland et al. (2014) investigated the Fe(II)-accelerated transformation of ferrihydrite to goethite and found that the sorbed Fe(II) is immediately oxidized to Fe(III) at ferrihydrite surface. Boland et al. (2014) observed that this freshly formed Fe(III) species transformed to secondary mineral and facilitated the continuous sorption of Fe(II) from solution by creating new surface sorption sites. Williams and Scherer (2004) had the similar finding that electron transfer between $\text{Fe(II)}_{\text{sorb}}$ and underlying Fe(III) induces growth of an Fe(III) layer on oxides surface that was similar to bulk oxides. Therefore, an explanation can be put forward to accounting for incomplete recovery of Fe(II) that electrons moved inside goethite and a new Fe(III) precipitate formed at goethite surface, preventing the recovery of Fe(II) in acidic extraction. However, considering that goethite is a thermodynamically stable mineral, question

arises how many electrons the bulk goethite can accommodate from $\text{Fe(II)}_{\text{sorb}}$ and to which extent the recrystallization of goethite occur under the studied conditions. Therefore, further investigation needs to be conducted to address this question.

4.5 Environmental implications

The disproportionation of elemental sulfur to sulfide and sulfate plays important role in the sulfur cycling in natural system which obtained considerable interest during the last decades (Belkin et al., 1985; Canfield and Thamdrup, 1996; Poser et al., 2013; Slobodkin et al., 2013; Thamdrup et al., 1993). In natural environments where iron oxides are ubiquitous, reduced sulfide can bind with Fe(II) to form FeS(s) , which further transforms to thermodynamically stable pyrite, contributing to the cycling of Fe and S (Canfield and Thamdrup, 1996). However, so far, most studies about sulfur disproportionation were conducted in biotic systems (Bak and Cypionka, 1987; Finster, 2008; Frederiksen and Finster, 2004; Slobodkin et al., 2013; Thamdrup et al., 1993). The abiotic disproportionation of elemental sulfur at iron oxides surface has not been reported in literature. This research is the first study to demonstrate the abiotic disproportionation of elemental sulfur at iron oxides surface under environmentally relevant condition. In natural system, formation of sulfate and especially the disproportionation of S derived by reactive Fe(III) species should also be taken into consideration to discuss the S cycle.

5 Conclusions and Outlook

5.1 Conclusions

The main goal of this study is to investigate the interaction between aqueous sulfide and iron oxides under the influence of Fe(II) and NOM at neutral pH under anoxic conditions. We observed that the main oxidation product of sulfide was elemental sulfur. The interaction between elemental sulfur and goethite/Fe(II) was also investigated under similar experimental conditions. We focused on the influence of Fe(II) and NOM on the oxidation of sulfide, and the reaction mechanism of S^0 with surface sorbed Fe(II). Therefore, the main sulfur species were monitored during the whole reaction process. The main conclusions are summarized as follows:

Firstly, during the reaction of aqueous sulfide and goethite, S^0 and Fe(II) were the main redox reaction products. The pre-existing of Fe(II) sorbing at goethite surface would affect the redox reaction. In the presence of Fe(II)_{aq}, a dynamic equilibrium between Fe(II)_{aq} and Fe(II)_{sorb} occurred during the reaction process, allowing Fe(II)_{sorb} keep fresh and reactive. The continuous regeneration of reactive Fe(II)_{sorb} enabled electron transfer between Fe(II)_{sorb} and structural Fe(III) in goethite, followed by the formation of unidentified reactive Fe(III) species at goethite surface, which contributed to the oxidation of FeS. While in the case of only Fe(II)_{sorb} present (without Fe(II)_{aq}), once the reactive Fe(III) species was consumed, the reaction between FeS and goethite stopped. Therefore in this case Fe(II)_{sorb} acted more as a coating, preventing the reaction between FeS and goethite. It is proposed that when Fe(II)_{aq} is present, Fe(II)_{aq} can re-sorb at mineral surface forming new Fe(II)_{sorb} sites, allowing the Fe(II)_{sorb} keep reactive, thus plays a more influential role in the interaction. Therefore Fe(II)_{sorb} acts more as a stimulating role in the reaction between goethite and FeS in the presence of Fe(II)_{aq}. Apart from oxidation of S(-II) to S^0 , most spiked sulfide existed in the form of iron sulfide minerals. In the Fe(II)_{no} setup where there was no interference of Fe(II), one quarter of spiked sulfide (77 μM) was methanol extractable S^0 . The other S atoms combined with iron sulfide minerals, which cannot be released as acid volatile sulfide in 1 M HCl. In the Fe(II)_{high} setup where Fe(II)_{aq} and Fe(II)_{sorb} were present, the yield of S^0 was similar with that in the Fe(II)_{no} setup, but among the S binding to iron sulfide minerals, a large fraction of S (160 μM) were FeS, which was released in 1 M HCl, another quarter of sulfide (75 μM) was strongly bound to iron sulfide mineral neither can be released in methanol nor in 1 M HCl. Under

conditions where there was only $\text{Fe(II)}_{\text{sorb}}$ but no $\text{Fe(II)}_{\text{aq}}$, the formation of S^0 took up small fraction of the initially spiked sulfide. Most S existed in the form of iron sulfide minerals: 62 μM was in the form of FeS, 218 μM was in the form of iron sulfide mineral.

Secondly, in goethite/Fe(II) suspension at neutral pH under anoxic conditions, AHA sorbed at goethite surface significantly and inhibited the redox reaction between sulfide with goethite, leading to a lower transformation products (thiosulfate and sulfate were not detected). In the case of high AHA concentration (40 mg C/L), the redox state played a minor role in the reaction between goethite and sulfide due to significant sorption of AHA at goethite surface. While in the case of low AHA concentration (10 mg C/L), the effect of redox state of AHA is very limited due to low concentration. Sulfide incorporated in AHA structure, regardless of the redox state. The $\text{S(-II)}_{\text{org}}$ cannot be completely recovered by acid treatment.

Thirdly, in goethite/Fe(II) suspension, elemental sulfur abiotically disproportionated to sulfide and sulfate at the goethite surface. The reduced sulfur species were sulfide and polysulfides. Due to the scavenging effect of goethite/Fe(II), the concentration of polysulfides stayed at 9 – 20 μM . The reduced sulfide precipitated with Fe(II) to form iron sulfide mineral. Simultaneously, the reactive surface Fe(III) species oxidized elemental sulfur to sulfate, highlighting the importance of abiotic disproportionation of elemental sulfur in natural system.

5.2 Outlook

In this study we added Fe(II) to goethite suspension first, followed by the addition of NOM. While, the sequence of addition of Fe(II) and NOM would affect the sorption of Fe(II) and NOM at mineral surface, thus alter the surface characteristic of iron oxides and subsequently affect the interaction of sulfide with iron oxides. In the future we can reverse the order to see how the interactions can be affected. We can also investigate the interaction of goethite/NOM with sulfide in the absence of Fe(II) to see how the presence of NOM affect the interaction of sulfide with iron oxides.

In this dissertation, all researches were conducted under well defined experimental conditions. However, in natural systems there are a variety of other inorganic and organic components, e.g. phosphate, metal ion and pesticide. All these components can sorb at mineral surface, competing with sorption of Fe(II) and NOM, thus altering the surface characteristics (Ali and Dzombak, 1996; Antelo et al., 2007; Weng et al., 2005). Therefore these components can affect the role of NOM in electron transfer at mineral surface in natural system. Thus the effect of

other sorbates on electron transfer at iron mineral surface can be further studied. Another important species are bacteria, which are ubiquitous in natural system. They can not only reduce iron oxides and sulfate to gain energy for growth, but also reduce NOM. In the presence of NOM-reducing bacteria, the reduced NOM can get oxidized by iron mineral, the resulting re-oxidized NOM can subsequently be reduced by bacteria again (Klüpfel et al., 2014). Under anoxic conditions, NOM can act as a regenerable electron acceptor in the presence of bacteria. To know more about the role of bacteria in reactions of electron transfer in natural environment, it is necessary to introduce bacteria into the future experiments.

In order to apply this research in field project for environmental remediation, the environmental pollutants (e.g. CCl_4 and toxic metal ions) can be added into future experiment to see their fate under the environment-like experimental conditions, in seek of establishing an efficient technology for environmental remediation.

6 References

- Aeschbacher, M., Sander, M. and Schwarzenbach, R.P. (2009) Novel electrochemical approach to assess the redox properties of humic substances. *Environ. Sci. Technol.* 44, 87-93.
- Aeschbacher, M., Vergari, D., Schwarzenbach, R.P. and Sander, M. (2011) Electrochemical analysis of proton and electron transfer equilibria of the reducible moieties in humic acids. *Environ. Sci. Technol.* 45, 8385-8394.
- Ali, M.A. and Dzombak, D.A. (1996) Effects of simple organic acids on sorption of Cu²⁺ and Ca²⁺ on goethite. *Geochim. Cosmochim. Acta* 60, 291-304.
- Amonette, J.E., Workman, D.J., Kennedy, D.W., Fruchter, J.S. and Gorby, Y.A. (2000) Dechlorination of carbon tetrachloride by Fe (II) associated with goethite. *Environ. Sci. Technol.* 34, 4606-4613.
- Amstaetter, K., Borch, T. and Kappler, A. (2012) Influence of humic acid imposed changes of ferrihydrite aggregation on microbial Fe (III) reduction. *Geochim. Cosmochim. Acta* 85, 326-341.
- Amstaetter, K., Borch, T., Larese-Casanova, P. and Kappler, A. (2009) Redox transformation of arsenic by Fe (II)-activated goethite (α -FeOOH). *Environ. Sci. Technol.* 44, 102-108.
- Antelo, J., Arce, F., Avena, M., Fiol, S., López, R. and Mac ís, F. (2007) Adsorption of a soil humic acid at the surface of goethite and its competitive interaction with phosphate. *Geoderma* 138, 12-19.
- Bak, F. and Cypionka, H. (1987) A novel type of energy metabolism involving fermentation of inorganic sulphur compounds. *Nature* 326, 891-892.
- Belkin, S., Wirsen, C.O. and Jannasch, H.W. (1985) Biological and abiological sulfur reduction at high temperatures. *Appl. Environ. Microbiol.* 49, 1057-1061.
- Ben - Yaakov, S. (1973) pH buffering of pore water of recent anoxic marine sediments. *Limnol. Oceanogr.* 18, 86-94.
- Benz, M., Schink, B. and Brune, A. (1998) Humic acid reduction by *Propionibacterium freudenreichii* and other fermenting bacteria. *Appl. Environ. Microbiol.* 64, 4507-4512.
- Boland, D.D., Collins, R.N., Miller, C.J., Glover, C.J. and Waite, T.D. (2014) Effect of solution and solid-phase conditions on the Fe (II)-accelerated transformation of ferrihydrite to lepidocrocite and goethite. *Environ. Sci. Technol.* 48, 5477-5485.
- Borch, T., Campbell, K. and Kretzschmar, R. (2009) How electron flow controls contaminant dynamics. *Environ. Sci. Technol.* 44, 3-6.
- Broderius, S.J. and Smith, L.L. (1977) Direct determination and calculation of aqueous hydrogen sulfide. *Anal. Chem.* 49, 424-428.
- Buchholz, A. (2009) Redox reactions and phase transformation processes at iron mineral surfaces studied by compound specific isotope analysis. Ph. D. thesis. Universität Tübingen.
- Canfield, D.E. and Thamdrup, B. (1996) Fate of elemental sulfur in an intertidal sediment. *FEMS Microbiol. Ecol.* 19, 95-103.
- Casagrande, D.J., Gronli, K. and Sutton, N. (1980) The distribution of sulfur and organic matter in various fractions of peat: origins of sulfur in coal. *Geochim. Cosmochim. Acta* 44, 25-32.

- Chakraborty, S., Favre, F., Banerjee, D., Scheinost, A.C., Mullet, M., Ehrhardt, J.-J., Brendle, J., Vidal, L.c. and Charlet, L. (2010) U (VI) sorption and reduction by Fe (II) sorbed on montmorillonite. *Environ. Sci. Technol.* 44, 3779-3785.
- Cline, J.D. (1969) Spectrophotometric determination of hydrogen sulfide in natural waters. *Limnol. Oceanogr.* 14, 454-458.
- Cline, J.D. and Richards, F.A. (1972) OXYGEN DEFICIENT CONDITIONS AND NITRATE REDUCTION IN THE EASTERN TROPICAL NORTH PACIFIC OCEAN1. *Limnol. Oceanogr.* 17, 885-900.
- Colón, D., Weber, E.J. and Anderson, J.L. (2008) Effect of natural organic matter on the reduction of nitroaromatics by Fe (II) species. *Environ. Sci. Technol.* 42, 6538-6543.
- Cornell, R.M. and Schwertmann, U. (2003) *The iron oxides: structure, properties, reactions, occurrences and uses.* John Wiley & Sons.
- Cornwell, J.C. and Morse, J.W. (1987) The characterization of iron sulfide minerals in anoxic marine sediments. *Mar. Chem.* 22, 193-206.
- Coughlin, B.R. and Stone, A.T. (1995) Nonreversible adsorption of divalent metal ions (MnII, CoII, NiII, CuII, and PbII) onto goethite: effects of acidification, FeII addition, and picolinic acid addition. *Environ. Sci. Technol.* 29, 2445-2455.
- Cui, D. and Eriksen, T.E. (1996) Reduction of pertechnetate by ferrous iron in solution: Influence of sorbed and precipitated Fe (II). *Environ. Sci. Technol.* 30, 2259-2262.
- Curtis, G.P. and Reinhard, M. (1994) Reductive dehalogenation of hexachloroethane, carbon tetrachloride, and bromoform by anthrahydroquinone disulfonate and humic acid. *Environ. Sci. Technol.* 28, 2393-2401.
- Dos Santos Afonso, M. and Stumm, W. (1992) Reductive dissolution of iron (III)(hydr) oxides by hydrogen sulfide. *Langmuir* 8, 1671-1675.
- Dunnivant, F.M., Schwarzenbach, R.P. and Macalady, D.L. (1992) Reduction of substituted nitrobenzenes in aqueous solutions containing natural organic matter. *Environ. Sci. Technol.* 26, 2133-2141.
- Duranceau, S.J. and Faborode, J.O. (2012) Predictive modeling of sulfide removal in tray aerators. *J Am Water Works Assoc* 104, E127-E135.
- Elsgaard, L. and Jørgensen, B.B. (1992) Anoxic transformations of radiolabeled hydrogen sulfide in marine and freshwater sediments. *Geochim. Cosmochim. Acta* 56, 2425-2435.
- Elsner, M., Haderlein, S.B., Kellerhals, T., Luzi, S., Zwank, L., Angst, W. and Schwarzenbach, R.P. (2004) Mechanisms and products of surface-mediated reductive dehalogenation of carbon tetrachloride by Fe (II) on goethite. *Environ. Sci. Technol.* 38, 2058-2066.
- Feitosa-Felizzola, J., Hanna, K. and Chiron, S. (2009) Adsorption and transformation of selected human-used macrolide antibacterial agents with iron (III) and manganese (IV) oxides. *Environ. Pollut.* 157, 1317-1322.
- Feng, X., Simpson, A.J. and Simpson, M.J. (2005) Chemical and mineralogical controls on humic acid sorption to clay mineral surfaces. *Org. Geochem.* 36, 1553-1566.
- Finster, K. (2008) Microbiological disproportionation of inorganic sulfur compounds. *J. Sulfur Chem.* 29, 281-292.

- Fonselius, S., Dyrssen, D. and Yhlen, B. (2007) Determination of hydrogen sulphide. *Methods of Seawater Analysis*, Third Edition, 91-100.
- Fox, P.M., Davis, J.A., Kukkadapu, R., Singer, D.M., Bargar, J. and Williams, K.H. (2013) Abiotic U (VI) reduction by sorbed Fe (II) on natural sediments. *Geochim. Cosmochim. Acta* 117, 266-282.
- Frederiksen, T.-M. and Finster, K. (2004) The transformation of inorganic sulfur compounds and the assimilation of organic and inorganic carbon by the sulfur disproportionating bacterium *Desulfocapsa sulfoexigens*. *Antonie van Leeuwenhoek* 85, 141-149.
- Glasauer, S., Langley, S. and Beveridge, T.J. (2002) Intracellular iron minerals in a dissimilatory iron-reducing bacterium. *Science* 295, 117-119.
- Glass, B.L. (1972) Relation between the degradation of DDT and the iron redox system in soils. *J. Agric. Food. Chem.* 20, 324-327.
- Gorski, C. and Scherer, M. (2011) Fe²⁺ sorption at the Fe oxide-water interface: A revised conceptual framework. *Aquatic Redox Chemistry* 1071, 477-517.
- Gorski, C.A. and Scherer, M.M. (2009) Influence of magnetite stoichiometry on FeII uptake and nitrobenzene reduction. *Environ. Sci. Technol.* 43, 3675-3680.
- Gregory, K.B., Larese-Casanova, P., Parkin, G.F. and Scherer, M.M. (2004) Abiotic transformation of hexahydro-1, 3, 5-trinitro-1, 3, 5-triazine by FeII bound to magnetite. *Environ. Sci. Technol.* 38, 1408-1414.
- Guo, X. and Jans, U. (2006) Kinetics and mechanism of the degradation of methyl parathion in aqueous hydrogen sulfide solution: investigation of natural organic matter effects. *Environ. Sci. Technol.* 40, 900-906.
- Haderlein, S.B. and Pecher, K. (1998) Pollutant reduction in heterogeneous Fe (II)-Fe (III) systems.
- Handler, R.M., Beard, B.L., Johnson, C.M. and Scherer, M.M. (2009) Atom exchange between aqueous Fe (II) and goethite: An Fe isotope tracer study. *Environ. Sci. Technol.* 43, 1102-1107.
- Handler, R.M., Friedrich, A.J., Johnson, C.M., Rosso, K.M., Beard, B.L., Wang, C., Latta, D.E., Neumann, A., Pasakarnis, T. and Premaratne, W. (2014) Fe (II)-catalyzed recrystallization of goethite revisited. *Environ. Sci. Technol.* 48, 11302-11311.
- Heijman, C.G., Grieder, E., Holliger, C. and Schwarzenbach, R.P. (1995) Reduction of nitroaromatic compounds coupled to microbial iron reduction in laboratory aquifer columns. *Environ. Sci. Technol.* 29, 775-783.
- Heijman, C.G., Holliger, C., Glaus, M.A., Schwarzenbach, R.P. and Zeyer, J. (1993) Abiotic reduction of 4-chloronitrobenzene to 4-chloroaniline in a dissimilatory iron-reducing enrichment culture. *Appl. Environ. Microbiol.* 59, 4350-4353.
- Heitmann, T. and Blodau, C. (2006) Oxidation and incorporation of hydrogen sulfide by dissolved organic matter. *Chem. Geol.* 235, 12-20.
- Hellige, K., Pollok, K., Larese-Casanova, P., Behrends, T. and Peiffer, S. (2012) Pathways of ferrous iron mineral formation upon sulfidation of lepidocrocite surfaces. *Geochim. Cosmochim. Acta* 81, 69-81.

- Henneke, E., Luther, G.W., De Lange, G.J. and Hoefs, J. (1997) Sulphur speciation in anoxic hypersaline sediments from the eastern Mediterranean Sea. *Geochim. Cosmochim. Acta* 61, 307-321.
- Hofstetter, T.B., Neumann, A. and Schwarzenbach, R.P. (2006) Reduction of nitroaromatic compounds by Fe (II) species associated with iron-rich smectites. *Environ. Sci. Technol.* 40, 235-242.
- Hofstetter, T.B., Schwarzenbach, R.P. and Haderlein, S.B. (2003) Reactivity of Fe (II) species associated with clay minerals. *Environ. Sci. Technol.* 37, 519-528.
- Huang, Y.H. and Zhang, T.C. (2016) Nitrate Reduction by Surface-Bound Fe (II) on Solid Surfaces at Near-Neutral pH and Ambient Temperature. *J. Environ. Eng.* 142, 04016053.
- Hunger, S. and Benning, L.G. (2007) Greigite: a true intermediate on the polysulfide pathway to pyrite. *Geochem. Trans* 8, 1.
- Jeon, B.-H., Dempsey, B.A. and Burgos, W.D. (2003) Kinetics and mechanisms for reactions of Fe (II) with iron (III) oxides. *Environ. Sci. Technol.* 37, 3309-3315.
- Jeon, B.-H., Dempsey, B.A., Burgos, W.D. and Royer, R.A. (2001) Reactions of ferrous iron with hematite. *Colloids Surf A Physicochem Eng Asp* 191, 41-55.
- Jiang, J. and Kappler, A. (2008) Kinetics of Microbial and Chemical Reduction of Humic Substances: Implications for Electron Shuttling. *Environ. Sci. Technol.* 42, 3563-3569.
- Kamyshny, A., Borkenstein, C.G. and Ferdelman, T.G. (2009) Protocol for Quantitative Detection of Elemental Sulfur and Polysulfide Zero - Valent Sulfur Distribution in Natural Aquatic Samples. *GEOSTAND GEOANAL RES* 33, 415-435.
- Kamyshny Jr, A., Zilberbrand, M., Ekeltchik, I., Voitsekovski, T., Gun, J. and Lev, O. (2008) Speciation of polysulfides and zerovalent sulfur in sulfide-rich water wells in southern and central Israel. *AQUAT GEOCHEM* 14, 171-192.
- Kang, X., Liu, S. and Zhang, G. (2014) Reduced inorganic sulfur in the sediments of the Yellow Sea and East China Sea. *Acta Oceanologica Sinica* 33, 100-108.
- Kappler, A., Benz, M., Schink, B. and Brune, A. (2004) Electron shuttling via humic acids in microbial iron (III) reduction in a freshwater sediment. *FEMS Microbiol. Ecol.* 47, 85-92.
- Kappler, A. and Haderlein, S.B. (2003) Natural organic matter as reductant for chlorinated aliphatic pollutants. *Environ. Sci. Technol.* 37, 2714-2719.
- Klausen, J., Haderlein, S.B. and Schwarzenbach, R.P. (1997) Oxidation of substituted anilines by aqueous MnO₂: Effect of co-solutes on initial and quasi-steady-state kinetics. *Environ. Sci. Technol.* 31, 2642-2649.
- Klausen, J., Trober, S.P., Haderlein, S.B. and Schwarzenbach, R. (1995) Reduction of substituted nitrobenzenes by Fe (II) in aqueous mineral suspensions. *Environ. Sci. Technol* 29, 2396-2404.
- Klüpfel, L., Piepenbrock, A., Kappler, A. and Sander, M. (2014) Humic substances as fully regenerable electron acceptors in recurrently anoxic environments. *Nat Geosci* 7, 195-200.
- Kosobucki, P. and Buszewski, B. (2014) Natural organic matter in ecosystems-A review. *Nova Biotechnologica et Chimica* 13, 109-129.
- Larese-Casanova, P. and Scherer, M.M. (2007) Fe(II) sorption on hematite: new insights based on spectroscopic measurements. *Environ. Sci. Technol.* 41, 471-477.

- Lawrence, N.S., Davis, J. and Compton, R.G. (2000) Analytical strategies for the detection of sulfide: a review. *Talanta* 52, 771-784.
- Liger, E., Charlet, L. and Van Cappellen, P. (1999) Surface catalysis of uranium (VI) reduction by iron (II). *Geochim. Cosmochim. Acta* 63, 2939-2955.
- Lohmayer, R., Kappler, A., Lösekann-Behrens, T. and Planer-Friedrich, B. (2014) Sulfur species as redox partners and electron shuttles for ferrihydrite reduction by *Sulfurospirillum deleyianum*. *Appl. Environ. Microbiol.* 80, 3141-3149.
- Lovley, D.R. (1997) Microbial Fe (III) reduction in subsurface environments. *FEMS Microbiol. Rev.* 20, 305-313.
- Luan, F., Xie, L., Li, J. and Zhou, Q. (2013) Abiotic reduction of nitroaromatic compounds by Fe (II) associated with iron oxides and humic acid. *Chemosphere* 91, 1035-1041.
- Luther, G.W. (1991) Pyrite synthesis via polysulfide compounds. *Geochim. Cosmochim. Acta* 55, 2839-2849.
- Meysman, F.J. and Middelburg, J.J. (2005) Acid-volatile sulfide (AVS)—a comment. *Mar. Chem.* 97, 206-212.
- Morse, J.W., Millero, F.J., Cornwell, J.C. and Rickard, D. (1987) The chemistry of the hydrogen sulfide and iron sulfide systems in natural waters. *Earth Sci Rev* 24, 1-42.
- Murad, E. (2010) Mössbauer spectroscopy of clays, soils and their mineral constituents. *Clay Minerals* 45, 413-430.
- Murad, E. and Cashion, J. (2004) Iron oxides, Mössbauer Spectroscopy of Environmental Materials and their Industrial Utilization. Springer, pp. 159-188.
- Neumann, A., Wu, L., Li, W., Beard, B.L., Johnson, C.M., Rosso, K.M., Friedrich, A.J. and Scherer, M.M. (2015) Atom exchange between aqueous Fe(II) and structural Fe in clay minerals. *Environ. Sci. Technol.* 49, 2786-2795.
- O'Loughlin, E.J., Burris, D.R. and Delcomyn, C.A. (1999) Reductive dechlorination of trichloroethene mediated by humic-metal complexes. *Environ. Sci. Technol.* 33, 1145-1147.
- Olson, K.R. (2005) Vascular actions of hydrogen sulfide in nonmammalian vertebrates. *Antioxid. Redox Signal.* 7, 804-812.
- Orsetti, S., Laskov, C. and Haderlein, S.B. (2013) Electron transfer between iron minerals and quinones: estimating the reduction potential of the Fe (II)-goethite surface from AQDS speciation. *Environ. Sci. Technol.* 47, 14161-14168.
- Pedersen, H., Postma, D., Jakobsen, R. and Larsen, O. (2005) Fast transformation of iron oxyhydroxides by the catalytic action of aqueous Fe(II). *Geochim. Cosmochim. Acta* 69, 3967-3977.
- Peiffer, S., Behrends, T., Hellige, K., Larese-Casanova, P., Wan, M. and Pollok, K. (2015) Pyrite formation and mineral transformation pathways upon sulfidation of ferric hydroxides depend on mineral type and sulfide concentration. *Chem. Geol.* 400, 44-55.
- Peiffer, S., Dos Santos Afonso, M., Wehrli, B. and Gaechter, R. (1992) Kinetics and mechanism of the reaction of hydrogen sulfide with lepidocrocite. *Environ. Sci. Technol.* 26, 2408-2413.
- Peiffer, S. and Gade, W. (2007) Reactivity of ferric oxides toward H₂S at low pH. *Environ. Sci. Technol.* 41, 3159-3164.

- Piepenbrock, A., Schröder, C. and Kappler, A. (2014) Electron transfer from humic substances to biogenic and abiogenic Fe (III) oxyhydroxide minerals. *Environ. Sci. Technol.* 48, 1656-1664.
- Polubesova, T. and Chefetz, B. (2014) DOM-affected transformation of contaminants on mineral surfaces: A review. *Crit Rev Environ Sci Technol* 44, 223-254.
- Poser, A., Lohmayer, R., Vogt, C., Knoeller, K., Planer-Friedrich, B., Sorokin, D., Richnow, H.-H. and Finster, K. (2013) Disproportionation of elemental sulfur by haloalkaliphilic bacteria from soda lakes. *Extremophiles* 17, 1003-1012.
- Poulton, S.W. (2003) Sulfide oxidation and iron dissolution kinetics during the reaction of dissolved sulfide with ferrihydrite. *Chem. Geol.* 202, 79-94.
- Poulton, S.W., Krom, M.D. and Raiswell, R. (2004) A revised scheme for the reactivity of iron (oxyhydr) oxide minerals towards dissolved sulfide. *Geochim. Cosmochim. Acta* 68, 3703-3715.
- Pyzik, A.J. and Sommer, S.E. (1981) Sedimentary iron monosulfides: kinetics and mechanism of formation. *Geochim. Cosmochim. Acta* 45, 687-698.
- Ratasuk, N. and Nanny, M.A. (2007) Characterization and quantification of reversible redox sites in humic substances. *Environ. Sci. Technol.* 41, 7844-7850.
- Rickard, D. and Luther, G.W. (2007) Chemistry of iron sulfides. *Chem. Rev.* 107, 514-562.
- Rickard, D. and Morse, J.W. (2005) Acid volatile sulfide (AVS). *Mar. Chem.* 97, 141-197.
- Saito, T., Koopal, L.K., van Riemsdijk, W.H., Nagasaki, S. and Tanaka, S. (2004) Adsorption of humic acid on goethite: Isotherms, charge adjustments, and potential profiles. *Langmuir* 20, 689-700.
- Schmidt, C., Behrens, S. and Kappler, A. (2010) Ecosystem functioning from a geomicrobiological perspective—a conceptual framework for biogeochemical iron cycling. *Environ. Chem.* 7, 399-405.
- Schulten, H.-R. (1995) The three-dimensional structure of humic substances and soil organic matter studied by computational analytical chemistry. *Fresenius J. Anal. Chem.* 351, 62-73.
- Shao, H. and Butler, E.C. (2007) The influence of iron and sulfur mineral fractions on carbon tetrachloride transformation in model anaerobic soils and sediments. *Chemosphere* 68, 1807-1813.
- Siegel, L.M. (1965) A direct microdetermination for sulfide. *Anal. Biochem.* 11, 126-132.
- Slobodkin, A., Reysenbach, A.-L., Slobodkina, G., Kolganova, T., Kostrikina, N. and Bonch-Osmolovskaya, E. (2013) *Dissulfuribacter thermophilus* gen. nov., sp. nov., a thermophilic, autotrophic, sulfur-disproportionating, deeply branching deltaproteobacterium from a deep-sea hydrothermal vent. *Int. J. Syst. Evol. Microbiol.* 63, 1967-1971.
- Stuedel, R. (2003) Inorganic Polysulfides S_n^{2-} and Radical Anions $S_n^{\cdot -}$: Top. *Curr. Chem.*, 127-152.
- Stuedel, R., Holdt, G. and Göbel, T. (1989) Ion-pair chromatographic separation of inorganic sulphur anions including polysulphide. *J. Chromatogr. A* 475, 442-446.
- Stookey, L.L. (1970) Ferrozine---a new spectrophotometric reagent for iron. *Anal. Chem.* 42, 779-781.

- Stumm, W. (1987) Aquatic surface chemistry: Chemical processes at the particle-water interface. John Wiley & Sons.
- Stumm, W. and Morgan, J.J. (2012) Aquatic chemistry: chemical equilibria and rates in natural waters. John Wiley & Sons.
- Stumm, W. and Sulzberger, B. (1992) The cycling of iron in natural environments: considerations based on laboratory studies of heterogeneous redox processes. *Geochim. Cosmochim. Acta* 56, 3233-3257.
- Tan, K.H. (2014) Humic matter in soil and the environment: principles and controversies. CRC Press.
- Thamdrup, B., Finster, K., Hansen, J.W. and Bak, F. (1993) Bacterial disproportionation of elemental sulfur coupled to chemical reduction of iron or manganese. *Appl. Environ. Microbiol.* 59, 101-108.
- Tratnyek, P.G., Grundl, T.J. and Haderlein, S.B. (2011) Aquatic redox chemistry. ACS Publications.
- Tratnyek, P.G., Scherer, M.M., Deng, B. and Hu, S. (2001) Effects of natural organic matter, anthropogenic surfactants, and model quinones on the reduction of contaminants by zero-valent iron. *Water Res.* 35, 4435-4443.
- Ulrich, G.A., Krumholz, L.R. and Suflita, J.M. (1997) A rapid and simple method for estimating sulfate reduction activity and quantifying inorganic sulfides. *Appl. Environ. Microbiol.* 63, 1627-1630.
- Usman, M., Byrne, J., Chaudhary, A., Orsetti, S., Hanna, K., Ruby, C., Kappler, A. and Haderlein, S. (2018) Magnetite and green rust: synthesis, properties, and environmental applications of mixed-valent iron minerals. *Chem. Rev.* 118, 3251-3304.
- Vindedahl, A.M., Stemig, M.S., Arnold, W.A. and Penn, R.L. (2016) Character of humic substances as a predictor for goethite nanoparticle reactivity and aggregation. *Environ. Sci. Technol.* 50, 1200-1208.
- Wan, M., Schröder, C. and Peiffer, S. (2017) Fe (III): S (-II) concentration ratio controls the pathway and the kinetics of pyrite formation during sulfidation of ferric hydroxides. *Geochim. Cosmochim. Acta* 217, 334-348.
- Wan, M., Shchukarev, A., Lohmayer, R., Planer-Friedrich, B. and Peiffer, S. (2014) Occurrence of surface polysulfides during the interaction between ferric (hydr) oxides and aqueous sulfide. *Environ. Sci. Technol.* 48, 5076-5084.
- Wang, F. and Chapman, P.M. (1999) Biological implications of sulfide in sediment—a review focusing on sediment toxicity. *Environ. Toxicol. Chem.* 18, 2526-2532.
- Wasmund, K., Mussmann, M. and Loy, A. (2017) The life sulfuric: microbial ecology of sulfur cycling in marine sediments. *Environ Microbiol Rep* 9, 323-344.
- Weng, L.P., Koopal, L.K., Hiemstra, T., Meeussen, J.C. and Van Riemsdijk, W.H. (2005) Interactions of calcium and fulvic acid at the goethite-water interface. *Geochim. Cosmochim. Acta* 69, 325-339.
- Williams, A.G. and Scherer, M.M. (2001) Kinetics of Cr (VI) reduction by carbonate green rust. *Environ. Sci. Technol.* 35, 3488-3494.
- Williams, A.G. and Scherer, M.M. (2004) Spectroscopic evidence for Fe (II)– Fe (III) electron transfer at the iron oxide– water interface. *Environ. Sci. Technol.* 38, 4782-4790.

Xue, Z. (2018) Redox Reactions and Sorption of Quinones and Natural Organic Matter at Iron Mineral/Fe(II) Interfaces. Ph. D. thesis. Universität Tübingen.

Yang, H., Lu, R., Downs, R.T. and Costin, G. (2006) Goethite, α -FeO (OH), from single-crystal data. *Acta Crystallogr. Sect. E: Struct. Rep. Online* 62, i250-i252.

Yu, Z.-G., Orsetti, S., Haderlein, S.B. and Knorr, K.-H. (2016) Electron transfer between sulfide and humic acid: electrochemical evaluation of the reactivity of Sigma-Aldrich humic acid toward sulfide. *AQUAT GEOCHEM* 22, 117-130.

Yu, Z.G., Peiffer, S., Gottlicher, J. and Knorr, K.H. (2015) Electron transfer budgets and kinetics of abiotic oxidation and incorporation of aqueous sulfide by dissolved organic matter. *Environ. Sci. Technol.* 49, 5441-5449.

Zhang, H. and Huang, C.-H. (2003) Oxidative transformation of triclosan and chlorophene by manganese oxides. *Environ. Sci. Technol.* 37, 2421-2430.

Statement of Personal Contribution

Here, I state clearly that the general concept of this thesis and the experimental ideas were proposed by Prof. Dr. Stefan Haderlein and me. The detailed laboratory work and data analysis were conducted by myself. Prof. Dr. Stefan Haderlein supported my experimental work and provided academic advice. The abstract was translated into German by my colleague Philipp Martin.

In Chapter 2, the initial idea of the work was proposed by Prof. Dr. Stefan Haderlein. I performed the experimental work and conducted the wet chemical analysis independently. Mössbauer spectroscopy analysis was conducted under the instruction of Dr. James Byrne. The dataset evaluation of acid volatile sulfide was also done by me following the discussion with Prof. Dr. Stefan Haderlein.

In Chapter 3, the initial idea was designed by Prof. Dr. Stefan Haderlein. The experimental work in the glovebox was carried out by myself. The reduction of Aldrich humic acid was conducted with the help of Edison and Trinh Duong. DOC measurements were performed by the technician Bernice Nisch from Prof. Dr. Peter Grathwohl's group. The data analysis was done by me and discussed with Prof. Dr. Stefan Haderlein.

In Chapter 4, the initial present idea was proposed by me and Prof. Dr. Stefan Haderlein. The experimental work was carried out by myself. The measuring of polysulfides was conducted by Regina Lohmayer from University of Bayreuth. The data analysis was done by me and discussed in detailed with Prof. Dr. Stefan Haderlein. Dr. Usman Muhammad gave fruitful of advice to improve the quality of the script.

Acknowledgement

First of all, I would like to thank Professor Stefan Haderlein for giving me the opportunity to study in Tübingen University. I received a lot of precious advices and inspirations from him. His patience, motivation, and immense knowledge help me get through this period of PhD study. My sincere thanks go to Dr. Usman and Dr. Chuanhe Lu for the thesis revision and to Phillip for the German translation of abstract.

I also would like to express my gratitude to Monika Hertel, Ellen Röhm for their technical and laboratory support. I am grateful to Dr. James M. Byrne for Mössbauer spectroscopy. I also thank the group members for their help and the fun throughout my PhD study. They are Dr. Daniel Buchner, Dr. Silvia Orsetti, Chen Tingting, Liao Dijie, Xue Zhengrong, Trinh Duong, Leyla Guluzada, Edisson Subdiaga, Johannes Büsing, Li Shun, Philipp Martin, Johanna Schlögl. I also want to thank the helps from University of Bayreuth: Wan Moli, Regina Lohmayer, Yu Zhiguo for their sampling analysis and discussion.

Thanks are also given to the China Scholarship Council (CSC) for their financial support.

I would like to express my sincere gratitude to my host family, the Schalls. During my stay in Germany, they helped me a lot whenever I encountered some problems. Living with them made my life in Germany enjoyable and memorable. Shuttling by bicycle between Wurmlingen and Tübingen has always been the most relaxing time of day, which I will remember forever.

I also would like to thank my previous supervisor Prof. Li Dongwei for the continuous concern during these years.

I am sincerely grateful to the support from my friends from China: Peng Dongqin, Kong Xiaming, Xu Zhonghui, Wang Kui.

Last but not the least, I would like to thank my parents, my sister and my brother-in-law for supporting me throughout the period of my study in Germany. I am also sincerely grateful to my sister, my brother-in-law and nephew for their care and companion to parents. **Thank you!**

Curriculum Vitae

Name	Shaojian Zhang
Date of Birth	22.12.1987
Place of Birth	Jingmen, Hubei, China
Current address	Ringstrasse 8, Rottenburg am Neckar, 72108 Germany

Education

Oct 2012 – present	Doctor candidate, Center for Applied Geoscience, Eberhard-Karls University Tübingen, Germany
Sep 2009 – Jun 2012	Master study in Environmental science and Engineering, College of resources and Environmental science, Chongqing University, China Master thesis: Study on Treatment of Heavy Metals Pollution of Copper Tailings by Air-lift Bio-reactor. Supervisor: Prof. Dr. Li Dongwei
Sep 2005 – Jun 2009	Bachelor study in Environmental engineering, College of chemical engineering, Harbin Engineering University, China Bachelor thesis: The preparation of Exfoliated graphite and its performance on oil adsorption. Supervisor: Prof. Dr. Fan Zhuangjun

Scholarships

Sep 2010	First class scholarship, College of resources and Environmental science, Chongqing University
Dec 2011	Scholarship of China Scholarship Council